DOE/IE/10574--T3

DOE/IE/10574--T3

DE90 008796

RADAR IMAGERY INTERPRETATION TO ASSESS THE HYDROCARBON POTENTIAL OF FOUR SITES IN THE PHILIPPINES

ARCI TR 8701-101

November 17, 1988

prepared by

ARKANSAS RESEARCH CONSULTANTS, INC

DISCLAIMER

DISCLAIMER

PREFACE

INTRODUCTION

Arkansas Research Consultants, Inc. (ARCI), conducted an extensive imaging radar survey of selected petroleum and geothermal sites in the Republic of the Philippines. The effort was supported by the United States Department of Energy (DOE), Grant Number DE-FG01-86IE10574.A000.

OBJECTIVES

The primary objectives of this work were (1) to further the goals of international energy development by helping the Philippine's Government improve its understanding of its energy potential, (2) to advance the economic and energy development of the Philippines and, (3) to increase the world's oil supply base. Secondary objectives were (1) to teach scientists and engineers in the Republic of the Philippines the fundamentals of radar image interpretation, and (2) to provide them with a data base for their continued research and analysis.

SCOPE

The work conducted was limited to acquiring SAR (synthetic aperture radar) data which included four potential petroleum resource basins and three areas of geothermal resources in the Republic of the Philippines, to interpreting the data acquired for hydrocarbon or geothermal potential, and to ranking the potential of various prospects identified.

EXECUTIVE SUMMARY

This Executive Summary relates the essential aspects of the work conducted for petroleum prospect evaluation and summarized here. A separate report has also been prepared to detail the work performed in the hydrocarbon analysis.[1] The geothermal investigation is reported in a separate document as well[2].

As with most nations of the world, the Republic of the Philippines is intensely interested in the identification, development, and conservation of natural resources. In keeping with this, the Government of the Philippines has recently completed a nation-wide sedimentary basin evaluation program to assess hydrocarbon potential and assist in future exploration activities. This study was directed by the Philippine Bureau of Energy Development (BED) with a significant portion of the work performed by the Philippine National Oil Company Exploration Corporation (PNOC EC). Since this work was completed, the BED has been reorganized and is now known as the Office of Energy Affairs (OEA).

This program of collection and interpretation of the radar imagery was designed to augment and complement the existing data base prepared by BED and PNOC EC. Hydrocarbon and geothermal sites were selected through the cooperative efforts of BED and PNOC EC scientific personnel. The primary objective of the project was to further the goals of international energy development by aiding the Republic of the Philippines in the assessment of potential petroleum and geothermal prospects within the areas imaged. Secondary goals were to assist the Republic of the Philippines in utilizing state-of-the-art radar remote sensing technology for resource exploration, and to train key Philippines scientists in the use of imaging radar data.

---

1 ARCI, 1988, ***Radar Imagery Interpretation to Assess the Hydrocarbon Potential of Four Sites in the Philippines***, ARCI TR 8701-101, Arkansas Research Consultants, Inc., November 17, 1988.

2 ARCI, 1988, ***Radar Imagery Interpretation to Provide Information about Several Geothermal Sites in the Philippines***, ARCI TR 8701-102, Arkansas Research Consultants, Inc., November 17, 1988.

RADAR'S UNIQUE CAPABILITIES

Because radar provides its own source of illumination, radar images can be produced that preferentially highlight geologic structure and surface detail. Radar images so constructed provide unique information about the local geology which may not be available from other sources. Such information is needed in the Republic of the Philippines because although the region has been extensively mapped via conventional techniques, large uncertainties in the petroleum resource potential of the area still exist.

Radar's unique capabilities include:

* All weather, day-night operation
* Control of look direction and look angle for improved geological interpretation
* Wide areal coverage-synoptic view
* High resolution comparable with most remote sensing systems
* Stereo capability allows rapid formulation of geologic models
* Sensitivity to vegetation at shorter wavelengths
* Terrain texture discrimination in non-vegetated regions
* Digital capability for image enhancement and multi-sensor integration
* Radar mosaic provides an accurate base map

DATA ACQUIRED

Radar imagery covering roughly 60,000 km^2 was acquired. These data were collected by Intera Technology, Inc., under subcontract from ARCI. ARCI provided mission planning and quality assurance for the program. Complete stereo coverage of five different regions was acquired. Within these five sites, the following seven different sets of data were collected, including four for hydrocarbon interpretation and three for geothermal evaluation.

Hydrocarbon Sites

* Bondoc Peninsula
* Cotabato Basin, Mindanao
* Mindoro Island
* Cebu Island

Geothermal Sites

* Mt. Apo, Mindanao
* North Negros Island
* South Negros Island

DATA PRODUCED

The final data products were (1) negative film and positive prints of each of 34 flight line strips, (2) computer compatible tapes (CCT) of each image strip, and (3) negative film and positive prints of radar mosaics of four petroleum sites at 1:250,000 scale. The Intera STAR-1 imaging radar system used to acquire these data operated at X-band, HH-polarization, with 12 m resolution. The final data set represents one of the best examples of radar imagery for resource exploration available anywhere.

Interpretive data products produced include (1) geologic maps, (2) lineament maps, and (3) prospect evaluations. Development of geologic maps and prospect evaluations included extensive use of surface and subsurface data furnished by BED and PNOC EC. Thus, the final evaluation is a synthesis of all data available rather than simply that obtainable from the radar imagery itself. This is perhaps the most significant aspect of the program in that it demonstrates the use of radar as a sensor in an integrated program for hydrocarbon and geothermal exploration. The imagery acquired is an excellent source of data that may be used to refine exploration strategy and define areas for more detailed investigation by ground survey and seismic data acquisition. The image analysis shows numerous areas of agreement with prospects developed from other data

sources such as field and geophysical surveys. In addition, a considerable number of structures and prospects were discovered, particularly in areas where other data sources were unavailable.

SUMMARY

This synthesis of all available data shows radar imagery to be an excellent survey tool in an integrated multilevel exploration. The radar by itself may be used to guide acquisition of more detailed data and develop a general exploration strategy. Where other survey data such as photography or LANDSAT are available, the unique response and illumination enhancement of surface structure obtainable with radar is seen to provide additional data complementary to other survey imagery.

Important new prospects and prospect areas have been identified which will provide a focus for further follow-up field and geophysical studies.

Especially for the Bondoc Peninsula and Cotabato Basin, Mindanao, radar imagery interpretation has provided an increase in the structural information by several orders of magnitude over existing data, and the fault and lineament patterns reveal structural complexity not previously recognized.

Hydrocarbon Prospects

* **Bondoc Peninsula** - Seven prime hydrocarbon prospects have been identified. It is recommended that these potential plays be refined with seismic data. The region is considered to have good potential for both oil and gas. Average field size should range from 5-50 MMBBLS of oil, and 50-500 BCF of gas.

* **Cotabato Basin** - Five prime hydrocarbon prospects have been identified. Two of these plays are in the central part of the basin where relatively large reserves are possible. The region is considered to have poor to fair oil potential. Average field size should be in the range of 5-20 MMBBLS of oil.

* **Mindoro Island** - Only the coastal margins on the southern two-thirds of Mindoro Island are considered favorable for hydrocarbon accumulation. Five prime hydrocarbon prospects

and two additional prospect areas have been identified. Although the geologic maps provided by PNOC EC are of good quality for delineating fold patterns, the structural complexity of fault and lineament patterns has been revealed for the first time on the radar imagery. The Mindoro region is considered to have fair to good potential for predominantly gas plays. Average field size should be in the range of 5-50 MMBBLS of oil, or 50-500 BCF of gas.

* **Cebu Island** - Southern Cebu has received considerable seismic exploration effort; however, the northern half of the island has not been mapped in detail. Ten prime hydrocarbon prospects have been identified with more than half of them being located in the poorly explored northern portion part of the island. Cebu is considered to have good potential for both oil and gas. Average field size should range from 5-50 MMBBLS of oil, or 50-500 BCF of gas.

HIGHLIGHTS

* A significant number of new onshore prospects have been identified in this project that these warrant new seismic investigations.

* The radar data and this project have significantly improved the knowledge of stratigraphy and structure, and in many cases have provided data for updating existing geologic maps.

* The radar geologic maps produced, while important by themselves, can be used to complement existing geoscience data and can provide new map products tailored to support exploration activities.

* An important aspect of radar investigations is that reconnaissance radar images facilitate field work in remote and impassable areas.

* The baseline survey and interpretation were conducted at a scale of 1:250,000, but the data support increasing the scale to 1:50,000.

* A training course on radar interpretation and SAR fundamentals has been provided to Philippines geoscientists, and they have become enthusiastic in the potential application of using radar images for this and other important investigations such as land cover mapping (forestry or other vegetation covers), land use mapping, hydrology, and ground-water exploration.

RECOMMENDATIONS

* Detailed field studies should be conducted to determine the precise locations of prime prospects and then correlate with all available subsurface data. Prospects that do not have supporting surface or subsurface data should be refined with seismic interpretation. More subtle structural targets, such as fault traps and geomorphic anomalies should receive exploration attention using seismic data to confirm the radar imagery-defined plays.

* Additional radar imagery should be acquired over a much larger region of the Philippines, especially within those sedimentary basins where radar can contribute significant data to the development of an integrated exploration strategy for hydrocarbons.

Table of Contents

Table of Figures

Table of Tables

1 INTRODUCTION

1.1 Objectives

The Republic of the Philippines is not well endowed with hydrocarbon reserves, and the Government of the Philippines is anxious to spur more petroleum exploration. For both the Philippines National Oil Company Exploration Corporation (PNOC EC) and Bureau of Energy Development (BED), it has been an important goal to upgrade available geological information on various sedimentary basins in the interest of attracting foreign firms to invest or explore for hydrocarbons. The Government of the Republic of the Philippines has invited new bids from international companies to explore for oil and gas in onshore and offshore sedimentary basins. To assist the private oil industry in the evaluation of the petroleum potential of these basins, the Government, with the assistance of a loan from the World Bank, has completed a nation-wide basin evaluation program.[3]

The collection and interpretation of radar imagery is designed to augment and complement the existing data base prepared by PNOC EC and BED. The primary objective of the project is to further the goals of international energy development by aiding the Republic of the Philippines in the assessment of potential petroleum prospects within the areas imaged. Secondary goals are to assist the Republic of the Philippines in utilizing state-of-the-art radar remote sensing technology for resource exploration, and to train key Philippines scientists in the use of imaging radar data.

---

3 Sedimentary Basins of the Philippines - Their Geology and Hydrocarbon Potential (BED et al., 1987).

1.2 Project Description

Specific project accomplishments include:

(1) Side-looking airborne radar (SLAR) imagery of certain key regions within the Republic of the Philippines has been acquired.

(2) The SLAR data have been processed into images and the separate images have been mosaicked.

(3) Most of the SLAR data have been interpreted for petroleum prospects.

(4) Final geologic maps have been prepared for each petroleum prospect region and are enclosures with this report. These show structural, lithologic, and stratigraphic detail.

(5) This technical report describes the geological details of the regions covered by the maps.

(6) An Executive Summary highlighting the results of this study has been written for a non-technical audience.

(7) A percentage of the data have been reviewed for geothermal prospects and this work and recommendations is presented in a separate report.

(8) A training course in the methods of interpreting SLAR images, the relative merits of SLAR vs other forms of images, and the results of the interpretation of images used for this project was prepared. The training course, approximately one week in length, was conducted for Philippines geoscientists in Manila in May, 1988.

2 BACKGROUND

Key personnel from Arkansas Research Consultants, Inc (ARCI) and the U. S. Department of Energy (DOE) traveled to the Republic of the Philippines (March 1987) to explore the possibilities of scientific and technical interchange in conducting a SAR (synthetic aperture radar) mapping campaign in the Philippines. The proposed project would involve acquiring SAR data of selected sites in the Philippines, processing the data, preparing mosaics, and interpreting and analyzing the resultant image data for hydrocarbon resource exploration potential.

2.1 Synopsis of Meetings

Meetings were held during the week of March 16-20, 1987 in the Republic of the Philippines. The primary objectives of these meetings were: 1) to be introduced to the Minister of Energy and geoscience personnel from PNOC EC and BED; 2) to propose a SAR mapping campaign to the Philippines officials which could help them assess their petroleum potential and; 3) to present a brief overview of the proposed project.

DOE personnel presented to the Philippines officials and scientists present at the meetings an outline of our proposal to conduct a SAR mapping campaign in the Philippines to aid in understanding their petroleum resource potential. ARCI personnel summarized the project, keyed issues for discussion, identified data acquisition and analysis plans, and requested help in selecting and prioritizing sites. ARCI discussed preparations to acquire SAR image data for certain selected regions in the Philippines, and asked for local Philippines experts to aid in deciding which specific areas should

be imaged, and in prioritizing the areas selected. It was further indicated that ARCI would require certain geologic data from previous Philippines studies to be integrated into the total interpretation package.

2.2 Potential Hydrocarbon Areas

The Philippines Archipelago (a group of islands) consists of 11 major and more than 7000 smaller islands. The Archipelago is located between Taiwan on the north and the Indonesian Archipelago to the south (Fig. 2.1). It is separated from the Asiatic continent by the deep basin of the South China Sea to the west, and is bounded on the east by the Philippines Sea. The territory is enclosed roughly by 5° and 21°N latitudes and 116° and 127°E longitudes. Thirteen potential hydrocarbon areas (sedimentary basins) have been identified (Fig. 2.2).

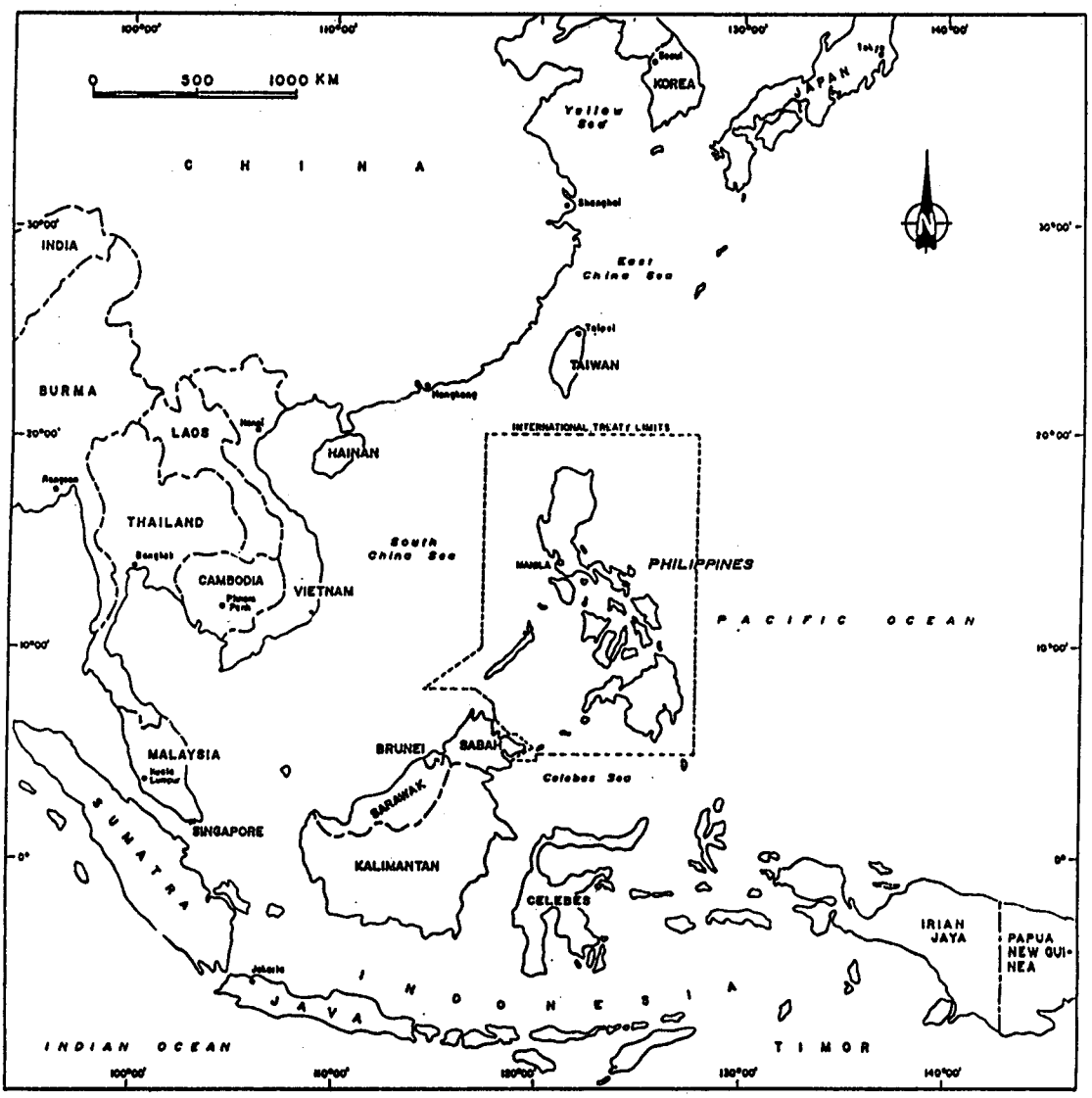

Figure 2.1: Location map. (After BED et al., 1987)

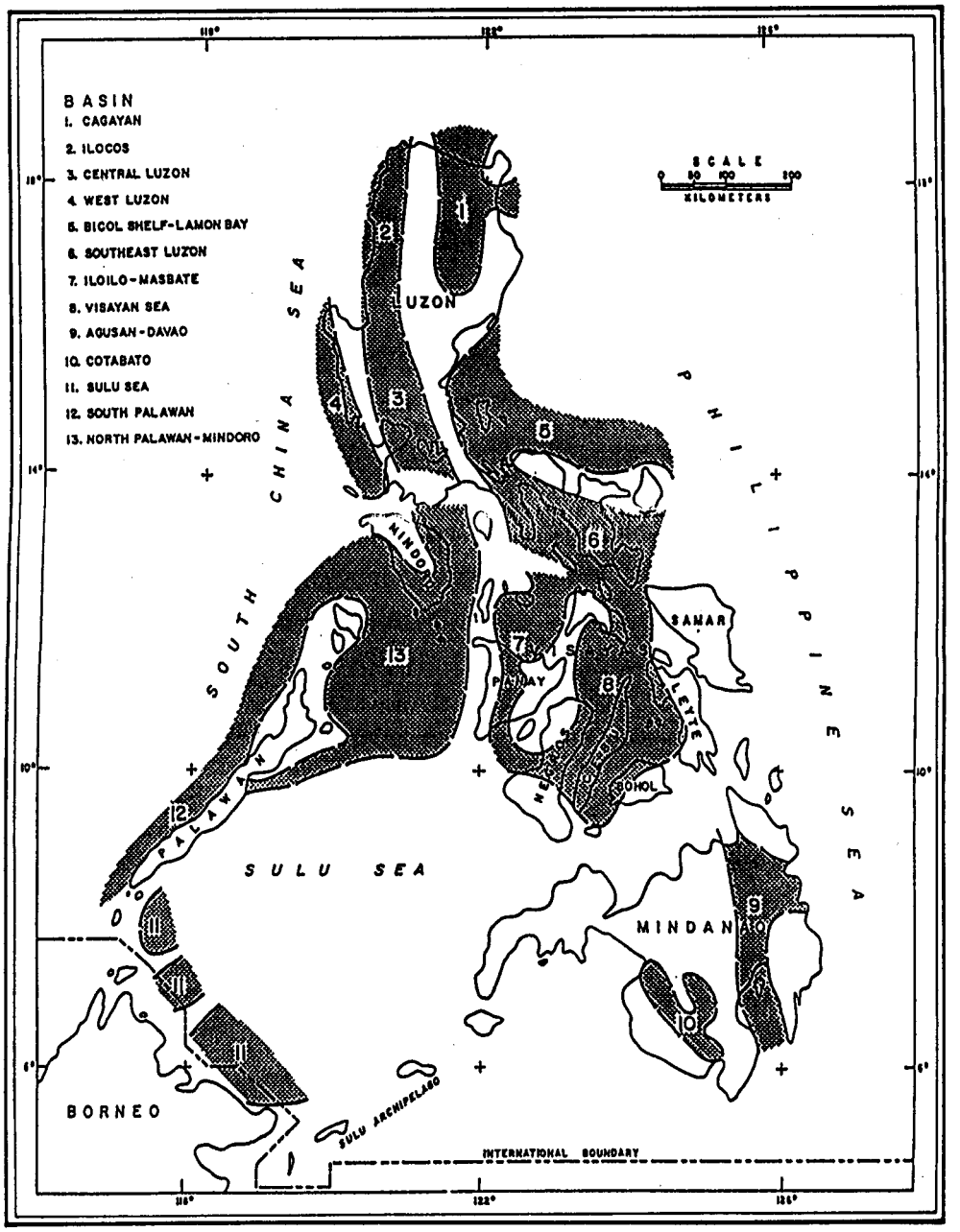

Figure 2.2: Sedimentary basins of the Philippines. (Modified from PNOC EC, 1987a)

3 IMAGING RADAR PRINCIPLES, INTERPRETATION TECHNIQUES, AND IMAGERY ACQUISITION

3.1 Radar Principles

Imaging radars were first developed in the early fifties as incoherent side-looking airborne radars (SLAR) for high-resolution remote sensing, and by 1969 SLAR surveys were available on a commercial basis. In parallel with SLAR exploitation, the coherent imaging radar or SAR (synthetic aperture radar) was in the making; first with the early fifties experiments by Carl Wiley of the Goodyear Aircraft Corporation, and later at the Universities of Illinois and Michigan (MacDonald, 1980). The SAR makes use of the Doppler phase history of the backscattered radiation from natural targets to synthesize an effective along-track aperture which is much larger than the real aperture, thereby permitting fine along-track resolution without the need for an impractically long antenna.

Since the late 1960's, large parts of the world have been surveyed by airborne side-looking radar. Most of these surveys were carried out in Third World countries where the complete lack of any type of map severely hampered development progress. The "Radam" project in Brazil is the best known example and the largest in areal extent (4.5 million km^2). The survey was later expanded to cover the entire Brazilian territory of 8.5 million km^2. With other radar surveys over the Colombian, Ecuadorian, Peruvian and Bolivian Amazon areas, the largest cartographic blank in the world (the South American Amazon area) was filled in by the fast method of data acquisition (independent of weather conditions) and the synoptic view provided by radar mosaics, which permitted relatively rapid reconnaissance surveying.

3.1.1 Terminology Significant to Interpretation

The term radar is an acronym for the phrase *radio detection and ranging*. Radar is a remote-sensing device that is active (i.e., it provides its own illumination energy). It transmits pulses of microwave energy and then receives reflections of the signal from a target. The reflected component is called the echo or backscatter. By providing its own illumination, radar operates entirely independent of sunlight, and equally effective missions can be conducted by day or night. In addition, the angle and direction of microwave illumination for imaging radars can be controlled to enhance features of special interest.

Radar systems operate in the microwave portion of the electromagnetic spectrum, where wavelengths range from a few millimeters to more than a meter. Radars are monochromatic-type sensors because they use microwave energy of single wavelengths as does a laser. Figure 3.1 provides the subdivisions of the microwave spectrum, letter codes, and the frequencies and wavelengths that have been used for imaging radars; the random letter designations are a carryover from the military when radar development was classified.

An antenna is positioned laterally (in the azimuth or along-track direction) at the velocity of the aircraft. Through this fixed antenna, pulses of microwave energy are propagated outward in a perpendicular plane at the speed of light in the range, look, or across-track direction. Slant range is the line-of-sight distance measured from the antenna to the terrain target, while ground range is the horizontal distance measured along the surface from the ground tract or nadir line to the target. The

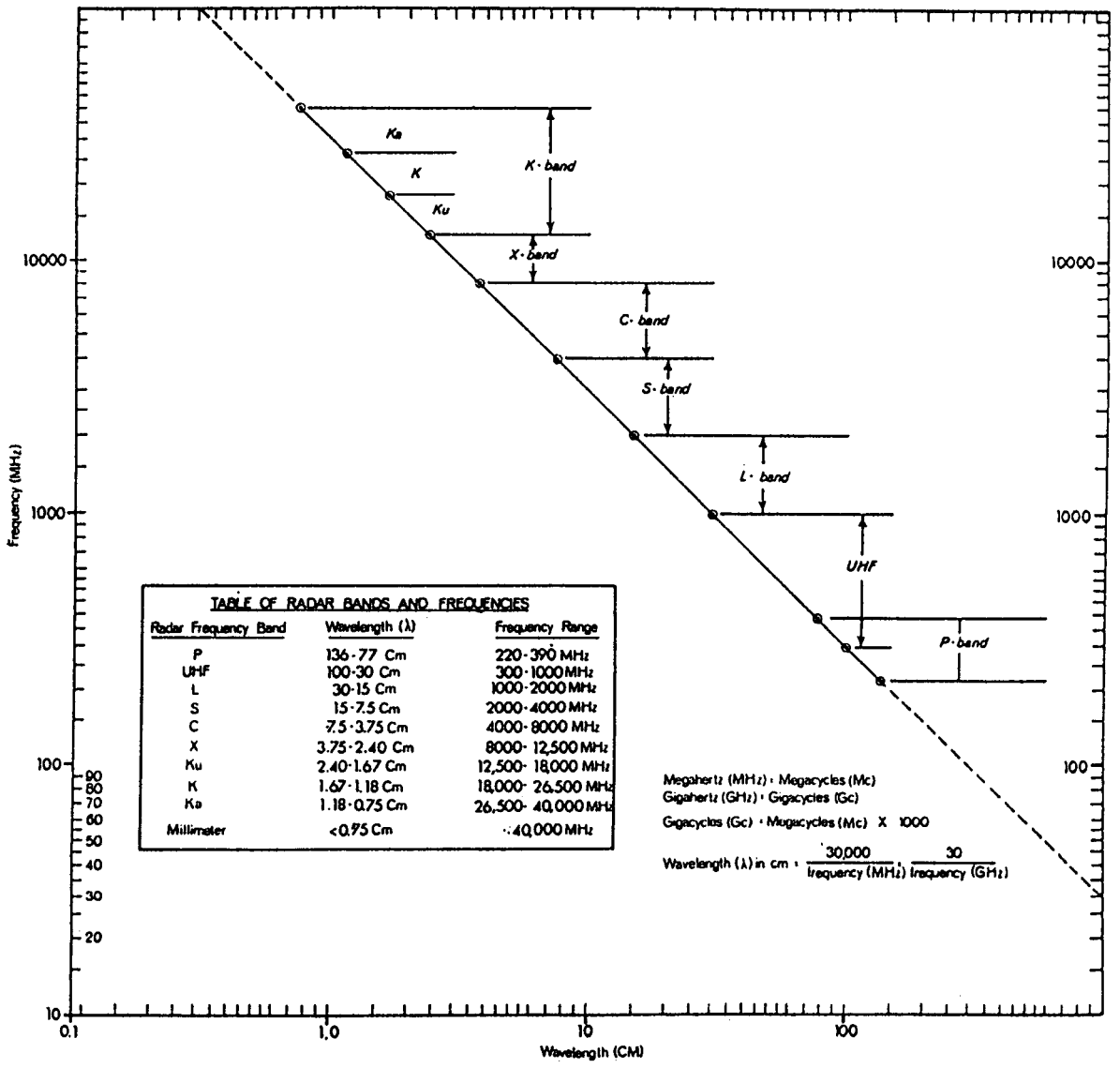

Figure 3.1: Radar frequencies and wavelength bands.

area closest to ground track where a radar pulse intercepts the terrain is the near range, and the area of pulse termination farthest from ground track is the far range.

The angle measured between a horizontal plane relative to the Earth's surface and the radar beam defines the depression angle (Fig. 3.2). Far range and near range represent the minimum and maximum depression angles, respectively, over the entire image swath. The angle measured from a vertical plane to the radar beam is the look angle off ground track. The depression angle and look angle are complementary angles. The local angle of incidence is the angle measured between the beam and the normal to the local surface. Unlike the look angle and depression angle, which are fixed, the local incidence angle varies in accordance with the slope of the terrain. The look angle and incidence angle are equal only in the special case where the terrain is level (Fig. 3.2).

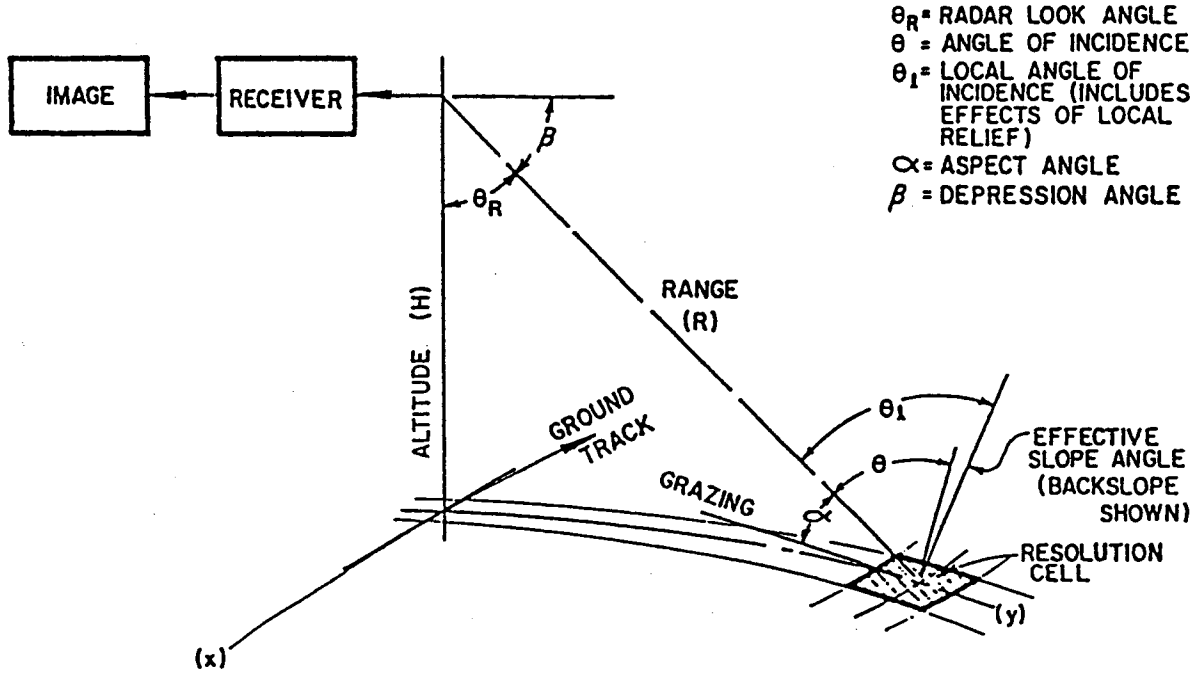

Figure 3.2: Side-looking radar geometry. (After Kaupp et al., 1982.)

3.1.2 Geometric Characteristics

Certain geometric effects related to variable elevation in the target scene result in nonrecoverable ambiguities or distortions of the image. These include shortening, layover, and shadowing. If a surface were perfectly flat, surface elements closer to the subnadir point of the SAR would be illuminated and reflect the radar signals before surface elements farther from the subnadir point. Thus, the signals would reflect from "near" - range to "far" - range elements progressively in time. However, if a surface element is elevated relative to its surroundings, it will intercept the radar signal sooner and appear in the radar image to be closer than in actuality. Figure 3.3 (a) illustrates how this effect results in an apparent shortening of slopes inclined toward the radar; i.e., slope AB appears in the radar image as shortened slope A'B'. The "radar image plane" in the figure is a geometrical representation (a right-angle projection) of the conversion between target range and location on the resulting image. For extreme cases of relief displacement (Figure 3.3 (b)), the ordering of surface elements on the radar image is the reverse of the ordering on the ground; i.e., B' appears at a nearer range than A', while actually A is at a nearer range than B. This is known as "layover." The elevated element can also stop the radar signal from illuminating elements in its shadow (Figure 3.3 (c)).

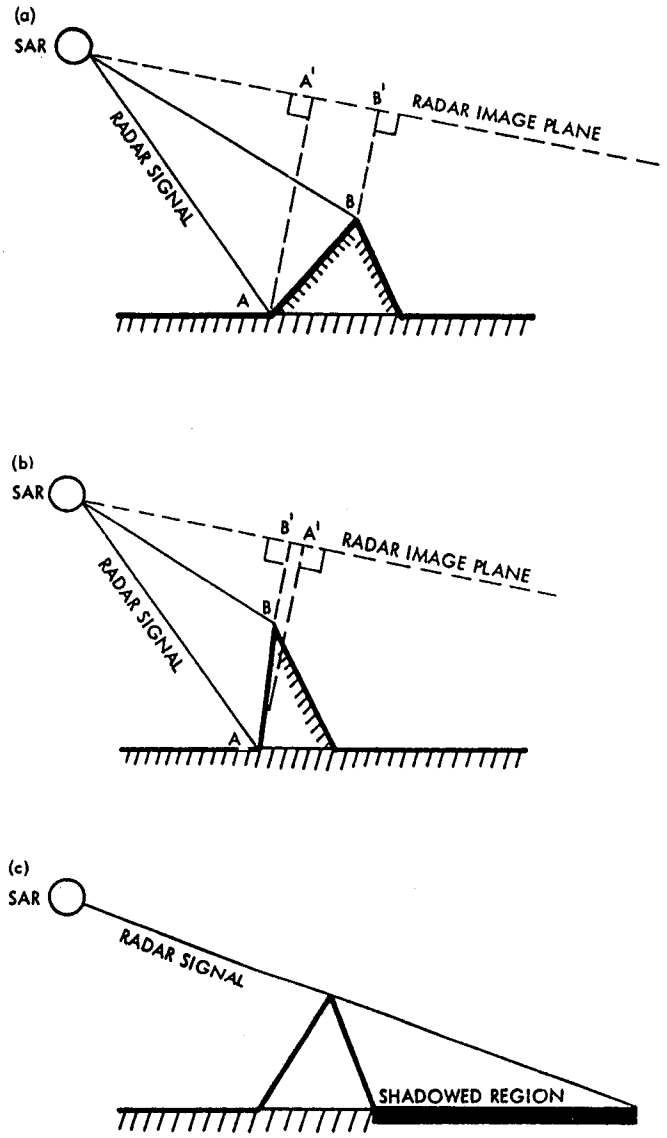

Figure 3.3: SLAR geometric characteristics and the effects of surface height variations. (a) foreshortening, (b) layover, (c) shadowing (after Pravdo et al., 1983)

3.1.3 Radar Return and Image Tone

The SAR image is a measure of the radar backscatter (reflectivity) of the target scene. The backscatter depends upon slope, roughness-size scale of the surface material, and sometimes the composition of the terrain materials/cover. Bright regions on the imagery can be caused by surface roughness on a size scale comparable to the radar wavelength, terrain orientation and slope, and when present, large changes in the dielectric properties of the surface (and sometimes subsurface) materials.

The strength of radar return and, hence image tone are primarily influenced by key terrain and radar system parameters. These are listed in Table 3.1.

Table 3.1: Ground and radar system parameters.

Ground Parameters	Radar System Parameters
Terrain slope	Frequency (wavelength)
Surface roughness	Radar look angle (depression angle)
Complex dielectric	Antenna look direction
Terrain feature orientation	Polarization

The last two decades have provided rapid technological progress in radar remote sensing. Imaging radars that were relatively unknown to geologists only a few years ago are now used for extensive geologic mapping in many parts of the world. Aircraft radar images have proven valuable for geologic interpretation in a wide range of terrain environments. In

fact, most of the proven benefits to date from radar remote sensing have been derived from geologic interpretation for non-renewable resources. Radar's unique capabilities are listed in Table 3.2.

Table 3.2: Radar's unique capabilities. Why use radar for non-renewable resource exploration?

*	All weather, day-night operation
*	Control of look direction and look angle for improved geological interpretation
*	Wide area coverage-synoptic view
*	High resolution comparable with most remote sensing systems
*	Stereo capability allows rapid formulation of geologic models
*	Sensitivity to vegetation at shorter wavelengths
*	Terrain texture discrimination in non-vegetated regions
*	Digital capability for image enhancement and multi-sensor integration
*	Radar mosaic provides an accurate base map

3.2 Interpretation Techniques

Geologists within the user community have done an impressive job of image interpretation and of development of geologic models from image recognition elements such as tone, texture, pattern, shadow, size, shape, and context. The geologic models developed by these geologists are not unlike the three-dimensional concepts achieved in the field, where outcrop observations provide information for a geologic map (plan view) and structural cross-sections of the subsurface. Radar imagery enables the

geologist to analyze systematically the visual pattern elements of the terrain (drainage, vegetation, landforms, etc.) for geologic significance, from which geologic models can often be developed rapidly. Model implementation ultimately provides the geologist with an insight into the three-dimensional geologic environment (i.e., inference about landform type and origin, rock characteristics, and structural complexity).

3.2.1 Recognition Elements

Recognition elements are important considerations for interpretation of radar imagery and contribute to the extraction of geologic data. Recognition elements include tone, texture, shape, pattern, shadow, size, and context.

3.2.1.1 Tone

Tone on radar imagery is the shade of gray recorded for the signal returned from each resolution cell on the ground. When a transmitted radar signal interacts with the ground, a certain percentage of the incident energy will be reradiated from each resolution cell back to the radar. This return signal is processed for resolution and noise averaging, and the resulting signal is ultimately recorded on photographic film as a shade of gray, or tone, pixel by pixel.

The strength of the signal returned to the radar from each resolution cell will vary according to the character of the terrain or target area. The strength of the returned signal determines the tone, or shade of gray recorded for the intensity of a point on the radar imagery. High intensities representing strong return signals appear as light or bright tones on positive imagery prints, whereas low intensities, or low return signals appear as dark tones on the imagery.

Although tone is a basic recognition element for imagery interpretation, it is highly system dependent. For example, both the brightest and darkest radar imagery tones (other than shadow) are generally caused by the influence of specular reflection. In specular reflection, the surface from which the reradiation occurs is essentially smooth or has a surface roughness about ten times smaller than the wavelength of the incident radiation. Strongest returns occur when such a smooth surface is oriented so that a major part of the energy is returned to the radar (i.e., oriented essentially perpendicular to the incident radiation). Conversely, weakest returns occur when such a surface is tipped away from the incident radiation (i.e., oriented essentially parallel to the incident radiation) allowing only a small percentage to be returned to the radar.

If the surface is rough relative to the wavelength of the impinging radar energy (i.e., has a roughness scale greater than a wavelength), reradiation will occur in many directions. This type of surface produces what is called diffuse reflection and may produce a broad range of tones in radar imagery. A perfectly rough surface spreads the incident energy in all directions. Most rough surfaces have a preferential orientation and the return from such a surface has both a specular and diffuse component.

Features imaged in proximity to a specular surface commonly allow rapid identification because of marked tonal contrasts. Water is typically a specular reflector. The signal returned from land near water produces a striking tonal contrast with the signal from the water. Land/water boundaries then produce striking interfaces on radar imagery which are advantageous for the delineation and mapping of coastal features.

3.2.1.2 Texture

Texture can be described as the frequency of tone change within an image, and is produced by an aggregate of unit features too small to be clearly discerned individually on the image. The scale of an image would obviously have an important bearing on this definition of texture.

When considering the natural terrain where landforms have developed, texture can also be defined as the degree of erosional dissection which results in an aggregate of unit features reflected in the terrain configuration. The distribution and tone of individual resolution elements form an image texture. While average or representative tone of a small area indicates the general reflecting characteristic of the local terrain surface, image texture yields evidence of variability of reflection within that unit.

Imagery texture can be evaluated as fine, smooth, coarse, grainy, speckled, mottled, irregular, etc. SLAR image texture is generally used to permit identification and delineation of unit areas contained within boundaries of homogeneity. This concept of texture contrasts with the recognition of imagery pattern (to be discussed later) which refers to an ordinary spatial arrangement of geologic, topographic, and vegetation features.

3.2.1.3 Shape

In the interpretation of medium or large scale photographic images, the shapes of objects are configured in terms of planimetric geometry and are primary factors in their analysis. The planimetric geometry of individual scene objects is expressed in terms of differences in configuration, i.e., object A is round and object B is square, therefore object A is not the same as object B. This reliance on shape is reinforced in large or medium

scale aerial photographs by the interpreter's familiarity with objects. In aerial photographs, objects retain their natural shapes, thus the individual scene units are recognizable in themselves. An individual scene unit is the basic unit perceived by an interpreter which, when aggregated, comprises a scene. For instance, a building, a smokestack, a cooling tower and a transformer yard are individual scene units which, when assembled, become a power station. With imaging radars, the basic scene unit loses its shape, and thus its object context. This occurs in radar more often than in photography because of resolution considerations, fading noise, geometric distortion, and the backscattering properties of the individual scene objects.

The shape of natural objects depends on their genesis and consequently, shape can be defined as a spatial form with respect to a relatively constant contour or periphery. Because cultural features generally have regular geometric shapes, the radar image interpreter can usually distinguish natural from cultural features. Even though many elements of the landscape usually have irregular outlines, numerous geologic features can be interpreted by their shape alone, i.e., alluvial fans, volcanic cones, river terraces, many glacial features, and folded strata are but a few examples.

3.2.1.4 Pattern

Pattern can be defined as the arrangement of geologic, topographic, or vegetation features; that is, areas or groups of areas throughout a region with recurring configuration. Patterns resulting from particular distributions of gently curved or straight lines are common and are frequently of structural significance; they may represent faults, joints, bedding, and so forth. The distribution of straight and then gently curved ridges provide classic indicators of folded sedimentary rock units.

Drainage pattern analysis provides the geologist with an extremely important geomorphic and structural interpretive technique. Drainage patterns (spatial relationships) generally reflect at the surface the underlying structure and rock type. In addition to drainage patterns, vegetation and soil patterns commonly reflect structural conditions, lithologic character of rock type, and distribution of surficial materials.

3.2.1.5 Shadow

The interpretation of subtle terrain configurations is often improved by radar shadow. Shadows on radar, in contrast to those on photography, are black (no return), and while radar shadowing may aid in determining the shapes of certain terrain features, it also limits stereoscopic interpretation. The length of shadows will, under the similar constrains of shadow measurement on single aerial photos, allow for the determination of the height of certain features. Shadow frequency can also be used to infer relative relief, whereas the shapes of radar shadowing may allow the interpreter to infer information about the relative relief of the terrain. For example, the length of a radar shadow can be used for determining the height of some objects, and shadow shape may be used for inferring spatial form. Where relief is relatively rugged and radar depression angles are shallow (small), the shadow outlines commonly reveal more about terrain configuration than do the crestlines or summits which are portrayed on the radar imagery.

3.2.1.6 Size

The measurement of length, width, area, and volume of basic scene objects has long been a major interpretation element in photo-interpretation of cultural features; however, the surface or volume dimensions of an object

have been used only in a qualitative way on radar imagery. Because of image obliquity and geometric distortions, size measurement is seldom determined using SLAR imagery. Greater interest in measurement data has recently developed as a consequence of improved SLAR ground range image presentation and rectification. This is particularly true where the objects are sizeable enough to exceed system resolution.

As a general rule, size is used in a qualitative way as an image recognition element for non-renewable resource exploration. The size of known features on the imagery provides a relative evaluation of scale and dimensions of other terrain features.

3.2.1.7 Context

The geographic, geomorphic, and geologic characteristics of the surrounding area contribute to the "background" information provided in a radar image. The interpretive expertise is of considerable importance in determining the significance of this recognition element. The importance of context explains why automated mapping and interpretation has advanced slowly. Machine systems can easily register tonal differences between adjacent pixels and have some success in texture recognition, but they face a difficult problem in equaling the interpreter's experience and his ability to appreciate spatial relationships.

3.2.2 Lithology and Structure

Detailed observation of the terrain is required for all phases of applied geology which includes exploration for non-renewable resources. Determining surface geology from radar images has found more practicality than perhaps any other usage. The interpreter who utilizes radar images for geologic synthesis usually has four ultimate objectives: (1) correlation of

outcrops from one location to another, (2) determination of the stratigraphic sequence, (3) delimitation of rock types or lithologic units, and (4) determination of geologic structure.

Radar images provide the geologist with a terrain format approximating a three-dimensional strip map that can reveal varying amounts of geologic information depending on the terrain environment and stage of erosional development. For example, in areas where rock type and structure are reflected in the topography, one may be able to recognize certain geological features quite unequivocally from the evidence provided by the radar images. However, in many areas of the world, where bedrock is obscured by surficial deposits or vegetation, and where underlying geologic conditions have little direct influence on the surface, the interpretive skill of the geologist to analyze landforms becomes the critical link for structural or even lithologic evaluation. The extent to which radar geological interpretation methods can be successful varies considerably depending primarily upon the geological and geomorphological character of the region.

Geological information that can be interpreted from radar images can be grouped broadly into two categories: (1) lithologic and (2) structural. Analysis of landforms provides valuable information on the composition and mode of origin of different terrains. Coupled with an understanding of the climatic influences on geomorphic processes, landform analysis is one of the most important techniques for lithologic and structural mapping.

3.2.2.1 Landform Analysis

Geologists commonly use **landform** to describe the geomorphic characteristics of a region. Landforms are the physical features of the Earth's surface that have resulted from constructional or erosional (destructional) processes that when found under similar conditions (such as climate,

weathering, erosion, structural attitude etc.) will exhibit a definite range of visual and physical characteristics. In geological analysis, it is generally impossible to consider drainage and landform development as separate processes. Drainage is analyzed according to its pattern type and its texture or density of dissection.

Landform and drainage analyses are extremely important in the recognition and mapping of numerous geologic structures. Examples might include:

(1) Characteristic landform shape or form that allows for the identification of many geologic features such as domes, cinder cones, volcanos, plunging folds, etc.

(2) Topographic highs and lows in areas of little relief and low dip that are indicative of subsurface structure.

(3) Abrupt changes in direction (strike) of topographic features such as ridges which may be indicative of faulting.

(4) Recognition of slope asymmetry where infacing escarpments are towards the structurally high part of an anticline; and conversely, outfacing escarpments are indicative of synclines.

(5) Contrast of slopes on opposite sides of a ridge or valley related to dipping strata.

(6) Marked changes in slope orientation which may be related to jointing or fracturing.

(7) Areas where the surface is more intensely eroded than the surrounding area resulting in differing slope orientations and drainage patterns or textures.

(8) Drainage contrasts on opposite sides of a ridge or a valley.

Radar's sensitivity to changes in surface slope is particularly useful for highlighting landforms, thus improving geologic interpretation. Examples listed above provide evidence that recognition of slope changes significantly impacts geological interpretation.

3.2.2.2 Lithologic Analysis

Lithologic mapping experiments involve the use of radar data to obtain information concerning the roughness and dielectric properties of natural surfaces. Researchers have reported mixed results in attempts to correlate radar signatures with specific rock types or lithologic units. The results have ranged from no correlation (Ford, 1980), to good correlation using co-registered data (Rebillard and Evans, 1983). Several investigators have successfully used tone and texture to differentiate lithologic units (Elachi et al., 1980; Blom and Daily, 1982; Canoba, 1983; Wadge and Dixon, 1984; and Podwysocki et al., 1985). Daily et al. (1978), have accomplished a nearly complete discrimination of surficial geologic units in Death Valley, California, using dual frequency and polarization imaging radar data.

Rebillard and Evans (1983) report that texture and backscatter information provided by radars with different illumination geometries improves discernability and classification accuracy of geologic units over Landsat images alone, or combinations of Landsat images and radar images obtained at a single incidence angle. Blom and Daily (1982) have used radar data filtering methods to improve rock-type discrimination, but not for specific rock-type identification. Curlis et al. (1986), reported that computer enhancement techniques applied to the Shuttle Imaging Radar-A (SIR-A) data from Lisbon Valley area in the northern portion of the Paradox Basin increased the value of the imagery in the development of geologically

useful maps. The enhancement techniques include filtering to remove image speckle from the SIR-A data and combining these data with Landsat multi-spectral scanner data. A method well-suited for the combination of the data sets utilized a three-dimensional domain defined by intensity-hue-saturation (IHS) coordinates. Such a system allows the Landsat data to modulate image intensity, while the SIR-A data control image hue and saturation. Whereas the addition of Landsat data to the SIR-A image by means of a pixel-by-pixel ratio accentuated textural variations within the image, the addition of color to the combined images enabled isolation of areas in which gray-tone contrast was minimal. This isolation resulted in a more precise definition of stratigraphic units.

The discrimination of lithic type, as discussed in the preceding two paragraphs, was generally successful only in those regions where arid or semi-arid climatic conditions prevailed. In these regions of little precipitation where the weathered material is not excessively leached, a close relationship of soil to lithic type may occur. Where this close association of lithology to residual soil exists, the distribution of different vegetation types or terrain textures may facilitate the mapping of lithology. However, the extent to which radar can be applied to lithologic mapping may vary widely.

In tropical climatic regions of abundant rainfall such as the Philippines, soils are usually leached of salts, and there is a tendency for soils from different parent formations to become more similar with maturity. Thus, differences in vegetation as related to specific lithic types will be less developed under these climatic conditions, except for those plant associations that may depend primarily on the physical characteristics of the soil rather than chemical. Consequently, landform discrimination, and differences in drainage patterns and terrain texture may be the only indicators of certain lithic types. For example, Longoria and Jimenez (1985) using visual analysis

of SIR-A images in northeastern Mexico, recognized morphostratigraphic units (lithic packages) which maintain their textural expression in the images throughout the region. Their identification on the radar images was considered vital for recognizing mappable units comparable to lithologic discrimination during ground mapping.

3.2.2.3 Structure

Structural information is generally extracted from radar imagery for non-renewable resource exploration by empirical correlation between landform units and a hypothetical geological model. Radar recognition elements (Section 3.2.1) are used in concert in the identification of landforms with special emphasis on examining drainage patterns, topographic relief, erosional characteristics, cover type, and land use. Certain patterns occurring either singly or in combination can be correlated with the actual presence of predicted conditions, and thus by analogy, unknown conditions can be inferred.

3.3 Radar Imagery Acquisition — Philippines Sites

In support of the hydrocarbon exploration program, radar imagery was acquired of four sites in the Philippines. These sites were selected in coordination with BED and PNOC EC personnel. Site selection was determined from evaluation of the extensive data base of hydrocarbon potential in the Philippines previously assembled by BED and PNOC EC. Selection criteria included not only hydrocarbon potential, but locations wherein it was felt the unique perspective of surface structure and features afforded by radar would best complement existing surface and subsurface data.

Site selection was further constrained by cost considerations. These dictated the total area imaged to be in the range of 30,000 to 60,000 km^2. The total amount to be spent on imagery acquisition was fixed; however, total coverage could vary significantly depending on the acquisition parameters specified. The major parameters affecting the total coverage available at a fixed price were the flight line spacings and the number of look directions specified.

In order to increase coverage and permit investigation of the maximum number of sites, ARCI recommended that coverage be acquired from only a single look direction. However, it was felt that because of the structural complexity of the Philippines sites, stereo interpretation was mandatory. Complete stereo coverage requires an image sidelap of at least 50%. Slight variations in ground swath coverage due to elevation differences and positional errors in flight line location must also be accommodated. Thus, flight plans for stereo mapping normally specify a 55% nominal image sidelap.

The previous considerations restricted the coverage area to approximately 45,000 km^2. Accordingly, four sites were selected whose total area met this constraint. Subsequent to these initial site selection negotiations, a request was received from the Philippines representatives that coverage of a few small geothermal sites be included in the program even at the expense of dropping one of the hydrocarbon sites selected. The image acquisition contractor agreed to cover three small geothermal sites for the fixed maximum price even though this coverage increased the total area to well beyond 45,000 km^2. It was stipulated these data were also to have complete stereo coverage, however, no mosaics were to be delivered for the geothermal sites. This essentially no-cost addition of coverage was possible at this stage by selecting geothermal sites that could be imaged during the same flights that hydrocarbon site imagery was collected and

in some cases by even sharing the same flight lines. The coordinates of the selected sites, both hydrocarbon and geothermal, are listed in Table 3.3. Sketch maps of the areas are shown in Figures 3.4 through 3.7.

It should be pointed out that the total coverage obtained is well beyond the total area of both hydrocarbon and geothermal sites. This is due, to the extent of the flight lines beyond the site boundaries and extra coverage required to provide full stereo sidelap. While much of this additional coverage is monoscopic, it still represents a significant and valuable addition to the total data acquired. Table 3.4 shows the approximate area of each site along with the additional coverage obtained.

Table 3.3: Site coordinates for Philippines radar survey project.

Hydrocarbon Site 1 - Bondoc Peninsula

Point	Coordinates	Point	Coordinates
1	13°55'N 121°41'E	4	13°13'N 122°48'E
2	13°31'N 122°18'E	5	13°52'N 122°31'E
3	13°08'N 122°35'E	6	14°17'N 121°57'E

Hydrocarbon Site 2 - Cotabato Basin, Mindanao

Point	Coordinates	Point	Coordinates
1	7°07'N 123°55'E	3	6°22'N 125°42'E
2	5°50'N 125°00'E	4	7°30'N 124°40'E

Hydrocarbon Site 3 - Mindoro

Point	Coordinates	Point	Coordinates
1	13°15'N 120°32'E	4	12°41'N 121°35'E
2	12°11'N 121°00'E	5	13°02'N 121°30'E
3	12°11'N 121°26'E		

Hydrocarbon Site 4 – Cebu

Point	Coordinates	Point	Coordinates
1	11°17'N 123°58'E	5	9°23'N 123°24'E
2	10°30'N 123°41'E	6	10°00'N 123°41'E
3	10°00'N 123°21'E	7	10°26'N 124°04'E
4	9°23'N 123°16'E	8	11°17'N 124°06'E

Geothermal Site A – North Negros

Point	Coordinates	Point	Coordinates
1	10°41'N 123°00'E	3	10°18'N 123°20'E
2	10°18'N 123°00'E	4	10°41'N 123°20'E

Geothermal Site B – South Negros

Point	Coordinates	Point	Coordinates
1	9°30'N 123°00'E	4	9°19'N 123°19'E
2	9°03'N 123°00'E	5	9°30'N 123°11'E
3	9°03'N 123°09'E		

Geothermal Site C – Mt. Apo, Mindanao

Point	Coordinates	Point	Coordinates
1	7°05'41"N 125°04'16"E	3	6°49'28"N 125°21'36"E
2	6°49'28"N 125°04'16"E	4	7°05'41"N 125°21'36"E

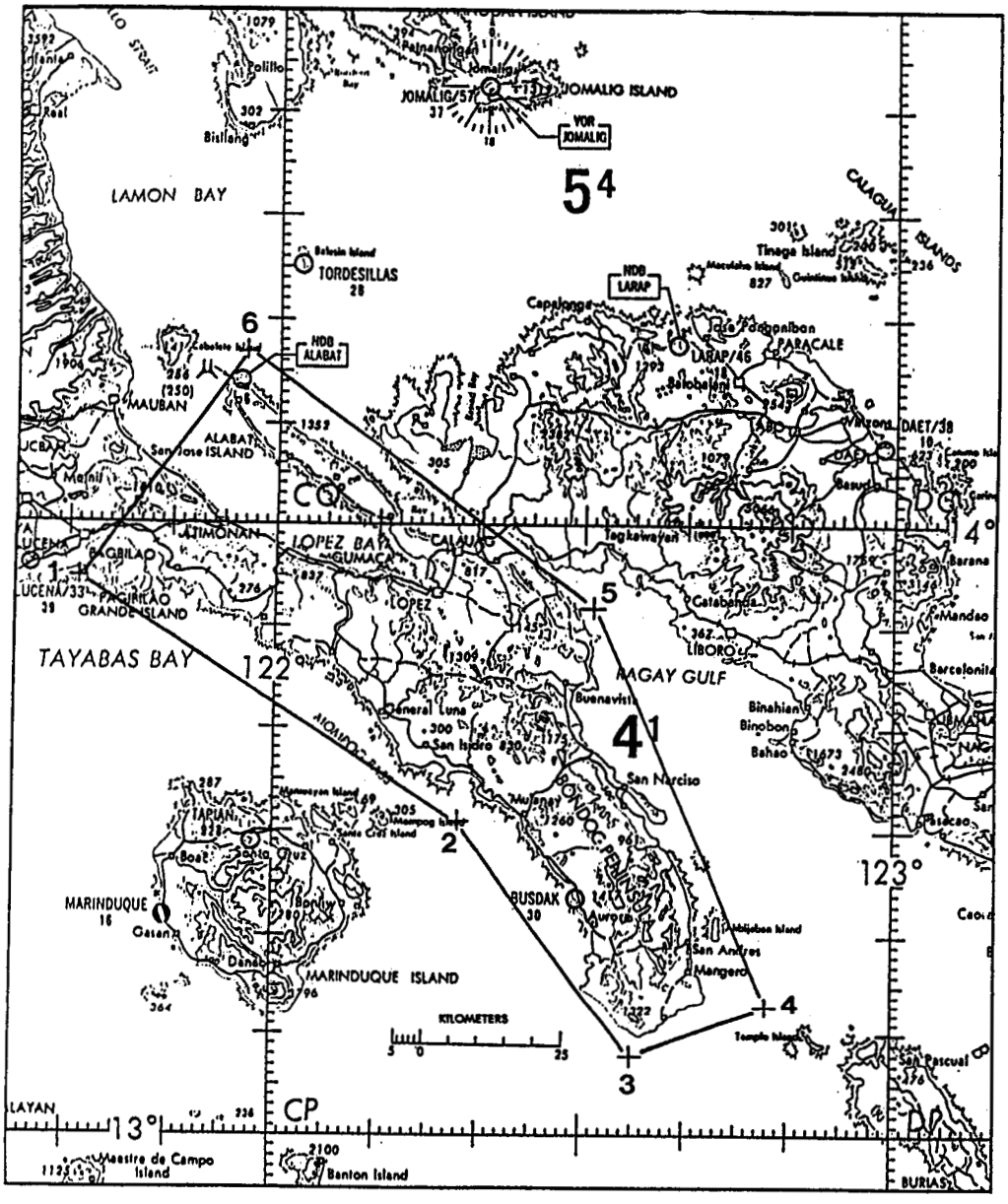

Figure 3.4: Bondoc Peninsula hydrocarbon site.

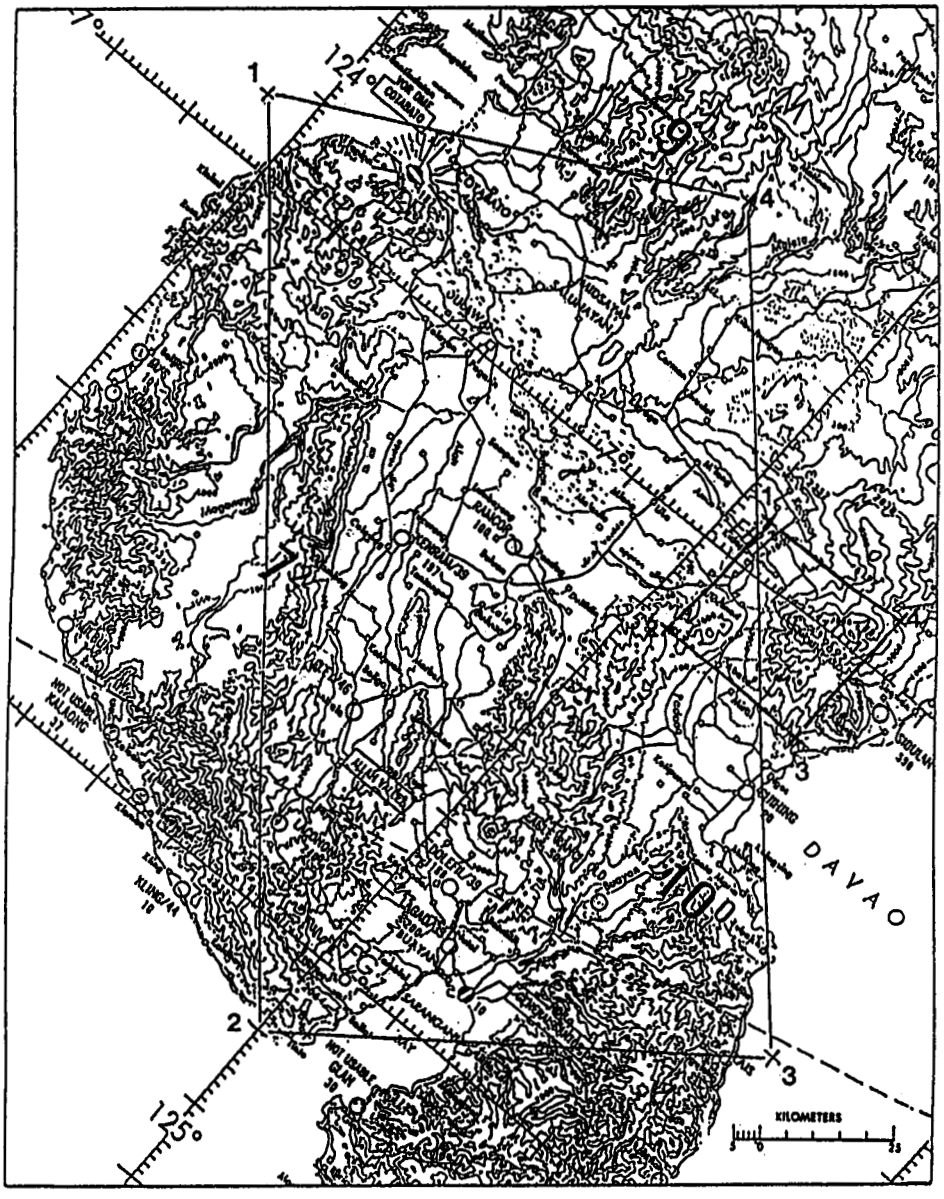

Figure 3.5: Mindanao hydrocarbon and geothermal sites.

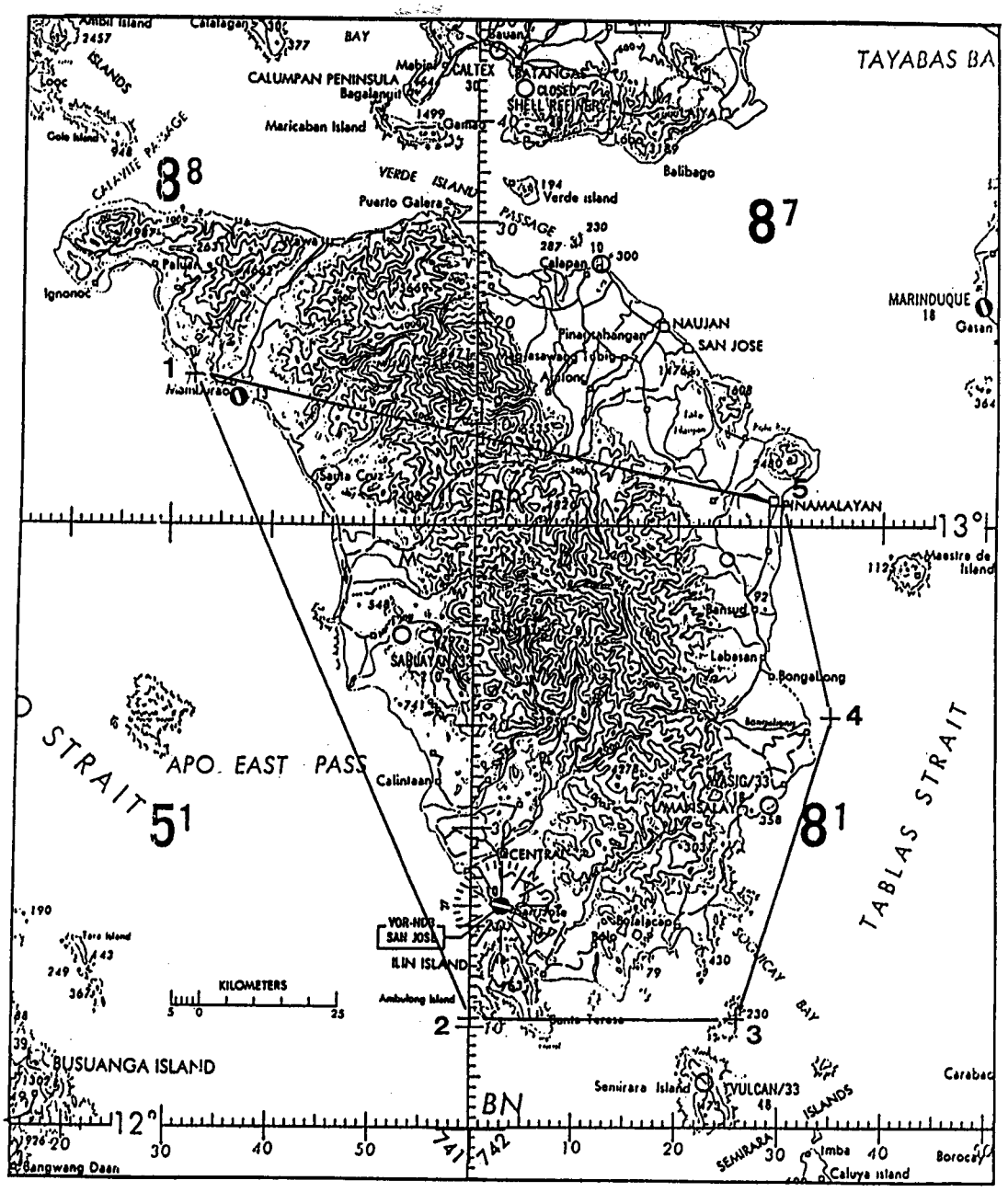

Figure 3.6: Mindoro hydrocarbon site.

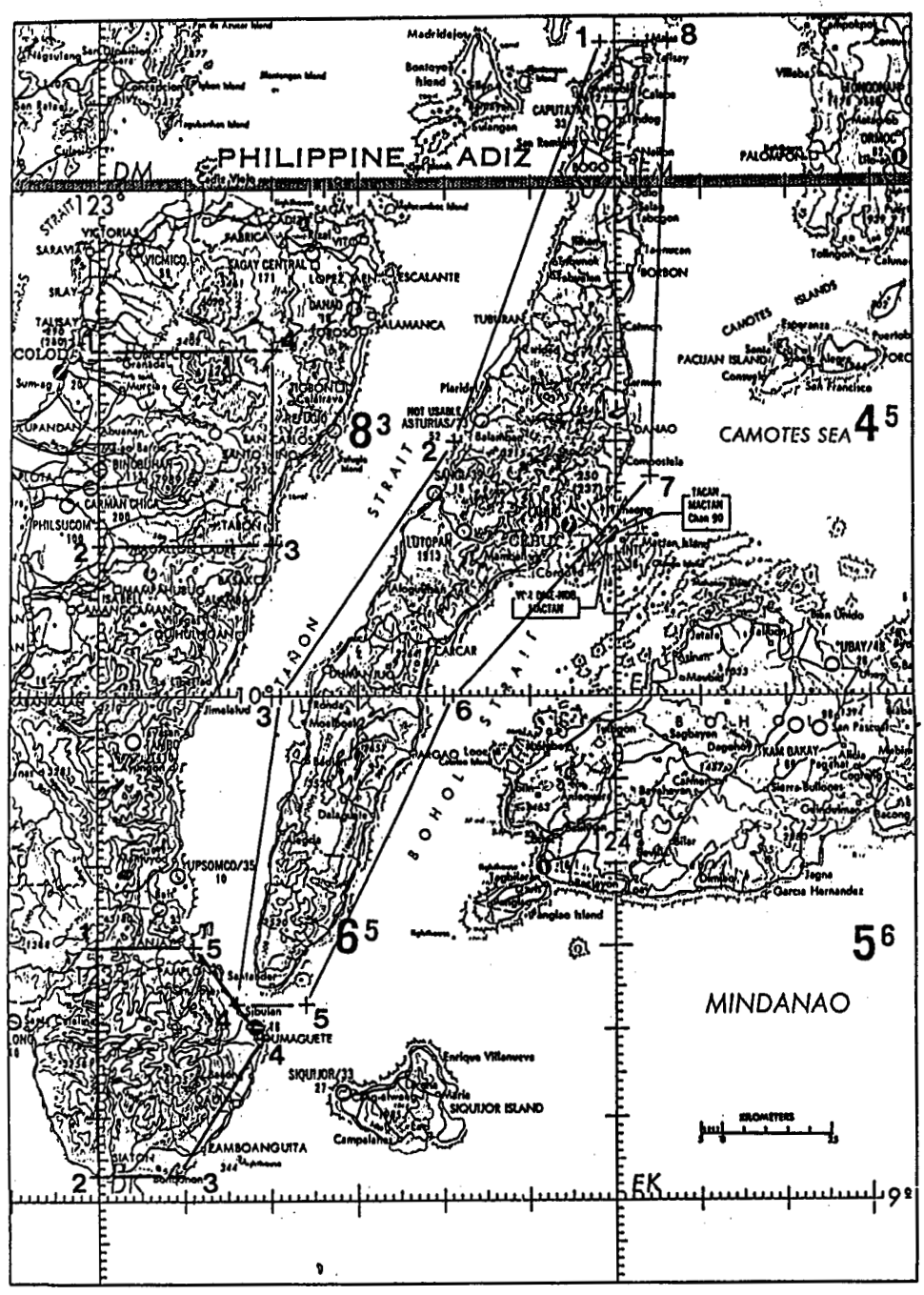

Figure 3.7: Cebu hydrocarbon site and Negros geothermal sites.

Table 3.4: Coverage for Philippines radar survey project.

HYDROCARBON SITES

Site	Area Contract (km^2)	Area Additional (km^2)	Area Total (km^2)
Bondoc Peninsula	6,250	2,010	8,260
Cotabato Basin, Mindanao	19,000	3,265	22,265
Mindoro	11,500	2,100	13,600
Cebu	7,525	400	7,925
Subtotal	**44,275**	**7,775**	**52,050**

GEOTHERMAL SITES

North Negros	1,325	2,600	3,925
South Negros	1,570	930	2,500
Mt. Apo	715	1,735	2,450
Subtotal	**3,610**	**5,265**	**8,875**
GRAND TOTAL	**47,885**	**13,040**	**60,925**

3.3.1 System Characteristics

The radar imagery for this program was acquired by Intera Technologies, Inc. (Intera) under subcontract from Arkansas Research Consultants, Inc.

As discussed previously, the radar system characteristics have a direct bearing not only on the quality of the data acquired but on the interpretation of these data as well. The characteristics of the STAR-1 system used by Intera to collect the imagery are shown in Table 3.5. Comments on the characteristics particularly significant for mission planning and quality control are contained in the following paragraphs.

The Philippines radar survey was conducted using exclusively wide swath coverage. According to the Table of Specifications this yields a resolution of 6x12 m (azimuth x range) and an incoherent averaging of approximately 8 independent samples. The actual operation of the system and the processing of the data is somewhat different than this, leading to some modification of both the swath width and number of samples averaged. In general, the azimuth resolution is subsequently averaged to near the same value as the range resolution. For wide swath coverage this produces a resolution cell of approximately 12x12 m and on the order of 24 independent samples.

For mission planning it is critical that the actual swath width be known along with the incidence angles at the swath limits. Let us consider how the swath width of the imagery is controlled in actual system operation. Figure 3.8 shows the side-looking geometry of the SAR system. The near range of the swath is set by means of a time delay which corresponds to the slant range to the near edge of the swath. The swath extent is controlled by the sweep duration, again in time or slant range. The swath width in the ground plane is a function not only of the time delay and sweep extent of the system, but also the altitude of the aircraft.

Table 3.5: STAR-1 system parameters.

Parameter	Value	
Frequency	X-Band (9.375 GHz)	
Average Power Output	160 W	
Antenna Length (Physical)	1.0 m	
Viewing Direction	Left or Right	
Antenna Stabilization	3-Axis	
Operating Altitude	to 10,000 m (33,000 feet)	
Maximum Ground Speed	350 knots	
	Narrow	**Wide**
Swath Coverage	25 km	50 km
Resolution		
- Range	6 m	12 m
- Azimuth	6 m	12 m
Averaging		
- Range	1	2
- Azimuth	7	14
Minimum Detectable Reflectivity	-30dB across swath	
Recording	Digital HDDT (on-board full-bandwidth)	
Display	Real-time (on-board dry silver paper)	
Scale	1:250,000	

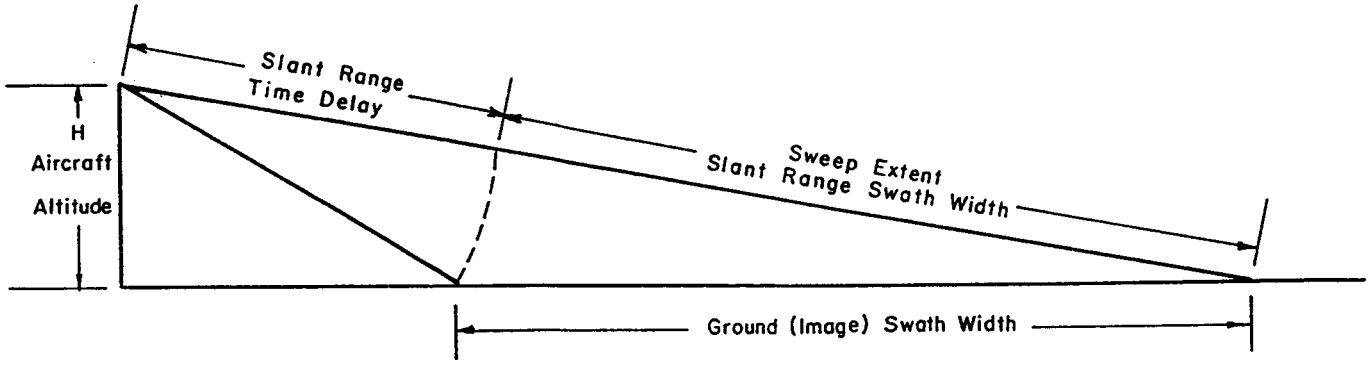

Figure 3.8: Swath coverage of SAR system.

The processor used in the STAR-1 system is capable of digitizing 4,096 range samples; and with a range resolution (in the slant plane) of 12 m, the resulting range sweep extent is 4,096x12 = 49.1 km. The system is operated such that the far range incidence angle is approximately 80°, which corresponds to a ground swath width of approximately 49.9 km. Note this gives a ground range resolution of just slightly over 12 m, the exact amount varying over the swath with changing incidence angle. This is obviously the basis for the 50 km swath width listed in the STAR-1 Table of Specifications.

The fashion in which Intera operates the system is slightly different from that described above and implied by the Table of Specifications. The Intera mode of operation is a compromise between not only swath width and sensitivity, but also selection of the optimum range of incidence angle for terrain enhancement, the characteristics of the specific antenna used, and ease of adjustment in field operations. This compromise results in basic operation over the angular range of approximately 60° to 80° incidence at normal operating altitudes. To maximize sensitivity, the antenna vertical beam width is only slightly greater than this range.

The STAR-1 system is operated with a fixed sweep extent in the slant range of approximately 44.7 km. This results in slightly better resolution in the slant plane and thus at least 12 m resolution in the ground plane for all but the near range edge of the image. Adjustment of the incidence angle range necessitated by altitude changes is accommodated by varying the slant range delay time. A limited range of tilt is possible in the antenna elevation angle permitting the beam to be centered over the range used.

After all this it must be pointed out that the exact incidence angles over the swath width are not really fixed. This is because these angles are determined by the altitude above the terrain rather than above a

reference such as mean sea level. This altitude may vary widely along the flight line and even across the swath, particularly for relatively mountainous regions such as much of the area covered by the Philippines radar survey. Note the aircraft altitude with respect to a reference level must be held constant along the flight line to permit formation of the synthetic array providing the azimuth resolution.

In theory, the radar operator estimates the mean terrain elevation for a given flight line then sets the range delay time to obtain the optimum angular range over the image swath. The antenna tilt angle may be adjusted to insure the complete swath remains within the antenna beam even as the terrain elevation and consequently the incidence angle vary. This also maximizes the system sensitivity for the specific configuration.

In actual practice, the flight altitude with respect to a barometric reference and the slant range delay are usually selected for an entire imaging mission and rarely changed unless dictated by flight operations. The only adjustment then, is of the antenna tilt angle. While this significantly eases operation and operator training, it does sacrifice line-to-line optimization and permits increased angular variation and scale changes which must be rectified in mosaic construction.

For the Philippines survey, Intera operated consistently at a barometric altitude of 29,000 feet (8,840 m) and a slant range delay of 18 km. For sea level operation this results in an incidence angle range of 60.6° to 81.9° with a ground swath width of 46.4 km. Obviously, the altitude above the terrain is variable and in many cases quite substantially less than the above figure. However, with operation at these relatively high incidence angles the swath width is not greatly sensitive to altitude changes. For instance, at an altitude of 24,000 feet (7,370 m) above the terrain the incidence angle range becomes 66.0° to 83.3° with a ground swath width

of 45.8 km. The most significant parameter changes from the standpoint of flight planning are the increased incidence angles which increase the data loss due to terrain shadowing.

A significant advantage of the Intera STAR-1 system, particularly in comparison with previous orbital radars such as Seasat, SIR-A, and SIR-B, is the large number of independent samples averaged at this resolution (in the range of 20 to 25). This degree of averaging greatly reduces the coherent fading or speckle common to radar and laser imaging systems. This significantly improves the effective resolution of the imagery (that useable for interpretation) and thus increases the range of image scale that may be used.

The imagery used for this survey was printed at a scale of 1:250,000 and transferred to base maps of the same scale. However, much of the detailed interpretation was performed by viewing the flight strips in stereo and under magnification. The high degree of averaging in these data permit viewing under magnifications up to 5 or 6 to 1. This means the data will support interpretation even at a scale of 1:50,000. Satellite imagery typically has 3 or 4 sample averaging, however, even if acquired at the same resolution, interpretation is effectively limited to a scale of 1:250,000. Only slight magnification can be used with such data before the coherent fading becomes too distracting for interpretation.

3.3.2 Flight Planning

The objective of flight planning should be to not only insure coverage of the survey area, but to do so in a fashion that optimally enhances the terrain and minimizes data loss due to geometric and radiometric distortions as well as shadowing. While this objective appears quite simple, cost considerations dictate that satisfaction of the objective is inevitably a

compromise between the cost of data acquisition and the quality of the data obtained. Where the organization collecting the data is likewise responsible for its interpretation, this compromise is usually weighted toward improved data quality and arrived at by internal negotiations between individuals directing flight operations and those charged with data analysis and application. The far more common situation is where data collection is contracted from the organization responsible for interpretation to one responsible solely for data collection. In this case, the contracting document becomes the mechanism for effecting this compromise. While major items such as the amount of coverage, overlap, look direction(s), etc. are easily documented, others are quite site and application specific and require detailed flight planning. Unfortunately, the detailed flight plan is normally not prepared until contract award and is in fact a portion of the effort covered by the contract.

To insure optimum data quality within the bounds of the contract specifications the contracting organization should reserve the right to participate in preparation of and approve the detailed flight plan. Without this reservation, flight plan compromises between acquisition cost and data quality will inevitably be weighted toward cost reduction. This obviously means the contracting organization must have detailed familiarity with the flight planning process and its effect on the quality of the data. In this section we shall describe the nominal process of flight planning, the flight plan used for the Philippines survey, and point out those areas of concern.

Specification of the area to be covered is self explanatory. The only caution to be exercised is to not bound the area too closely. Many features of geological interest are best evaluated by their placement in a regional

perspective. However, particularly where stereo coverage is specified, the monoscopic coverage extending beyond the bounds of the specified area may be used to extend this regional perspective at no additional cost.

As with aerial photography surveys, radar coverage is obtained by flying parallel flight paths over the area. The major difference with radar is that the area covered is offset to the side of the flight line by a considerable distance. For the Intera STAR-1 system this offset is generally on the order of 15 to 20 km. Cost considerations generally dictate that the number of flight lines be minimized, thus they are normally oriented parallel to the largest dimension of the defined area. However, this should definitely not be the criterion used to orient the flight path. One of the major advantages of radar is in its enhancement of structural and particularly linear features oriented parallel to the flight path. Where the region to be imaged has a definite structural orientation, or grain, the flight direction should be oriented parallel to this trend. In many cases these requirements for flight line orientation will be in close agreement as areas tend to be defined longer parallel to the direction of structural grain. However, where conflict arises, the orientation with respect to structural grain should take precedence. To prevent such conflict, the flight line orientation should be contractually specified along with the definition of the area.

The look direction perpendicular to the flight path is less critical but should also be specified. The radar enhancement of structure comes at the expense of incurring data loss from shadowing due to the oblique look angle. Terrain back slopes (measured in the plane of incidence) exceeding the compliment of the incidence angle will be in shadow, with the shadow length a function of the relative relief of the feature. For the relatively high incidence angles of the STAR-1 system (roughly 60° to 80°) this means

back slopes of 10° to 30° will be in shadow depending on their placement in the swath. Thus, in relatively rugged terrain such as much of the Philippines survey area there will be some unavoidable data loss due to shadow for single look direction imagery. Where it is known which side of the dominant structural grain is of most interest, the look direction should be specified toward this side to minimize data loss due to shadow for the more critical region. This specification of look direction (left or right) after specification of flight path will normally not impact acquisition time or cost, however, it should likewise be contractually specified with the area definition to prevent later misunderstanding.

As pointed out above, there is some inevitable data loss in relatively high relief-high slope regions due to the oblique perspective of radar imagery. This oblique perspective, that may be selectively oriented to complement the terrain structure, is also one of the major advantages of radar imagery in its enhancement of structure. This does mean, however, that complete radar data coverage is not possible in high relief areas with a single look direction. In many cases the percentage of the area affected may be quite small and trends in the affected areas may be inferred and extrapolated from the surrounding area. The additional information provided by a second look direction must be weighed against the cost of acquisition. Although this cost will vary between regions and contractors, one may roughly estimate that complete coverage of the same type with a second look direction will increase the total acquisition cost by 50%. Obviously, reduced coverage of selected regions would cost less, however, the reduction may not be a simple linear function of area coverage.

The decision as to single or multiple look coverage should be made by the organization contracting the data acquisition and responsible for analysis of the data, subject as always to their own cost constraints. While

the decision is greatly influenced by cost, it is also very definitely a function of the specific site(s), the particular application(s), and the acquisition system characteristics. This trade-off should be evaluated in conjunction with the original site specification and obviously must be specified in the original contract.

The trade-off involved in the Philippines survey was basically how best to spend the fixed sum available for data acquisition. ARCI, in consultation with BED and PNOC EC personnel, felt that for an initial survey the weighting should be toward coverage of more sites rather than filling in the small percentage of lost data for fewer sites. Accordingly, the contract with Intera called for single look coverage.

Although multiple look direction coverage was not recommended for this survey, it was strongly recommended by ARCI that the data be flown with sufficient sidelap to permit stereo viewing of the complete defined area(s) (exclusive, of course, of shadowed regions). The three-dimensional perspective afforded by stereo viewing is an invaluable aid to interpretation in regions of pronounced structural definition. This is the only means of discriminating relatively subtle slopes and even moderate slopes not oriented normal to the flight line. Even with the relatively low vertical exaggeration provided by the STAR-1 high incidence angle imagery, the three-dimensional view greatly aids formation of three-dimensional terrain models for inference of subsurface conditions. The added benefit of stereo coverage is only slightly less for radar imagery than for photographic reconnaissance, where stereo has become virtually standard for serious exploration surveys.

Obviously, complete stereo coverage requires the entire survey area to have duplicate coverage at two incidence angles. This duplication of coverage is somewhat more significant with radar than with photography. With photography, the number of flight lines required to cover the area

is essentially the same whether the frame overlap is 5% or 75%. The major difference is basically one of film and processing cost. Radar, due to the fact that coverage is lapped to the side rather than along the flight line, requires a near doubling of the required flight lines. Even with this, the cost differential between monoscopic and stereo coverage should not exceed 50% as fixed mobilization charges are a significant fraction of the cost for moderate surveys. In addition, staging costs will be significantly less when simply extending the time in the area.

Obviously, stereo coverage requires a minimum sidelap of 50%. The data acquisition contract awarded to Intera specified the imagery to be flown with a nominal sidelap of 55%. The additional 5% sidelap is to absorb errors in flight line positioning and the variation of swath width with elevation discussed previously. In order to simplify flight operations, Intera typically flies all lines at the same barometric altitude (thus a varying altitude with respect to the ground) and maintains both the slant range delay and sweep extent constant as well. Note that the relatively high incidence angles employed in the STAR-1 system tend to minimize the swath width variation with altitude above the ground. Even for an altitude range of 20,000 feet (6,100 m) to the maximum operating altitude of 33,000 feet (10,060 m) the swath width remains between 45 to 47 km.

Due to this relatively small variation of swath width with altitude, Intera chooses to further simplify flight planning and operation by spacing all flight lines equally. This spacing is chosen to provide sufficient sidelap under worst conditions. Typically, and for the entire Philippines survey, the flight line spacing is 10 nautical miles. Taking a worst case swath width of 45 km this provides a sidelap of 59%. This is certainly adequate

and provides considerable margin for possible errors in flight line positioning. While no exact figures for positioning errors are available, it is felt that the inertial navigation system (INS) used by Intera provides accuracy well within these bounds.

With the STAR-1 characteristics and procedures used, the requirements for stereo sidelap are met quite well. The safety margins used are adequate in normal operation and the only problems should stem from incorrect calculation or setting of the coordinates and possibly equipment (INS) malfunction. The minimum sidelap measured for all imagery collected during this survey was 55%. Even though no problem was encountered in obtaining complete stereo sidelap, it is recommended that any future contracts be worded to call for a minimum 55% sidelap rather than nominal. Any failure to obtain stereo coverage, whether by error or malfunction, is completely the responsibility of the contractor and should be acknowledged as such.

The flight line coordinates used for the Philippines survey are listed in Table 3.6 and shown on the sketch maps of Figures 3.9 through 3.12. The swath coverage is likewise indicated for a few lines to give some perspective.

Table 3.6: Flight line coordinates for Philippines radar survey project.

Hydrocarbon Site 1 - Bondoc Peninsula

Line No.	Start	Stop
1	14°12'N 121°46'E	13°53'N 122°05'E
2	13°18'N 122°54'E	14°20'N 121°52'E
3	14°28'N 121°59'E	13°25'N 123°02'E
4	13°33'N 123°09'E	14°36'N 122°05'E
5	14°44'N 122°12'E	13°45'N 123°12'E

Hydrocarbon Site 2 and Geothermal Site C - Cotabato Basin and Mt. Apo, Mindanao

Line No.	Coordinates	Coordinates
1	6°56'N 123°34'E	5°29'N 124°48'E
2	5°35'N 124°55'E	7°03'N 123°41'E
3	7°08'N 123°50'E	5°42'N 125°02'E
4	5°49'N 125°10'E	7°13'N 123°59'E
5	7°17'N 124°08'E	5°56'N 125°17'E
6	6°01'N 125°26'E	7°22'N 124°17'E
7	7°00'N 124°49'E	6°34'N 125°12'E
8	6°40'N 125°20'E	7°06'N 124°57'E

Hydrocarbon Site 3 - Mindoro

Line No.	Coordinates	Coordinates
1	13°20'N 120°57'E	12°40'N 120°57'E
2	12°20'N 121°07'E	13°20'N 121°07'E
3	13°17'N 121°17'E	12°05'N 121°17'E
4	12°05'N 121°27'E	13°15'N 121°27'E
5	13°14'N 121°37'E	12°05'N 121°37'E
6	12°05'N 121°47'E	13°13'N 121°47'E
7	13°10'N 121°57'E	12°10'N 121°57'E

Hydrocarbon Site 4 and Geothermal Sites A and B - Cebu and Negros

Line No.	Coordinates	Coordinates
1	10°46'N 123°21'E	10°13'N 123°21'E
2	10°13'N 123°31'E	10°46'N 123°31'E
3	10°46'N 123°41'E	10°13'N 123°41'E
4	9°29'N 123°32'E	8°52'N 123°16'E
5	8°49'N 123°26'E	11°16'N 124°24'E
6	11°12'N 124°33'E	8°45'N 123°36'E
7	9°14'N 123°59'E	10°55'N 124°37'E

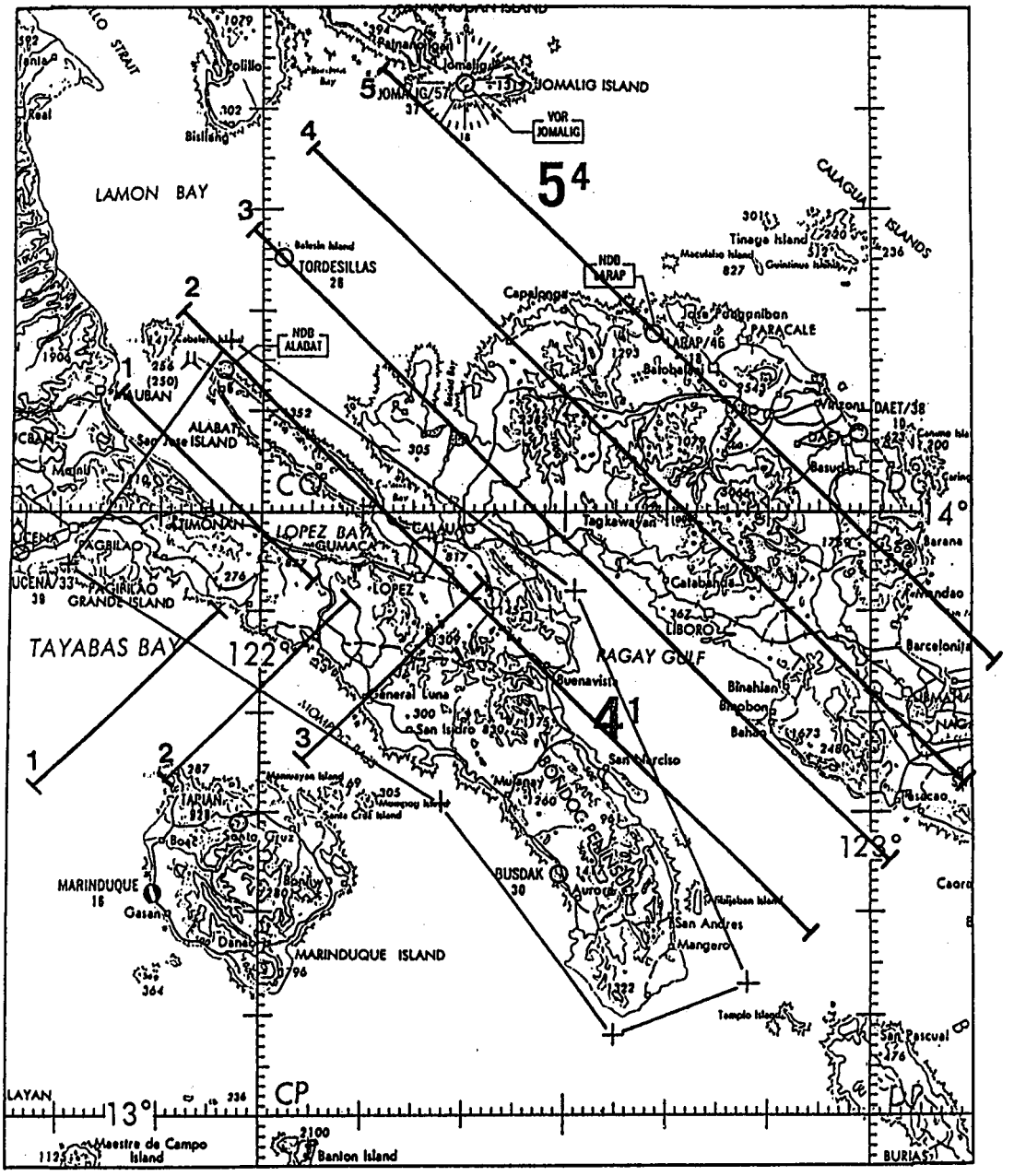

Figure 3.9: Flight lines for Bondoc test site.

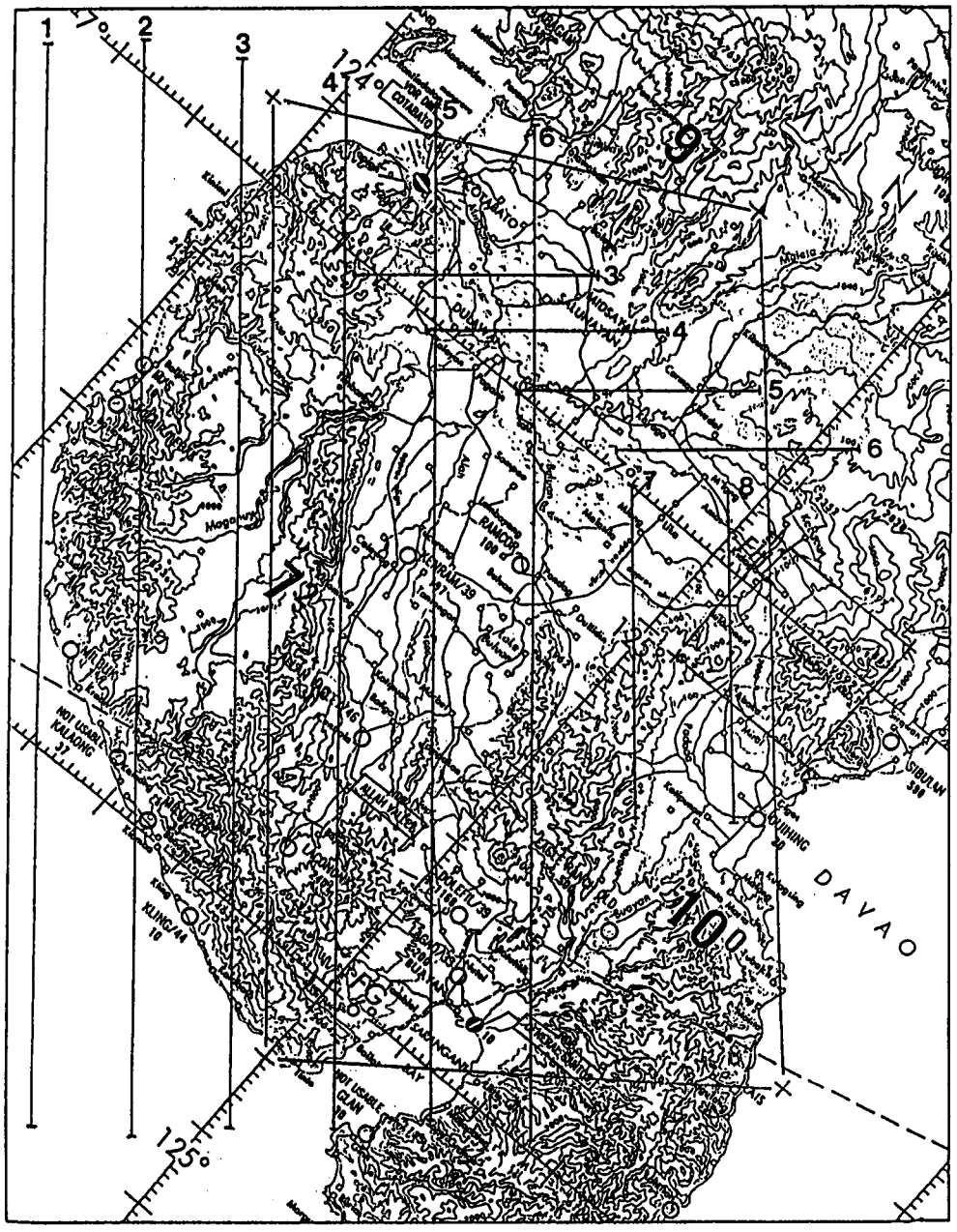

Figure 3.10: Flight lines for Mindanao test site.

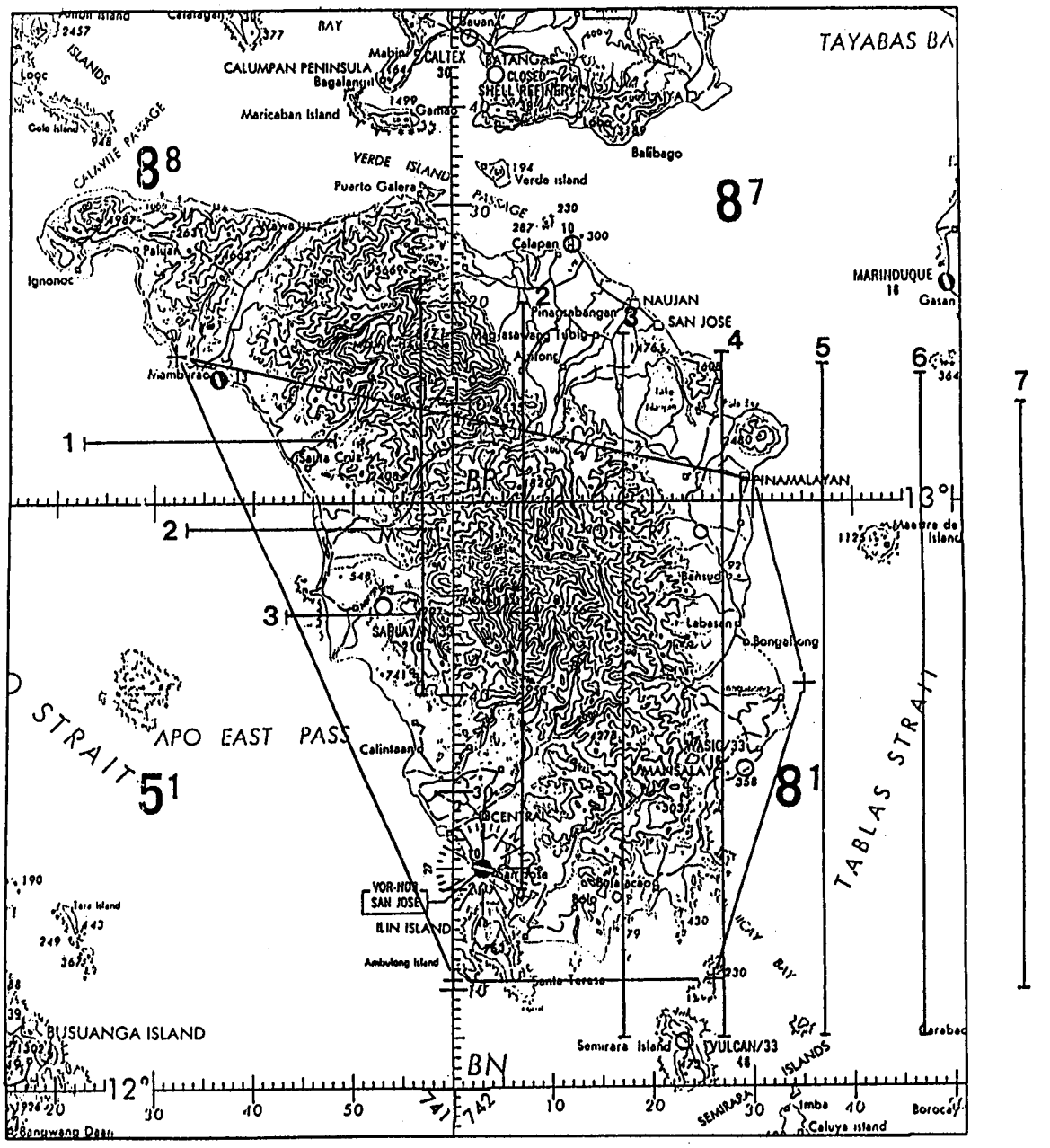

Figure 3.11: Flight lines for Mindoro test site.

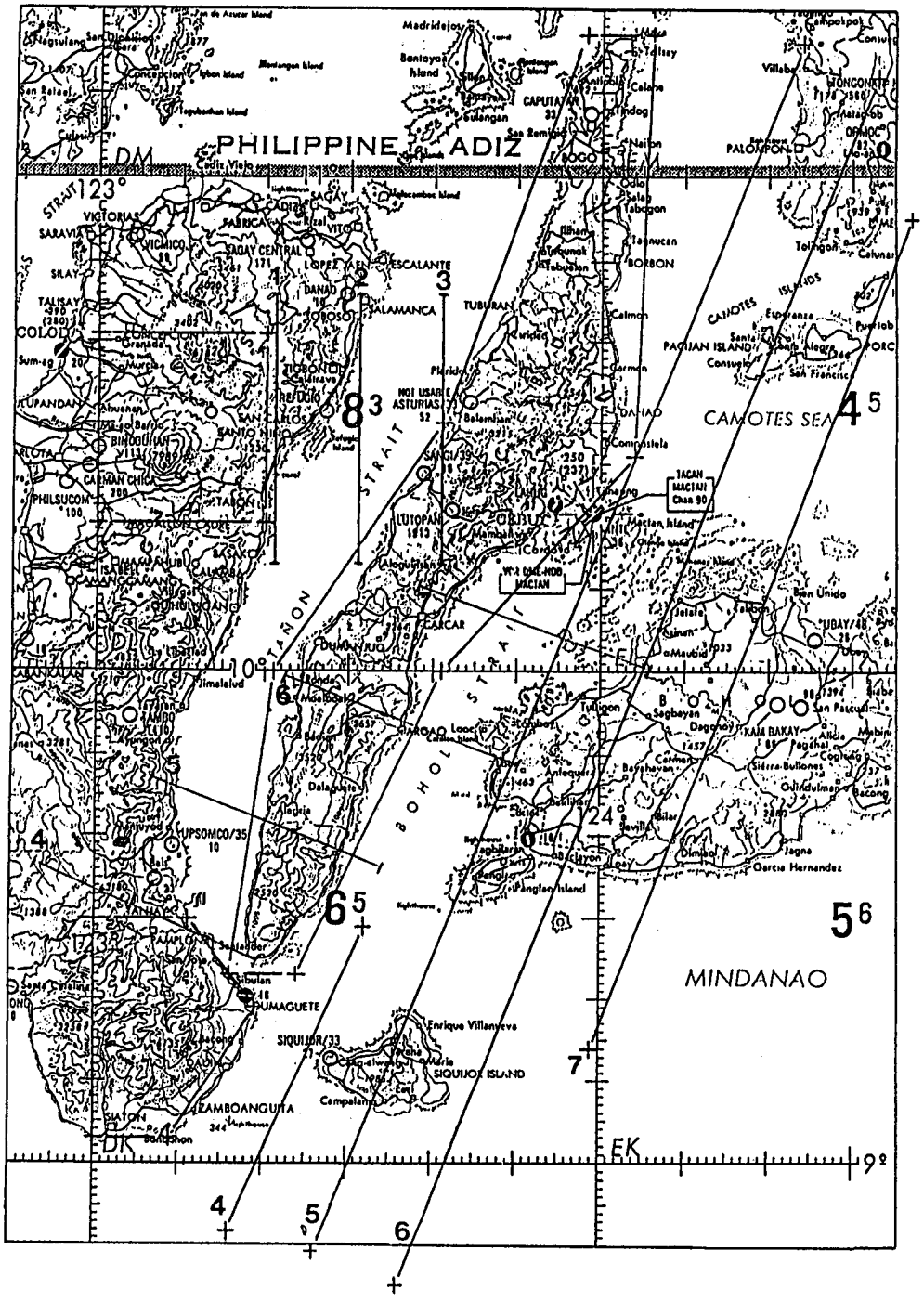

Figure 3.12: Flight lines for Cebu and Negros test sites.

The preceding discussion describes the extent of the flight planning conducted by Intera for this survey, and is a fair representation of that conducted by other firms or agencies conducting radar surveys. Most neglect another important consideration. This is in not making an effort to minimize the data loss due to shadowing which is increasingly important as the system is operated at higher incidence angles. For example, consider the nominal coverage used by Intera for this survey; 29,000 foot (8,840 m) altitude with approximately a 46.4 km swath width. The near and far range incidence angles are approximately 60.6° and 81.9° for the reference elevation. More importantly, however, the mid-swath angle is 77.4°. Thus, the near range portion of the imagery spans nearly 17° while the far range is confined to less than 5° in the region above 77.4°. This means backslopes exceeding 12.6° will be in shadow and these shadows may be quite extensive depending on the relative relief. This obviously precludes stereo viewing. A region imaged first near mid-swath (77.4°) will next be imaged close to the near range limit (60.6°), and if the slopes do not exceed 29.4°, at least monoscopic coverage is obtained. However, a region imaged first close to the far range limit (81.9°) will next be imaged near mid-swath (77.4°). In this case not even monoscopic coverage is obtained for slopes exceeding 12.6°.

This situation can be alleviated slightly by increasing altitude, however, going to the maximum operating altitude of the STAR-1 aircraft only increases the mid-swath angle by approximately 2°. This may also be alleviated somewhat by decreasing the slant range delay thus decreasing the incidence angles over the swath. However, this will incur some increase in slant range compression and relief distortion as well as decreasing the enhancement of more subtle slopes. Still another means of improving this situation would be decreasing the flight line spacing or increasing the

sidelap such that each area is imaged at least once at a lower incidence angle. This obviously impacts acquisition cost, and if used for more than a few sub-regions would have to be contrasted with the cost increase to obtain coverage at a different aspect angle.

Under a standard fixed price contract there is little flexibility in adding additional flight time. Thus, it is critical that the basic parameters of altitude, slant range delay, and sweep extent be chosen based on the known characteristics (slope and relief) of the area to be imaged. Even after arriving at compromise values for these parameters, the flight line placement should be reviewed for location with respect to any known critical areas. Minor offsets of flight lines and/or spacing changes should be negotiated to insure best coverage of known critical areas.

In summary, one must conclude that approval of the detailed flight plan including operating parameters of the system and coordinate location of all flight lines should, in the future, be a contract requirement. Generation of the plan and approval by the contracting agency should be conducted prior to aircraft mobilization. This will prevent expenditure of any significant funds prior to agreement on all details of the flight plan that could be construed to impact the contract cost.

3.3.3 Quality Assurance

Quality assurance encompasses all actions taken to insure the final data products are the best obtainable under the particular set of cost, system, and operational constraints. The quality assurance activity may be separated into the three distinct phases listed below:

(1) Mission planning
(2) On-site review of interim data products
(3) Detailed review of final data products

3.3.3.1 Mission Planning

The first and perhaps the most critical step in assuring the data collected are optimum for performance of the particular application is in definition of the data acquisition contract and formulation of the detailed flight plan. This step was covered in detail in the preceding section. Not as much control as desired could be exercised at this stage for the Philippines survey by virtue of the position as an add-on contract to an existing mission. Standard contract terms were accepted in order to minimize cost and assure collection of these data at the start rather than the end of a lengthy aircraft deployment. Note, however, it is strongly recommended that under normal circumstances the standard data acquisition contract be modified to require full stereo coverage and approval of the detailed flight plan before aircraft deployment.

3.3.3.2 On-Site Review of Interim Data Products

The second step, on-site review of interim data products, is where the Intera STAR-1 system has a decided advantage over most other radar imaging systems. With most other radar systems, the data are not reduced to image form until well after completion of the mission. This depends to some extent on the size of the survey which in turn determines the amount of support equipment moved to the staging area. However, for relatively small surveys such as this, the image data are normally not available for review until well after completion of the aircraft mission. This means quality assurance of the data is completely dependent upon system readings monitored by the radar operator. If marginal or unacceptable segments are subsequently found in the image data, the aircraft must return to

the site at some later time for reflights. This is an extremely costly step in terms of both time and money. Unless substantial penalties for late delivery, incomplete coverage, and image quality have been incorporated into the contract, negotiation of reflights is extremely difficult. Note this problem is primarily due to timing. A reflight for a questionable data strip while the aircraft is on-station for the mission is relatively inexpensive and thus considerably easier to negotiate. Once the aircraft has departed the area, the cost of returning for the same reflight is many times that while on-station.

With the Intera STAR-1 system, the SAR data are fully correlated in real time and an interim image product produced on dry silver paper. Since this image is produced from the digital data recorded on the high density digital tape (HDDT), it provides a complete check of the system through reception of the signal, correlation, and recording. While this paper image has degraded spatial and gray tone resolution, it still permits a detailed quality review of the data both in real time by the radar operator and immediately after each flight by the quality assurance (QA) representatives of the contractor and contracting agency.

It would be difficult to overemphasize the importance of this immediate post-flight review of the data by the QA representative of the contracting agency. Approval of the data by the contracting agency QA representative at this time should definitely be written into the data acquisition contract. Contract definition should provide substantial payment penalty for lack of this approval. This will insure cooperation on both sides in resolving any disputes over the adequacy of the data. Note again how critical it is to resolve questions involving possible reflights at this time. The cost to the contractor of reflying a line as a portion of the next flight is relatively minor. Thus, the possibility of incurring even a small penalty is sufficient

inducement for reflying. Once the aircraft has left the nearest staging area this cost goes up substantially, and once it has departed the complete survey area it escalates even more. At this point, the penalty for even a small data loss would have to be a substantial portion of the contract amount to balance the cost of returning the aircraft and crew to the survey site.

Now let us consider the items which the contracting agency QA representative may check in reviewing the interim dry silver paper imagery. These fall into two general categories: coverage of the contract area and quality of the recorded data. Specific items to be checked are listed in Table 3.7. Detailed monitoring of the items listed in Table 3.7 will insure that the basic data recorded on the High Density Digital Tape (HDDT) is of acceptable quality while the aircraft and crew are still on-site and available for reflights.

Review of the coverage items is quite straight forward and relatively rapid if prior preparations have been made. The nominal acquisition scale of the imagery is 1:250,000 and the final image strips will be adjusted exactly to this scale. The interim real-time paper images will not have all scale corrections incorporated to produce an exact 1:250,000 scale, however, the scale will be relatively close to this. The QA representative should have on-site a set of 1:250,000 maps with the survey area, flight lines, swath extent, and critical areas plotted. Superposition of the interim image strips on these maps permits rapid verification of the coverage requirements.

Review of the quality items is more time consuming and requires some familiarity with radar imagery, system operation, and the image appearance of various operational deficiencies. Flight line annotation by the radar operator of the occurrence of both rain and turbulence greatly aids this operation by pinpointing regions needing more detailed inspection. However,

Table 3.7: Items for on-site review of interim data products

I. Coverage of Contract Area

1.	Flight lines located and oriented as defined by mission plan.
2.	Look direction correct
3.	Flight lines extend beyond the bounds of the contract area on both ends
4.	Near and far range extremes of contract area covered. Coverage of range extremes of area must appear on two flight lines to provide stereo.
5.	Flight line sidelap meets specified minimum
6.	Critical areas are not excessively shadowed.

II. Quality of Flight Strips

1.	Areas of high return not correlated with surface features indicating return from intense rain cells within the range sweep.
2.	Areas of low return not correlated with surface features indicating power loss due to intense rain cell located in range delay interval.
3.	Periodic banding extending across the full image swath in the range direction. This is due to oscillations in the antenna motion compensation system normally excited by turbulence.
4.	Antenna pattern banding producing alternate light and dark strips in the near range extending along the length of the image or in the azimuth direction. This banding is due to antenna pattern ripples in the elevation plane.
5.	Areas of low return at water-to-land transitions. These may occur due to time delay of the clutter-lock system in tracking large transitions in the center of the received doppler spectrum.

even with this, each image strip should be examined in its entirety for any evidence of rain effects or periodic range bands due to turbulence. Land-water transitions occupying a large swath extent should also be examined in detail for shifts in average gray scale due to synchronization delay of the clutter-lock system.

Evidence of antenna banding in the azimuth dimension due to gain ripples in the antenna pattern at low elevation angles is best detected through examination of the near range portion of the imagery in regions along the flight path that are relatively flat and also at a lower elevation. While the antenna pattern is a basic design characteristic of the system that cannot be changed in field operation, this does not mean that the effects of antenna banding cannot be minimized. The low elevation angle ripples of the antenna pattern are a function of the ground plane mounting, thus vary with slight changes in the azimuth pointing direction. The antenna is pointed perpendicular to the velocity vector along the flight track. Under normal conditions, the flight velocity vector and the aircraft axis are near parallel, thus the antenna pointing direction is perpendicular to the axis of the aircraft. However, under crosswind conditions the axis of the aircraft and the flight velocity vector may differ by a substantial "crab" angle. To maintain perpendicularity to the velocity vector, the antenna must be pointed off broadside to the aircraft axis. This slight alteration of the ground plane and particularly reflections from the engine nacelle, cause significant perturbations (ripples) in the elevation pattern particularly at low angles.

This effect may best be minimized by reflying under low crosswind conditions or by changing look direction (so crab angle adjustment of azimuth pointing is toward aircraft tail). In many cases, other requirements dictate the look direction, thus it may not be possible to change this parameter. Also in regions of prevailing wind conditions it may not be practical to wait for decreased crosswinds. Under these conditions, it may still be possible to move operation to higher elevation angles of the pattern by adjusting the combination of aircraft altitude, slant range delay, and elevation tilt angle. While these adjustments may not totally eliminate the

banding, they may significantly reduce the effect. In general, imagery with substantial antenna banding should not be accepted until reflights have demonstrated the problem has been minimized through adjustment of system parameters.

3.3.3.3 Detailed Review of Final Data Products

The final data products normally produced are:

1) Digital tape (CCT) of each image strip.

2) Negative film and positive print of each image strip at 1:250,000 scale.

3) Negative film and positive print of radar mosaic of each area at 1:250,000 scale.

Let us consider the sequence of production of these products and the inspection needed for quality assurance at each step.

The first step in this process is transcription of the HDDT recorded on board the aircraft to a computer compatible tape (CCT). The data are resampled and, for wide swath operation, a three-line incoherent average is performed. The basic pixel size is set by the on-board SAR correlator, however, small errors in the along-track dimension are cumulative along the flight line. As many of the flight lines exceed 150 km, these cumulative errors may produce a significant scale change in the azimuth (along-track) dimension. During this resampling and averaging conversion, tie points between the image and base map are identified and the scale adjusted to 1:250,000.

Errors in the range dimension are obviously not cumulative along the flight track and consequently are much less severe. However, there is some uncertainty in this dimension due to varying relief displacement across the swath. These errors are normally corrected in the mosaicking process. Where a lay-down process (as opposed to digital) is used, as on this program, the image strips are printed at a slightly reduced cross-track scale. During the mosaicking process, this dimension is continuously stretched along the strip to meet tie points on the base map.

The general format description of the CCT produced by either of the Intera systems is shown in Table 3.8. The resulting CCT may be checked for readability and parity, however, this is implicitly performed by using the tape in the next step of the process; to produce an image strip negative. A digital controlled film laser writer is used to produce the strip negative from the CCT. There should be no substantial change between these strips and the interim paper strips inspected on-site, other than greatly improved resolution and gray-scale. However, each strip should be inspected for the same coverage and quality items as the on-site inspection and should also be compared with the interim product to insure no reduction of coverage or quality in the tape transcription and negative printing process. There are three additional items that should now be checked at this stage. These are:

1) Scale in both range and azimuth should be 1:250,000 or very slightly smaller.

2) There should be a continuous range of gray-tones for the regions of interest and these should span the full range from bright to dark.

3) The tonal distribution should be relatively well centered on the mid-grey level and should not significantly vary between regions and strips covering similar terrain.

Table 3.8: Format description for computer compatible tapes of STAR radar data

STAR-1 and STAR-2 data are recorded on 9-track, 2,400 foot computer compatible tapes (CCTs) at 6250 bpi, in one of several formats described below. Each CCT contains records of 4096 bytes with an EOT mark after the last record on the tape. The first record contains the ASCII annotation record. The subsequent records each consist of one range line of radar data (4096, 8-bit pixels), presented in one of the following formats. In every case, one line = one block.

STAR-1 Standard

4064 bytes | 16 bytes | 16 bytes

STAR-1 with ADMU Annotation

64 bytes ADMU | 4000 bytes | 16 bytes | 16 bytes

STAR-2 With ADMU

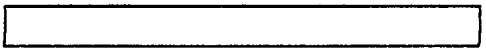

4096 bytes

STAR-2 With ADMU Modified to provide annotation data

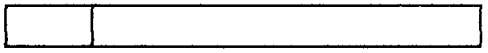

64 bytes ADMU | 4032 bytes

For the 6250 bpi CCTs, one block of data is written as follows:

$$4096\left[\frac{bytes}{line}\right]\times 1\left[\frac{line}{block}\right]\left[\frac{1}{6250 bytes/inch}\right]=0.65\left[\frac{inches}{block}\right]$$

The inter-record gap is 0.5 inches, thus giving a total of 0.65 + 0.5 = 1.15 inches/block. For a 2,400 foot tape, the maximum number of records is therefore:

$$\left[\frac{2,400\times 12}{1.15}\right]=25,043 \text{ records}$$

The maximum amount of data contained on one CCT is thus:

NEAR-SQUARE PIXEL FORMAT (WIDE SWATH)

System	records/tape	x	line/record	x	m/line	=	km/tape	or	nm/tape
STAR-1	25,043		1		12.6		315.5		170.4
STAR-2	25,043		1		18.0		450.8		243.4

RAW STANDARD PIXEL (FULL) FORMAT (WIDE SWATH)

STAR-1	25,043		1		4.2		105.2		56.8
STAR-2	25,043		1		6.0		150.3		81.1

RAW HIGH RESOLUTION FORMAT (NARROW SWATH)

STAR-1	25,043		1		4.2		105.2		56.8
STAR-2	25,043		1		6.0		150.2		81.1

REPRESENTATION OF STAR DATA ON CCT

Data on the CCTs represent ground distances in the across-track and along-track directions as follows:

DISTANCE	STAR-11		STAR-22	
	Std. Res.	Hi Res.	Std. Res.	Hi Res.
1 Line across track (Range)	46.6 km 11.4m/pixel	23.8 km 5.8m/pixel	63.3 km 15.5m/pixel	16.7 km 4.0m/pixel
1 Line along track (Azimuth)				
Near Square	12.6 m	-	16.2 m	-
Full Res.	4.2 m	4.2 m	5.4 m	5.2 m

Notes:
1. Altitude = 33,000 feet
   Range Delay = 20 km
2. Altitude = 33,000 feet
   Range Delay = 15 km

The first byte of each line represents the leftmost pixel, while the last byte of each line represents the rightmost pixel. Thus, if the radar is looking right out of the aircraft platform, the first byte of each line recorded represents the near edge of the swath and the last byte represents the far edge. If the radar is looking left, the reverse is true: the first byte of each line represents the far edge of the swath, and the last byte the near edge.

Contact prints produced from these negatives should also be inspected for the above three items. The primary concern here is that the exposure control preserve the dynamic range of gray tones and hence the discrimination of regions with differing scattering characteristics.

The preparation of the mosaic is covered in considerable detail in the next section. Insofar as inspection is concerned, this is performed on the positive print produced from the mosaic negative. The items checked and the concerns are the same as for the image strips except the measured scale should now be 1:250,000 within the allowable error tolerance.

3.3.4 Base Map/Mosaic Construction

Base maps used for the Philippines radar survey and preparation of radar mosaics were United States Defense Mapping Agency (DMA) 1:250,000 Joint Operation Graphics (JOG sheets). Copies of these maps, plotted on stable base film, were procured from DMA. The planimetric detail and drainage compiled on these maps provide an abundance of check points used to initially compute the true scale of each flight strip. The scale ratios computed are used in an optical projector to print tone and scale matched prints for mosaic construction. The optical projector can accommodate flight strips up to 45 inches (114 cm) in length, thus most flight strips can be printed and mosaicked in one piece, minimizing the number of cut-and-join lines in the mosaic. The strips for mosaic construction are printed on Ilfobrom fiber base paper. Surface IP glossy is used because of its ability to retain fine gradations of tone and its resistance to edge chipping.

Mosaic assembly is made at 1:250,000 scale on tempered masonite boards. The DMA maps, plotted on stable base film and with Transverse Mercator (TM) grid lines, serve as the Base Manuscript for mosaic construction.

Control overlays on stable base film were constructed from the Base Manuscript. These overlays are simply separations obtained from the Base Manuscript containing only prominent features used for checking scale and registration. This stable base film overlay is punched and pin registered to the mosaic assembly board so it can be rolled back as new strips are pasted to the mosaic board and then returned in position over the board to check the registration of the radar strip to the detail on the control overlay. The adhesive used allows time for final movement of the print, and careful adjustments are made until the strip is completely registered. Adjacent strips are tied one-to-another so the entire project area is covered with continuous tone-matched radar imagery.

Each completed mosaic sheet is set on a specially designed camera easel and optically copied at 1:1 to produce a copy negative, scale 1:250,000. The film used for the negative is Kodak Commercial Film coated on a .007 inch Estar base. This emulsion is by far the best in its class because of the even coating, long tonal range, excellent anti-halation backing, safelight tolerance, and range of contrast possible with varied development time. The most valuable assets for this purpose are, (1) the long tonal range, providing a D-LogE curve with a straight line portion from .30 to 3.0 density; and (2) a Gamma ranging from 0.90 to 1.10 with standard developer Kodak DK-50.

In order to produce an accurate 1:1 copy negative each time, a Robertson 26x32 inch Floor Camera is specially modified so it may be accurately set and locked in copy position without having to rely on visual focusing and aligning of the optical image for each setup. The copy easel is designed to have side-to-side movement with pin locks which allows a board containing four mosaic sheets to be positioned so that the center of each sheet to be copied automatically falls exactly on the center of the lens axis. The

process mosaic negative is checked for scale by aligning the corners of the sheet with the plotted corners on the Base Manuscript. The process Gamma (contrast) of the mosaic negative is controlled to 1.0 plus or minus 10%. Note how well Kodak Commercial Film fits this requirement with a Gamma range of 0.90 to 1.10.

All information required in the border area of the mosaic sheet: corner coordinates, scale bar, date of image acquisition, and all descriptive nomenclature is set up at the same scale as the mosaic and copied onto Kodak Ortho Type 3 Film, coated on a .007 inch Estar base. The border negative is punched and pin registered to the camera mosaic negative so that the film couplet is the Master Image Mosaic. The result is a master mosaic negative with fine reproduction of tonal differences in the radar mosaic and crisp, high density type in the border area.

3.3.5 Interpretive Products

The final interpretive products are positive prints of each flight line strip and mosaics of each project area. The negatives of these products serve as the working data masters.

From the individual flight line negatives, positive glossy prints are produced by vacuum contact printing on Kodak Polycontrast Rapid II Resin Coated (RC) Paper. The glossy surface enhances the appearance of the data giving it a visual "sharpness" that cannot be achieved using a matte-surfaced paper. The RC paper also provides an excellent dynamic range of tonal contrast and is reasonably stable dimensionally.

The positive strip prints are the basic data from which virtually all interpretation is performed. Interpretation is normally performed by viewing each area in stereo and under some degree of magnification. Overlays produced on the strips are subsequently transcribed onto the area mosaic.

The radar mosaics are normally printed on a stable base Cronopaque material to prevent swelling or shrinkage over long term use. These mosaics serve as the masters for transcription of all data obtained from the radar survey. The complete process flow of the image data along with the points of quality inspection are shown in Figure 3.13.

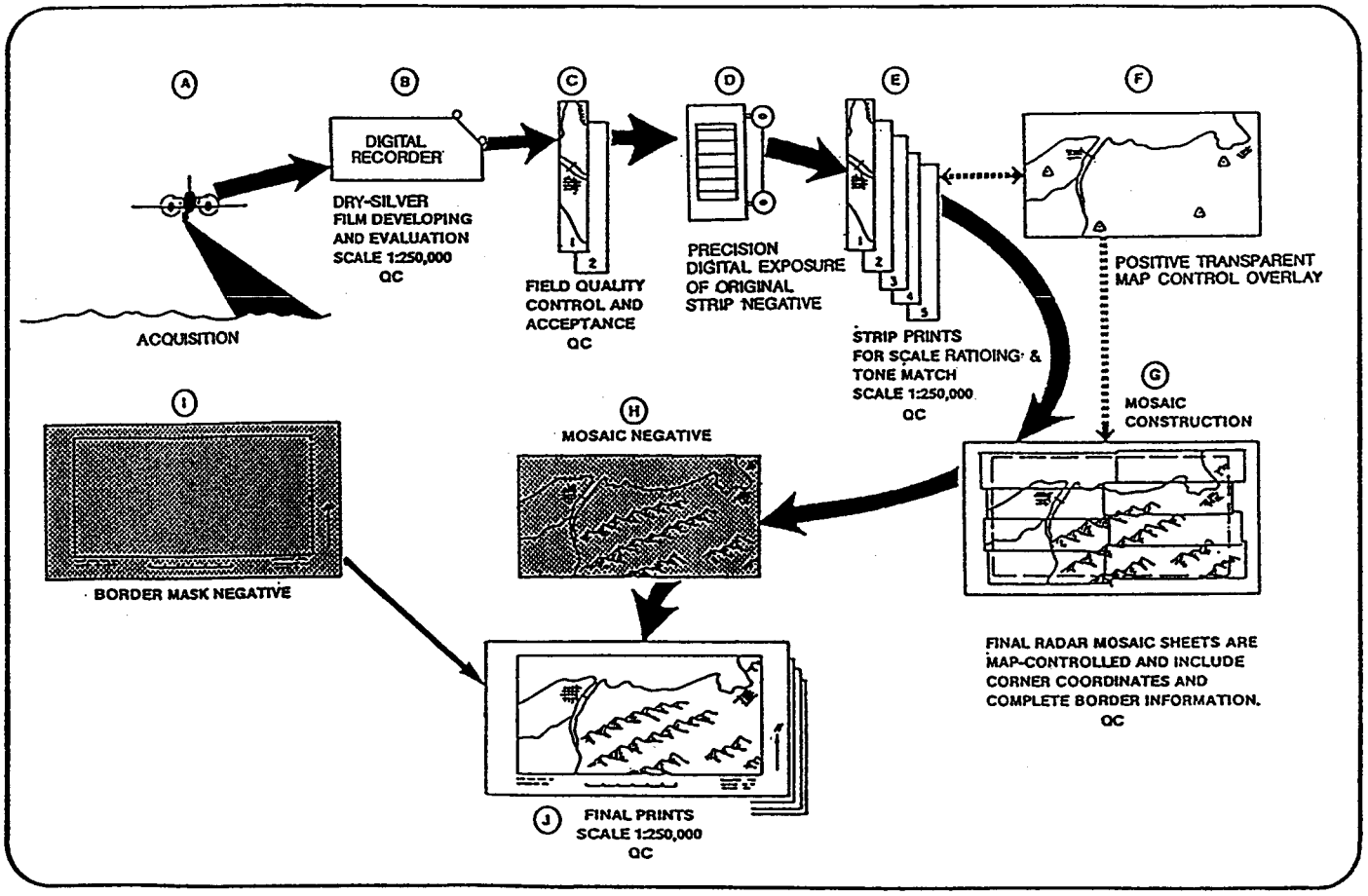

Figure 3.13: Process flow of image data.

This page is intentionally left blank.

4 INTERPRETIVE STRATEGY

Prior to interpretation of the imagery, an extensive literature search was conducted. This review allowed image interpreters to become familiar with the geologic history, rock types, and structural styles within each area. In the initial phase of the interpretation procedure, monoscopic analysis of the radar mosaic allowed the analysts to develop a comprehensive familiarity of the study area and determine the regional geology. Regional geology in an interpretive sense refers to the relationship between large scale geologic features that can be readily identified on the imagery. Coastlines and major rivers were then transferred from the radar mosaic to an overlay of stable-base drafting film. These features are easily identified on radar imagery due to a large tonal contrast between land and water boundaries. The overlay served as a base for geologic interpretation and provided points of reference between the imagery and published maps of the area.

The most comprehensive part of the initial interpretation procedure was the determination of local geology. Stereo radar imagery was used to enhance interpretation capabilities. Stereoscopic viewing of radar imagery produces a three-dimensional impression which creates the illusion of depth. The three-dimensional mental impression obtained from stereoscopic analysis is seldom an accurate replica of the terrain because of vertical exaggeration. In most cases, relief will appear more severe than it is in nature; however, vertical exaggeration increases the interpreter's ability to identify many subtle geologic features. For example, terrain slope, dip direction, strata thickness, surface morphology, and relief displacement due to faulting become more visually apparent under stereoscopic examination. Magnification (up to 10X) was used during the stereoscopic analysis in areas of greater

geologic complexity or to more clearly define subtle terrain features. Through the use of stereoscopic viewing, numerous previously unmapped structural features (folds, faults, lineaments) were recognized.

The second phase of the interpretation procedure entailed the synthesis of the two individual geologic interpretations to produce an integrated set of preliminary overlays. This was accomplished through a cooperative inspection and evaluation procedure involving the two imagery analysts. The preliminary overlays were then reviewed by a consultant and a final editor. After further revisions and refinements, a final set of overlays was drafted. The final interpretive products consisted of 1) a radar-geologic map which included lithologic boundaries, faults, lineaments, folds, form lines, and geomorphic anomalies, and 2) a radar-lineament map.

4.1 Radar – Geologic Map

Part of the overall interpretive strategy was the examination and incorporation of known geologic data. Available geologic maps aided in providing a general geographic location of lithologic boundaries and previously recognized structural features. Geologic literature provided lithologic descriptions which were used to acquire an understanding of the interrelationship between rock type and the corresponding radar image appearance.

Age relationships between geologic units were initially assumed to be correct as previously mapped; stratigraphic information was derived from the existing geologic maps of the Philippines, and the legends for the radar-geologic maps are a result of the combination of the legends of these previously published maps. In the identification of lithologic units, if the tone-texture signature on the radar suggested that the observed lithology contrasted with published information, a change was made to conform with

the evidence interpreted from the radar imagery. Characteristic tone-texture signatures were selected from areas which appear to relate accurately to mapped units, while allowing for variations due to topographic relief, lithologic variations within the unit, partial masking by transported material, slope, and structural variations within the unit. These characteristic signatures were used as guides for determining the areal extent of each unit.

Abrupt changes in drainage patterns were also assumed to suggest changes in composition or structure of the underlying rocks and were mapped as lithologic contacts. Unless a rock unit has developed particular tone-texture-topographic signature that contrasts with adjacent units, or unless it was sufficiently distinct to permit positive identification and isolation, it was not mapped. Thus, only those units that were clearly expressed on the radar imagery were compiled on the interpretation overlays. This does not mean or imply that the unit is not sufficiently unique in composition to be identified on the ground.

It was assumed that the available geologic maps were based on field data, whereas units on the radar-geologic maps were delineated only if they were detectable on the radar imagery. Hence, some outcrops mapped on the existing geologic maps, may not appear on the radar-geologic maps because the areal extent of the outcrops is small, or the small scale of the radar imagery does not lend itself to such fine discrimination.

Geologic maps provided by PNOC EC and BED were used as the primary source of geologic information in areas where excessive terrain relief produced adverse radar shadowing, or where tonal, textural, or morphologic changes were not sufficiently expressed on the radar imagery to provide accurate delineation of lithologic boundaries.

It is sometimes possible to discern movement across faults and confidently identify these features. Further, it is possible to identify the sense of movement and consequently the type of fault on only a small percentage of these features. In determining fault movement, a problem which leads to confusing evidence in the imagery arises when older faults have experienced different senses of movement at different times. Unfortunately, for most faults, there is no clear evidence of offset. However, many of the lineaments in recent volcanic material and associated alluvial fans, terraces, etc., show evidence of recent disturbances. Folds and faults shown on the radar-geologic maps were inferred from the radar imagery and their actual location and orientation relates directly to position on the radar mosaic.

4.2 Radar – Lineament Map

According to O'Leary et al. (1976), a lineament is a "mappable, simple or composite linear feature of a surface, whose parts are aligned in a rectilinear or slightly curvilinear relationship and which differs distinctly from the patterns of adjacent features and presumably reflects a subsurface phenomenon." Important elements of the definition are that it is naturally occurring, it is mappable, and it is presumed to represent or reflect some subsurface phenomenon. Fractures in hydrocarbon-bearing strata have been recognized as factors affecting migration, accumulation, and production of hydrocarbons. Because fractures are commonly propagated upward and are reflected at the Earth's surface as subtle lineaments, mapping of these surface features can be extremely important in many phases of petroleum exploration and development.

A wide variety of terrain features, such as straight stream segments, aligned stream offsets, straight scarps, valleys and ridges, tonal or textural boundaries or alignments, aligned terminations, or interruption of topographic fabric, etc., can manifest lineaments. In reality, many lineaments and most of the longer lineaments or zones mapped are composed of a combination of features. In the more rugged mountainous areas, straight valleys and ridges constitute many of the lineaments. In the lowland areas, tonal alignments and tonal or textural boundaries are more common. Drainage anomalies, either straight stream segments or aligned discontinuities or offsets, form lineaments in virtually any terrain.

In general, lineaments are more boldly displayed and confidently identified in the more rugged areas than in the lowlands. Much of this is the effect of shadow highlighting of aligned topographic features. In the lowlands, the subtle tonal or textural boundaries are more difficult to identify and confidently separate from agricultural practice or other cultural features.

4.3 Prospect Evaluation

The supreme achievement in petroleum exploration is the development of a prospect or play, and the eventual discovery of hydrocarbons that opens a new petroleum province. Upon what criteria should the geologic choice of the best area to drill be based? What evidence is significant? What kinds of geologic evidence can be used or is available in predicting where a petroleum discovery will eventually be found, and what weight should be given to each kind of evidence?

If we compare the geologic conditions that are found in the known petroleum producing areas we see that they are extremely diverse. Each area may have its own geologic history, its own characteristic deformation,

its own stratigraphy, and its own particular types of petroleum accumulation. It is doubtful whether many geologic conditions could be accurately anticipated for an unknown region in advance of drilling. Yet there are certain empirical characteristics that seem to be present in most productive areas, and that seem to carry more weight than others in a prediscovery evaluation of the prospects of a region. These characteristics might be classified as (1) sediment type, (2) source potential and maturity, (3) reservoir and seal type, (4) regional arching with associated pinch-outs and unconformities, and (5) nature of local traps.

5 RADAR–GEOLOGIC INTERPRETATION – BONDOC PENINSULA

The Southeast Luzon Basin embraces the Bondoc Peninsula. For purposes of radar flight line planning, the Bondoc radar mosaic includes approximately 6,250 km^2 of land/water coverage (see Bondoc Radar Mosaic which is an enclosure with this report).

5.1 Background and Petroleum Exploration Activities

5.1.1 Structure

The Bondoc part of the Geologic Map of the Bicol Shelf, Lamon Bay and Southeast Luzon Basins (BED, 1985), which was provided by the Philippines Bureau of Energy Development, was used to familiarize radar image interpreters with the regional geologic framework. The Bondoc Peninsula has been described structurally as a southeast plunging anticlinorium or structural high, with associated northwest-trending folds, and major longitudinal-type faults which parallel the trend of the Peninsula (Philippines Minerals and Fuels Division, 1976). However, based on recent analysis of aeromagnetic and seismic data, BED et al. (1987) suggest that a major part of the Bondoc Peninsula is within the Bondoc Graben, the central part of which is a probable diapiric zone that was uplifted during the Pleistocene. Consequently, the basement is relatively deep in this area.

The Bondoc Graben (Fig. 5.1) is one of eleven structural provinces corresponding to a series of parallel and elongate northwest-trending horst, graben, platform, and terrace features that make up the Southeast Luzon Basin. The structural highs (horsts, platforms, and terraces) are characterized by relatively thin sedimentary cover, generally less than 3 km

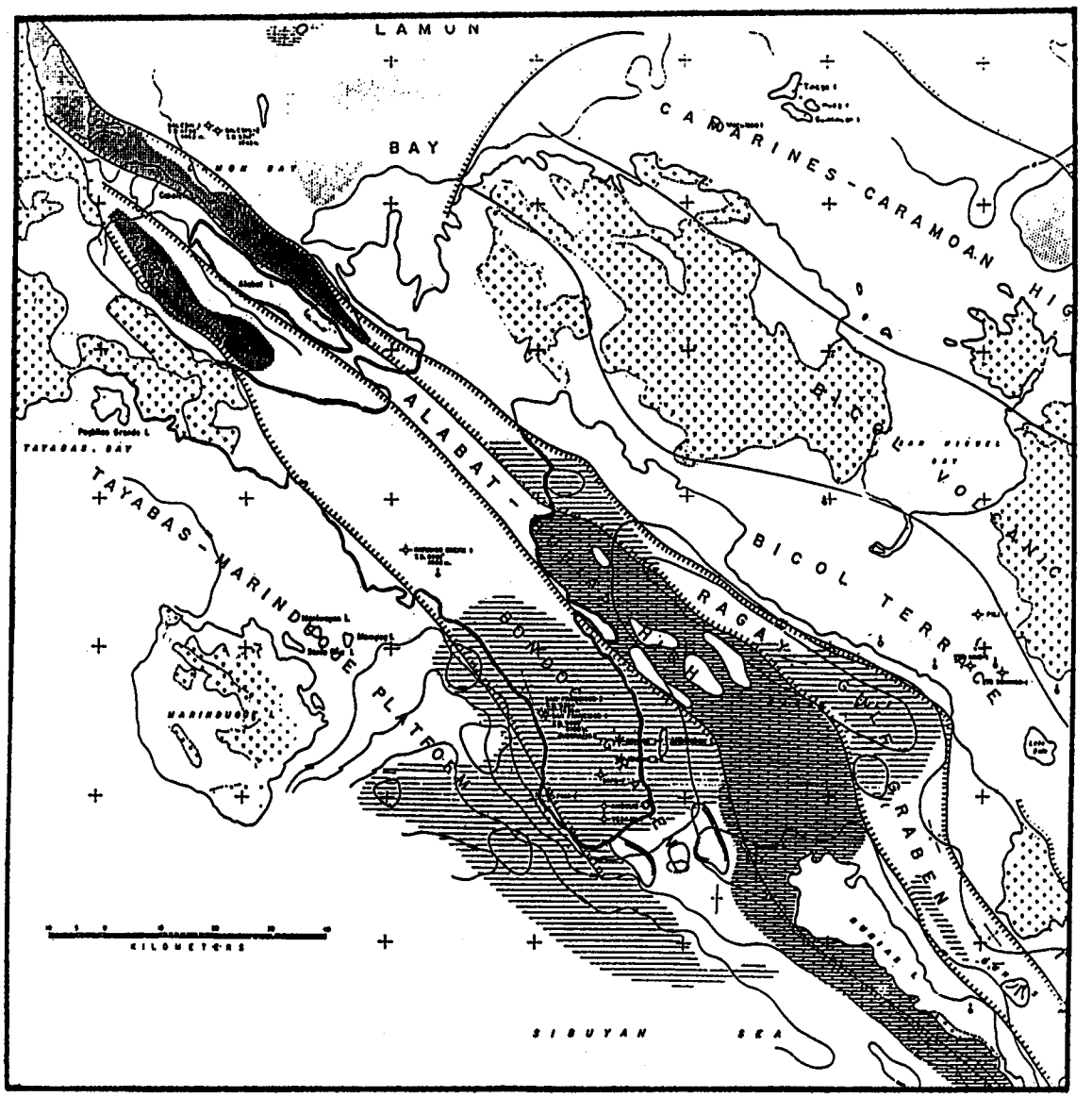

Figure 5.1: Structural provinces in the vicinity of the Bondoc Peninsula. (After BED et al., 1987)

thick, and/or exposures of basement rocks. The grabens comprise the major depocenters with probable maximum thickness of sedimentary fill of 8 km (BED et al., 1987). The Bondoc Graben which appears to plunge from northwest to southeast is bordered on the southwest by the Tayabas-Marinduque Platform, and on the northeast by the Alabat-Burias Horst and Ragay Gulf Graben (Fig. 5.1)

5.1.2 Stratigraphy

The stratigraphy of the Bondoc Peninsula has been described by BED et al. (1987), the Philippines Bureau of Mines and Geo-Sciences (1981), the Philippines Mineral Fuels Division (1976), and Robertson Research International Ltd. (1975). The following stratigraphic discussion is a synthesis of these reports. The section includes strata which ranges in age from Cretaceous to Pleistocene with Quaternary and Recent sediments.

The stratigraphic descriptions provided here include only those stratigraphic units that have been mapped on the Radar-Geologic Interpretation of the Bondoc Peninsula which accompanies this report. Stratigraphic units were selected from the 1985 Geological Map of the Bicol Shelf-Lamon Bay and Southeast Luzon Basins prepared by the Philippines Bureau of Energy Development.

Cretaceous

The Cretaceous section forms the stratigraphic basement and is composed of amphibolites, gneiss and spilitic rock groups. Pillow lavas, graywackes, and cherts have also been identified.

Eocene - Oligocene

This interval is represented by the deposition of the Unisan Volcanics which have been located in the vicinity of Unisan, Quezon. The formation consists of porphyritic andesite and amygdaloidal basalt with occasional interbeds of tuffaceous sandstone and conglomerate. Lithologic evidence and a faunal mix of planktonic and benthonic foraminifera indicate that this formation was probably deposited in an outer neritic to upper bathyal environment during a time of active volcanism.

Oligocene - Early Miocene

The Panaon Limestone, which unconformably overlies the Unisan Volcanics, has outcrops near Barrio Panaon and covers the whole Quezon National Park. The limestones may be massive to nodular or well bedded and are generally hard, dense, and tight. Fossiliferous portions are composed of whole tests and fragments of red algae, corals, benthonic and planktonic foraminifera, echinoids, molluscs, and occasional green algae.

The microfacies of the Panaon Limestone indicate variable environments of deposition. In most cases, the limestones were deposited in either lagoonal environments with open marine influences or foreslope to deep-shelf margin environments characterized by sedimentary brecciation.

Middle Miocene

Unconformably overlying the Panaon Limestone is the Middle Miocene Vigo Formation. This formation is predominantly a thick shale unit with sandstone interbeds and sandy or coralline fossiliferous limestone lenses. The shales are gray to brown and are soft, silty, and calcareous. The gray sandstones are medium to coarse grained and are moderately sorted.

Although late Early Miocene fossils have been identified in the basal portion of the formation, the occurrence of Globorotalia fohsi and Orbulina universa in the overlying beds gives a Middle Miocene age for the bulk of the Vigo Formation. This paleontological evidence along with sedimentary analysis indicates the Vigo Formation was generally deposited in a deep water, open marine environment. Formation thickness is approximately 6,560 feet (2,000 m).

Late Miocene - Pliocene

The Canguinsa Formation unconformably overlies the Vigo Formation. This formation was subdivided into two members by Santiago (1968) and the Philippines Oil Development Company (1978). The Late Miocene Lower Canguinsa is predominantly medium-to coarse-grained sandstone with interbedded siltstone, shale, and mudstone. Pebbles of conglomerate, found at local basal areas, are mostly of basalt and andesite and are cemented with a coarse sandy matrix. The Late Miocene - Pliocene Upper Canguinsa consists of finer-grained sandstone and siltstone. The formation as a whole can be described as rhythmically bedded sandstones, shales, and conglomerates with sandstones being predominant. Outcrops of the Canguinsa Formation are dark gray to brown, medium- to coarse-grained, friable sandstone. The sand grains are subrounded with a clay matrix.

Sandstones of the Canguinsa Formation contain abundant leaf imprints and fragments which are indicative of deposition in shallow to moderately deep water, perhaps near the outer shelf area. Formation thickness ranges from 6,560-9,840 feet (2,000-3,000 m). An open marine environment of deposition near the outer edge of the shelf has been suggested for the Canguinsa Formation.

Pliocene

The Hondagua Formation of Pliocene age is mostly siltstone with interbeds of shales and calcareous sandstone. This clastic sequence reaches an approximate thickness of 3,300 feet (1,006 m) and appears over a small area in northwestern Bondoc Peninsula. The sediments comprising this unit were generally deposited under deep water, open marine conditions.

Pliocene - Pleistocene

The Vinas Formation, which is conformable over the Hondagua Formation, is a sequence of coarse-grained sandstones and sandy shales with basal occurrences of gravelly limestone and conglomerate. Exposures of this formation are located northwest of Calauag town between Calauag Bay and Lopez Bay. The microfauna indicates the sediments of the Vinas Formation were deposited in a shallow marine, inner sublittoral, protected environment.

Pleistocene

The Malumbang Formation unconformably overlies several different formations and occurs as widespread exposures on the periphery of the Bondoc Peninsula. This Pleistocene formation is mostly limestone with occasional interbeds of sandstone, shale, siltstone, and marl in the lower portions. The limestone is bedded, sandy, crystalline, and porous with a measured thickness of over 4,000 feet (1,220 m) in the northern part of the Bondoc Peninsula; however, in southern Bondoc thicknesses vary from 425-1,000 feet (130-305 m).

The faunal assemblage found in the Malumbang Formation, which includes algae, echinoid spines, corals, molluscan shells and bryozoan fragments, indicates a warm, shallow marine, inner sublittoral environment of deposition.

Quaternary and Recent

Included in this group are all unconsolidated sediments. Deposits occur as floodplain alluvium, terraces, and colluvial flats within inland areas. Superficial sands appear as accumulations in depressions or along diffuse drainage channels.

5.1.3 Hydrocarbon Occurrences and Exploration Activity

The Bondoc Peninsula, because of the existence of several oil seeps, has long been recognized as a potential petroleum province. Many of the exploratory wells drilled on Bondoc have reported hydrocarbon shows, and a few have tested significant amounts of oil and gas (Table 5.1). Unfortunately, subsequent production testing has proven all prospective zones to be non-commercial. Figure 5.2 shows the approximate locations and Table 5.1 provides pertinent information for the exploratory wells drilled on the Bondoc Peninsula.

As indicated in Table 5.1, initial wildcat drilling took place on the Bondoc Peninsula in the early 1920's. Activity peaked between 1948 and 1960. In 1971, White Eagle Overseas Oil Company drilled the Aurora wells and penetrated hydrocarbon bearing sandstones in the Canguinsa and Vigo Formations (Philippines Minerals and Fuels Division, 1976). SEDCO Exploration Company drilled the most recent well in the area in 1980, the Katumbo Creek-1 well, in northwest Bondoc Peninsula. The well failed to encounter the prognosticated limestone target in a seismically defined anticlinal feature and was consequently plugged and abandoned as a dry hole (BED, et al., 1987). According to Petroconsultants (1988), an onshore Bondoc Peninsula wildcat well is planned for 1988.

Table 5.1: Exploratory wells and hydrocarbon occurrences - Bondoc Peninsula. (Modified from BED et al., 1987)

Well Name	Drilling Date	Total Depth m (ft)	Play Type	Defined by	Target	Age of Rock at T.D.	Results	Remarks
Bahay-1	1906 (?)	38.7 (127)	Fault structure	Surface mapping	No data	No data	Oil show	
Bahay-2	1910 (?)	91.4 (300)	Fault structure	Surface mapping	No data	No data	Oil show	
Irwin-2	1915 (?)	182.9 (600)	Anticline	Surface mapping	No data	No data	Oil show	
Amoguis-1 (Richmond)	1921	401.7 (1318)	Anticline	Surface mapping	Late Miocene ss	No data	Oil and gas shows	
Sapa-1 (Richmond)	1923	1143 (3750)	Anticline	Surface mapping	L/M Miocene ss	No data	Gas shows	
Yebaan-1 (Richmond)	1923	185.9 (610)	Anticline	Surface mapping	Late Miocene ss	No data	No shows	
Pina-1 (Richmond)	1924	1565.1 (5135)	Anticline	Surface mapping	L/M Miocene ss	No Data	Oil and gas shows	(886 - 903 m) 2600 m3 of gas per day
Maglihi-1 (Far East)	1938	138.7 (455)	Anticline	Surface mapping	No data	No data	Oil and gas shows	
Maglihi-2 (Far East)	1938	173.7 (570)	Anticline	Surface mapping	No data	No data	Oil and gas shows (165 - 173 m) 2 bopd	
Maglihi-2A (Far East)	1939	297.2 (975)	Anticline	Surface mapping	No data	No data	Oil and gas shows	
Maglihi-3 (Far East)	1940	189.9 (600)	Anticline	Surface mapping	No data	No data	No shows	
Maglihi-5 (Far East)	1940	317.0 (1040)	No data	No data	No data	E/M Miocene	Oil and gas shows	
Bondoc-1 (Far East)	1948	418.2 (1372)	Anticline	Surf. & seismic mapping	No data	? E/L Miocene	Oil and gas shows	
Bondoc-2 (Far East)	1948	723.0 (2372)	Anticline	Surf. & seismic mapping	No data	Late Miocene	Oil and gas shows	Tested 250 bopd at T.D.

(Table 5.1: Continued)

Well Name	Drilling Date	Total Depth m ft)	Play Type	Defined by	Target	Age of Rock at T.D.	Results	Remarks
Bondoc-3 (Far East)	1949	1691.0 (5548)	Anticline	Surf. & seismic mapping	No data	Middle Miocene	Oil and gas shows	Still small amount of oil & bubbly gas from open casing
Bondoc-4 (Far East)	1952	137.2 (440)	Anticline	Surface mapping	No data	(?) Early Miocene	Oil and gas shows	Few gas bubbles still coming from well head
Bondoc-5 (Far East)	1952	140.2 (460)	Anticline	Surface mapping	No data	(?) Early Miocene	Oil and gas shows	
Bondoc-6 (Far East)	1952	140.2 (460)	Anticline	Surface mapping	No data	(?) Early Miocene	Oil and gas shows	
Bondoc-7 (Far East)	1960	1299.1 (4262)	Anticline	Surface & data	Middle Miocene ss	Middle Miocene	Oil and gas shows	
Aurora-1 (White Eagle)	1971	2088.5 (6852)	Anticline	Surf. & seismic mapping	Middle Miocene ss	Late Miocene	Oil and gas shows	(398 - 1405 m) 1 meter flame / 20hrs
Aurora-2 (White Eagle)	1971	1103.4 (3620)	Anticline	Surface, seismic & well data	Middle Miocene ss	Middle Miocene	Oil and gas shows	9 meter flame for 15 minutes at T.D.
San Francisco-1 (White Eagle)	1977	2099.8 (6889)	Anticline	Surf. & seismic mapping	Late Miocene ss	Middle Miocene	Oil & gas shows; high pressure - low volume methane to butane at 701 - 915 m; DST at 1844 - 1852 m; 6 - 8' flame for 1 hr. recovered 2 gal. of 32° API gravity crude oil	Inconclusive test, off crest of anticline
San Francisco-2 (Richmond)	1977	1634.9 (5364)	Anticline	Seismic & well data	Middle Miocene ss	Middle Miocene	Dry well	Valid test, reservoirs lacking
Katumbo Creek-1 (SEDCO)	1980	1951.0 (6401)	Anticline	Seismic	Early Miocene ls	Early Miocene or older	Dry well	Test not valid, limestone target absent

SEDCO - SEDCO Exploration Company
White Eagle - White Eagle Overseas Oil Company
Richmond - Richmond Petroleum Co. (subsidiary of Standard Oil Co., CA.)
Far East - Far East Oil Dev'l Co. (Philippines Oil Development Company)

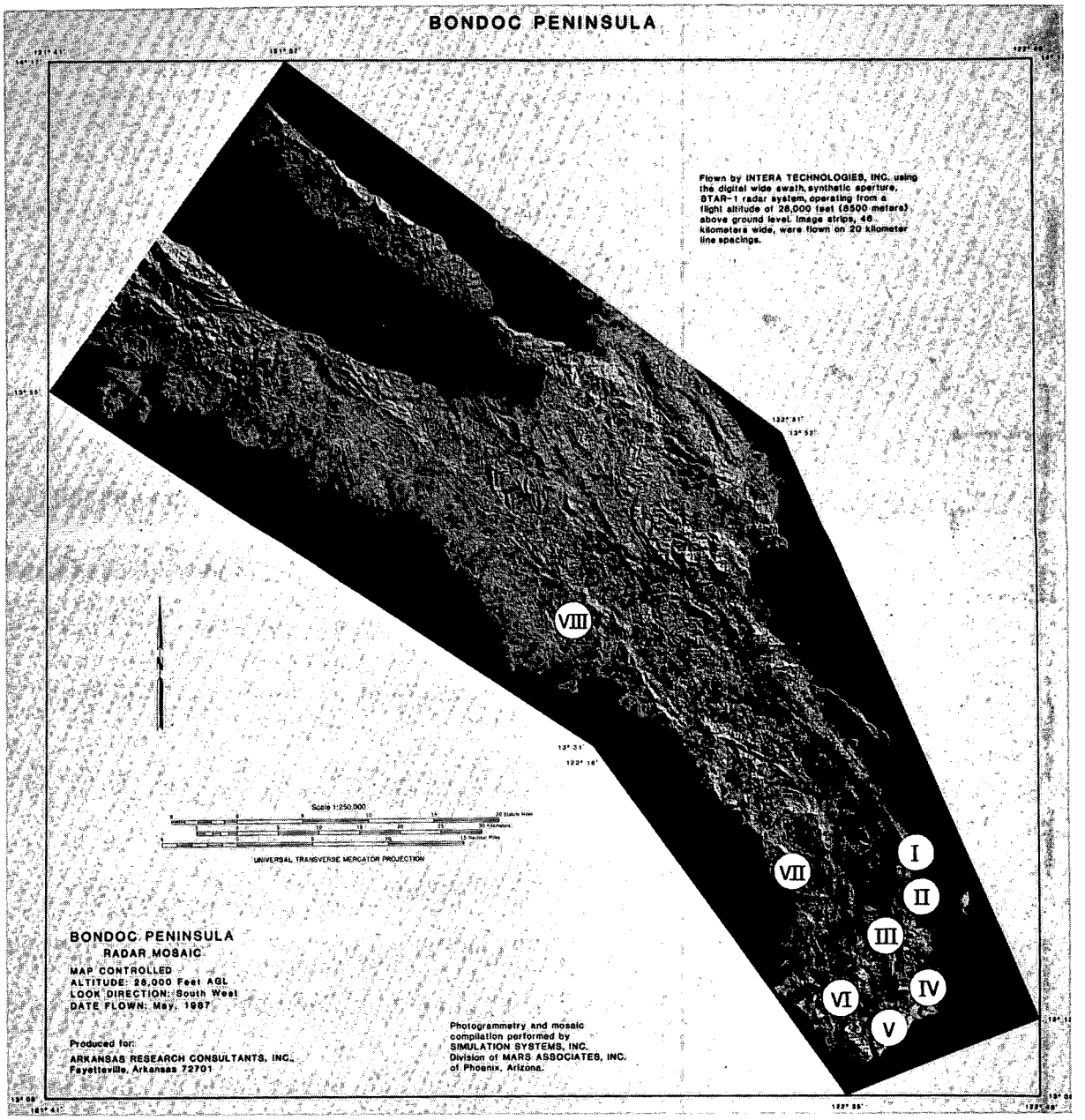

Figure 5.2: Approximate locations of petroleum exploration wells. I is Bondoc 1-7; II is Maglihi 1-5; III is Sapa-1; IV is Amoguis-1; V is Yebaan-1; VI is Pina-1; VII is Aurora 1-2 and San Francisco 1-2; and VIII is Katumbo Creek-1.

5.1.4 Reservoir Characteristics

Early to Middle Miocene age coarse grained sandstones and fossiliferous limestones which may be reefal in part could provide potential reservoir rocks. Middle Miocene sandstones encountered in Katumbo Creek-1 had log-calculated porosities ranging from 12 to 26 percent (BED et al., 1987). In some places, Late Miocene age sandstones and limestones also appear to have good reservoir characteristics. For example, according to Robertson Research International Ltd. (1975), Late Miocene sandstones in three wells in the southern Bondoc Peninsula area (Aurora-1 and -2, and Bondoc -3) exhibited good reservoir properties. Katumbo Creek-1 revealed Late Miocene sandstones with porosities ranging from 18 to 29 percent (Bed, 1987). More specific information on reservoir characteristics and sealing potential has been provided by BED et al. (1987).

5.1.5 Source Rocks

The evaluation of hydrocarbon source potential of Southeast Luzon Basin is based on the total organic carbon (TOC) and pyrolysis analysis results available for both San Francisco-1 and Katumbo Creek-1 wells and a number of field samples (BED et al., 1987). Based on the maturity data, the Recent, Pleistocene, Pliocene, Late Miocene and parts of the Middle Miocene sediments penetrated in this basin are immature for hydrocarbon generation. The Middle Miocene sediments penetrated in Katumbo Creek-1 are early mature, with middle maturity being attained in Early Miocene or older sediments. No significant oil-prone sources have been identified in any of the geochemical studies performed to date. Only thin gas-prone sources of fair to good quality have been recognized in San Francisco-1

well within the 1478-1722 m (4850 to 5650 ft) interval (Middle Miocene). However, these sources are not at sufficient maturity level to generate hydrocarbons.

According to BED et al. (1987), the occurrence of oil and gas shows reported in a number of wells, particularly on the Bondoc Peninsula, indicates the presence of significant hydrocarbon sources. It is assumed that these source rocks may occur in deeper and probably older formations of higher maturity than those penetrated. The kerogen is resin-rich type derived from land plant material. This is quite conceivable as the basin could, on the basis of seismic evidence, contain as much as 8 km of section of which only 2100 m has been penetrated by drilling (BED et al., 1987).

5.2 Interpretive Products

5.2.1 Radar-Geologic Map

The Radar-Geologic Map for the Bondoc Peninsula (which is an enclosure with this report) was developed through the analysis of radar imagery and review of 1985 geological and structural maps of the area provided by BED. The interpretive product contains lithologic boundaries, strikes and dips, faults, folds, and structural form lines.

5.2.1.1 Radar Map Units (Lithology)

The following is a description of the radar appearance of each lithologic unit within the area of interest.

Cretaceous Metamorphic Rocks and Intrusives (Bst)

The basement unit is exposed as a narrow strip along the western coast of Lopez Bay between Gumaca and Atimonan. Minor surface occurrences are also located on the eastern edge of Alabat Island. The rocks of this

unit form narrow symmetrical ridges of high relief with sharp continuous crestlines. This geomorphic expression produces parallel curvilinear areas of intermediate to bright radar tones from foreslopes and consequent areas of radar shadow on backslopes. The massive, highly resistant nature of this unit is responsible for the continuous gray tones exhibited across the radar-facing surfaces. Gray tones vary only where scarps produced by faulting are present which cause local areas of highlight and shadow.

Eocene - Oligocene Volcanics (Te-To)

The Unisan Volcanics occupy a small area in northern Bondoc Peninsula west of Lopez Bay and appear on radar imagery as featureless smooth-textured platforms. Gray tones are medium dark and continuous except for local areas where rougher pitted surfaces create small groups of subrounded light and dark tones. Faults in the area show significant displacement and cause abrupt tonal contrasts.

Oligocene - Early Miocene Limestone (To-Tme)

The Panaon Formation is exposed over a considerable portion of Alabat Island where cliff-forming ridges to the east yield high intensity radar returns. Moving westward, the formation produces highly variable gray tones which alternate from light to dark and are indicative of a highly weathered rough surface. Incident radar energy is strongly reflected from the edges of flatirons which have formed in great numbers on moderately sloped surfaces. This unit is sometimes difficult to distinguish from surrounding rock units that have responded to weathering in a similar fashion. Near Panaon, this unit is recognized by bright tones from a small area of subtle discontinuous ridges.

Middle Miocene Clastics (Tmm)

The Vigo Formation, a thick Middle Miocene shale and sandstone sequence, forms the interior surface of the Bondoc Peninsula from the south coast of Lopez Bay to N 13° 28'. The formation is also widely exposed in the northwest part of the peninsula west of Lopez Bay. This unit is easily recognized on radar imagery by an assemblage of terrain features which appear to have no preferred orientation. Ridges that are oriented perpendicular to the radar look direction are responsible for the brightest returns in the area. Radar shadow on backslopes is common in that many ridges are from moderate to high relief. The remainder of the area is characterized by continuous intermediate to dark tones which form a smooth texture. Local slopes control erosional characteristics and form the regional network of ridges and depressions.

Late Miocene Clastics (Tml)

This unit occurs as a small outcrop located in northeastern Bondoc Peninsula between Caua and Capuluan. This unit is rather featureless and is poorly distinguished from surrounding radar map units. Consequently, the interpreters had to rely solely on geologic map data to define radar map unit boundaries.

Late Miocene - Pliocene Clastics (Tml-Tp)

Surface exposures of the Upper Canguinsa Formation are widespread throughout the Bondoc Peninsula. In the southern tip of the peninsula this unit is difficult to distinguish from surrounding radar map units due to a high degree of variability in local gray tones. Severe faulting has created highly complex stratigraphic and morphological relationships. From the central to the northern part of the peninsula, the Upper Canguinsa appears as a thinly bedded unit which forms ridges that trend parallel

to the orientation of the peninsula. The linear bright tones produced by the ridges can be easily traced for many kilometers even though faulting has caused numerous discontinuities.

Pliocene Clastics (Tp)

The Hondagua Formation has limited surface exposure in the Bondoc Peninsula. On the radar imagery this unit appears as a flat-lying featureless surface with a smooth texture of intermediate to dark tones. Brighter tones are produced from small isolated areas of subtle relief.

Pliocene - Pleistocene Clastics (Tp–Qp)

The radar appearance of the Vinas Formation is one of consistent intermediate to bright tones, and is indicative of a moderately rough surface. This unit lacks any other distinguishing characteristics and consequently, the interpreters relied heavily on geologic map data to define radar map unit boundaries.

Pleistocene Limestone (Qp)

The Malumbang Formation appears in the southcentral portion and along both coasts of the Bondoc Peninsula. In the east, this unit takes the form of a symmetrical ridge with eastward dipping flatirons on the eastern flank. In its southcentral location, the unit forms the crestal part of a major anticline. Here the unit has been fractured by east-west trending faults, and near vertical scarps are responsible for high intensity radar returns. In the west, the unit trends parallel to the coast and extends nearly the entire length of the study area. The cliff-forming, east-northeast facing edge of the unit is easily discerned by radar returns of higher intensity. In all locations, the surface generally exhibits a rough

texture. Tones vary from medium dark to bright as incident radar energy is strongly reflected from the edges of small subrounded features that form the karst topographic surface of this limestone unit.

Quaternary Alluvium (Qal)

Alluvial deposits are easily recognized on radar imagery by their flat featureless appearance. Intermediate to dark gray tones form areas which exhibit a uniform smooth texture. In marshy areas or along river channels, this characteristic appearance may be disturbed by scattered patches of extremely dark tones caused by pools of water. Inland, these deposits fill depressions between surrounding areas of topographic relief.

5.2.1.2 Structure

The structural style consists for the most part of long, narrow, northwest-trending folds with axial orientations parallel to the long dimension of the peninsula. Faulting is prevalent through the entire study area. Major faults generally trend parallel to the coastlines of the peninsula. Both northwest- and northeast-trending faults traverse the major longitudinal faults except in southern Bondoc, where the faults become more west-trending.

The east-central part of the Bondoc Peninsula is characterized by broad northwest-trending folds. Several major faults which trend nearly parallel to these folds may be part of the Philippines Fault System. According to published reports (BED et al., 1987; and Robertson Research International Ltd., 1975), the northwest-trending Philippines Fault System runs the length of the southeastern Luzon region, including east-central Bondoc. Major

northeast-trending, strike-slip faults that have been inferred from the radar imagery transect fold axes and may be second order wrench faults also associated with the Philippines Fault System.

In southern Bondoc, the structure is dominated by major faults which, due to significant topographic displacement, are easily recognized on radar imagery. Abrupt morphological and image texture changes form continuous linear to curvilinear features which represent the surface expression of faults. Intersecting faults have created chaotic structural and stratigraphic relationships in this region. In the upper northwest Bondoc region, vertical displacement along major northeast-trending faults has exposed Cretaceous basement rocks over much of the area. The most conspicuous structural features on the radar imagery are fault blocks of basement rock which are clearly defined by parallel northeast-trending fault pairs.

5.2.2 Radar-Lineament Map

Lineaments in the Bondoc Peninsula study area have four general orientations. One group is oriented parallel to the long dimensions of the peninsula. These lineaments probably reflect fractures which are related to the major longitudinal faults. Two other groups of lineaments trend 1) northeast at angles 30°-45° east of north, and 2) northwest at angles 30°-45° west of north. The orientation of these lineaments corresponds with the orientation of the faults that traverse the major longitudinal faults of the Bondoc Peninsula. Other west-trending lineaments are scattered throughout the study area. A high concentration of lineaments with this orientation is located between N13°45" and N13°50", which may be associated with a zone of structural weakness.

5.3 Prospect Evaluation

Prospect evaluation evolved from 1) radar imagery analysis used in conjunction with corroborative data from sources previously discussed, 2) subdividing the area of radar coverage into different geologic terrain categories, and 3) defining prospects based on specific selection criteria. The Bondoc study area was subdivided into four geologic terrain categories which have been designated by Roman numerals (Fig. 5.3). The values of the numerals have no prioritization significance, but are provided to aid discussing the significant geologic aspects of the Bondoc Peninsula. The letters (A-G) indicate the approximate location of prospects with potential hydrocarbon accumulation and entrapment.

5.3.1 Geologic Terrain Category Criteria

AREA I

* Younger stratigraphic units appear at the surface indicating the possibility for a relatively thick sedimentary subsurface section.

* Contains several structural features that may provide potential sites for hydrocarbon accumulation.

AREA II

* Surface exposure of Middle Miocene strata and older stratigraphic units indicating a relatively thin sedimentary section.

* Poor seismic data because of shale diapirism.

AREA III

* Surface lithologies north of 13°52'N are predominantly volcanics, volcanic sediments, metamorphics and intrusives.

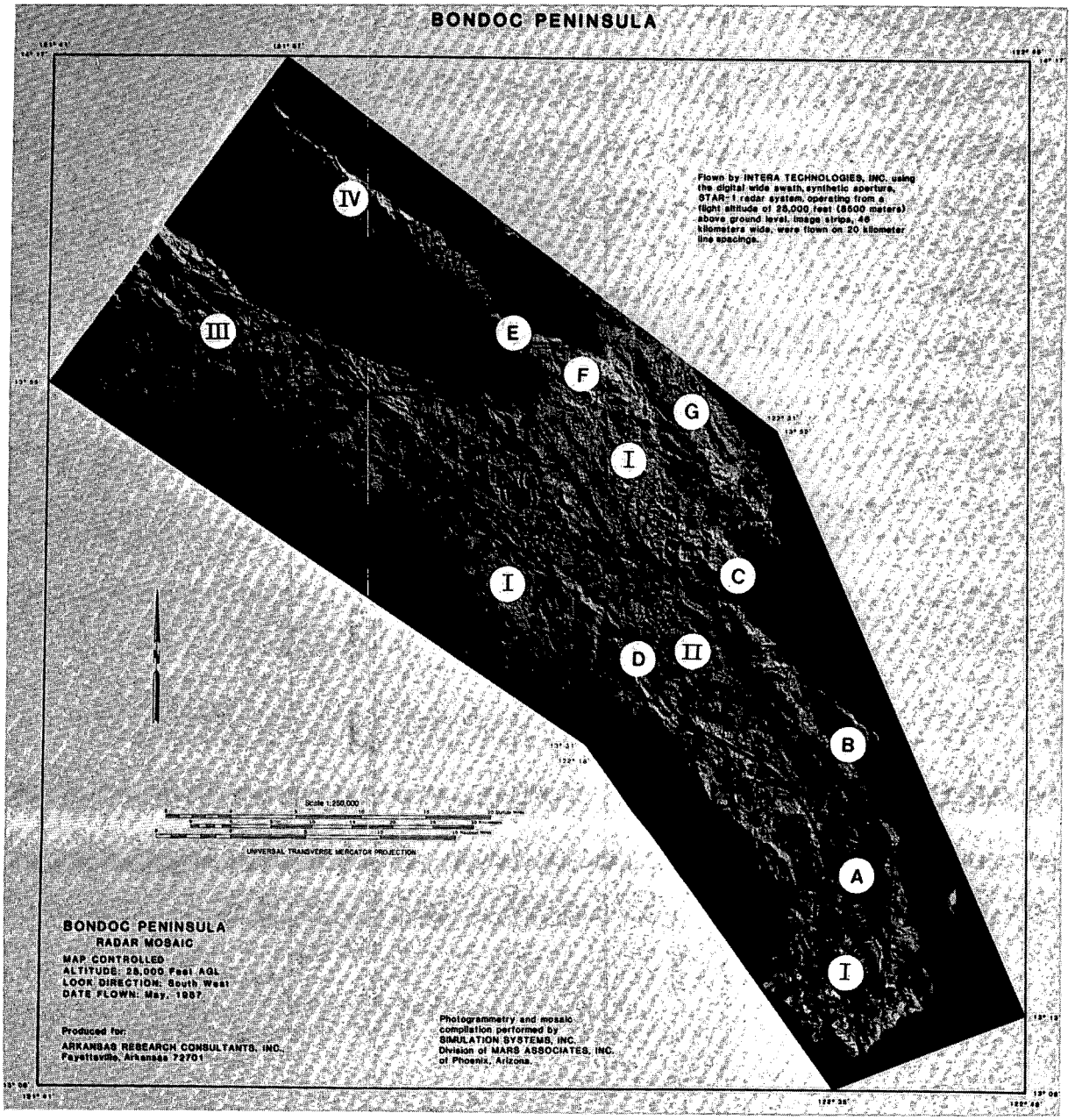

Figure 5.3: Terrain categories (I–IV) and prospects (A–G).

AREA IV

* The youngest rocks occurring at the surface are of Late Miocene age with rocks of Oligocene-Early Miocene and older exposed over the remainder of the area indicating a lack of suitable subsurface sedimentary section.

* No structural features considered to be potential prospects for hydrocarbon accumulation.

5.3.2 Prospects and Selection Criteria

Based on negative criteria, areas (III and IV) have been excluded as potential sites for hydrocarbon accumulation. Area II may become more favorable with additional seismic data. Area I is considered to have the most potential for hydrocarbon exploration. The following is a list of prospects and the selection criteria for each potential site.

Prospect A Anticlinal Crest (13°22'45"N, 122°36'00"E)

* Prospect is located within the southern part of the Bondoc Graben trend which should provide a relatively thick sequence of potential reservoir rocks.

* Numerous secondary structures (faults) located down dip from crest; potential for additional entrapment features and/or fracture porosity.

* Anticline is regionally expressed, extending over 14 miles (22.4 km) in length.

* Prospect is located between two areas which have demonstrated the presence of hydrocarbons.

* Structure is well expressed on radar imagery.

* Collapse feature located near anticlinal crest presents possible loss of near-surface closure.

Prospect B Anticlinal Crest (13°31'30"N, 122°34'00"E)

* Prospect is within proximity to the Bondoc Graben trend and may be located up-dip from potential source rocks.

* Secondary structures (faults) located down dip from crest; potential for entrapment features and/or fracture porosity.

* Anticline is regionally expressed, extending over 6 miles (9.6 km) in length.

* Structure is well expressed on radar imagery.

Prospect C Anticlinal Crest (13°43'20"N, 122°26'40"E)

* Secondary structures (faults) located down dip from crest; potential for entrapment features and/or fracture porosity.

* Structure is large in dimensions.

* Structure is moderately expressed on radar imagery.

* Prospect is on the Alabat-Burias High which may have a relatively thin sedimentary section; however, potential source rocks are located down-dip in a favorable position.

Prospect D Anticlinal Crest (13°36'40"N, 122°20'30"E)

* Prospect is located on the southwestern edge of the Bondoc Graben trend which is up-dip from potential source rocks.

* Subtle expression on radar imagery.

Three anticlinal features (E, F, and G) appear to have relatively large surface dimensions; however, they may not be attractive for hydrocarbon accumulation because of a high geothermal gradient in proximity to the Philippines Fault System. Conversely, there is a distinct possibility that faulting might have upgraded reservoir properties locally through increased secondary (fracture) porosity and permeability. Geothermal gradient and geophysical data are necessary for site evaluation.

Prospect E Anticlinal Crest (13°56'20"N, 122°18'30"E)

* Structure is well expressed on radar imagery.
* Structure is of large dimensions.
* Faults transverse anticlinal axis which could provide additional structural entrapment.
* Prospect is located within the Alabat-Burias High which will have a relatively thin sedimentary section.

Prospect F Anticlinal Crest (13°58'30"N, 122°12'15"E)

* Structure is moderately expressed on radar imagery.

Prospect G Anticlinal Crest (13°50'40"N, 122°25'30"E)

* Structure is well expressed on the radar imagery.
* Secondary structures (faults) located down dip from crest; potential for entrapment features and/or fracture porosity.
* Faults transverse anticlinal axis which could provide additional structural entrapment.
* Prospect is located along the Ragay Gulf Graben which should have a relatively thick sedimentary section.

5.4 Estimated Hydrocarbon Resources

The 13 sedimentary basins of the Philippines have been categorized into 6 classes based on relative oil and/or gas potential or prospectivity (BED et al., 1987). According to BED, the Southeast Luzon Basin which includes the Bondoc Peninsula is ranked as Class II, having good potential for both oil and gas. Average field size should range from 5-50 MMBBLS of oil, or 50-500 BCF of gas.

5.5 Recommendations

With sufficient seismic coverage, anticlinal fold structures whose subsurface axial positions may have been displaced by wrench or thrust faulting can usually be accurately delineated. In order to refine the prospects obtained from interpretation of the radar data, it is therefore recommended that:

* geophysical data be acquired and interpreted to confirm subsurface closure of prospects,

* the approximate thickness of the subsurface sedimentary section be inferred from the seismic data.

This page is intentionally left blank.

6 RADAR–GEOLOGIC INTERPRETATION – COTABATO BASIN, MINDANAO

The Cotabato Basin covers approximately 10,000 km^2 in southern Mindanao. For purposes of flight line planning and to include the adjacent Mt. Apo geothermal site, the Mindanao radar mosaic includes approximately 20,000 km^2 of land/water coverage (refer to the Mindanao Radar Mosaic which is an enclosure with this report).

6.1 Background and Petroleum Exploration Activities

6.1.1 Structure

Two geologic maps (scale 1:500,000) which were provided by the BED were used to familiarize radar image interpreters with the regional geologic framework; Geologic Map Agusan - Davao Basin and Cotabato Basin (1985), and Structural Framework Map of the Cotabato Basin (1985). The Cotabato Basin is a northwest-southeast oriented trough containing a sequence of sediments approaching approximately 14,000 feet (4,268 m) in thickness which range in age from Late Oligocene to Pleistocene. The basin boundaries include: the fault controlled basement rocks of the Tiruray Uplands and Southwest Coastal Range, on the west and southwest, respectively; the Cotabato Highlands on the north, the Central Cordillera on the east, and the Sarangani Peninsula on the southeast. According to the geologic maps previously mentioned, fold structures trend parallel to the basin axis in the south, whereas in the north folds are oriented nearly north-trending.

6.1.2 Stratigraphy

The Cotabato Basin on the island of Mindanao is a northwest-southeast area of deposition containing Pre-Oligocene to Pleistocene stratigraphic units which total an approximate thickness of 28,000 feet (8,537 m). The stratigraphy of the Cotabato Basin has been described by BED et al. (1987), the Philippines Bureau of Mines and Geo-Sciences (1981), the Philippines Mineral Fuels Division (1976), and Robertson Research International Ltd. (1975). The following stratigraphic discussion is a synthesis of these reports, but includes only those stratigraphic units that have been mapped on the Radar-Geologic Interpretation of the Cotabato Basin, Mindanao which accompanies this report. Stratigraphic units were selected from the 1985 Geological Map of the Agusan-Davao Basin and Cotabato Basin prepared by BED.

Pre-Oligocene

The basement complex of the Cotabato Basin is composed of a variety of metamorphic, volcanic, and intrusive rocks. Porphyritic andesite, basalt, agglomerate, schists, and metasediments are predominant. In local occurrences, quartzites, slates, and marbles have been intruded by peridotites, gabbros, and diorites. Sedimentary rocks affected by low grade metamorphism include argillaceous sandstones, siltstones, and calcareous siltstones. Porphyritic, finely crystalline rocks are present throughout the sedimentary sequence.

Late Oligocene

The Late Oligocene Maganoy Formation unconformably overlies the basement complex and represents the oldest exposed Tertiary sedimentary unit in the study area. The sequence is principally of marine origin and

measures at least 1,500 feet (460 m). Fossiliferous, well bedded marine limestones are the dominate rock type with orbitoidal, conglomeratic sandstones and volcanic conglomerates present as interbeds. Gray or green shale and occasional coal seams occur in the upper part of the formation.

Oligocene-Early Miocene

This lithologic unit consists of undifferentiated Oligocene-Early Miocene clastic rocks.

Early-Middle Miocene

This lithologic unit consists of undifferentiated Early-Middle Miocene clastic rocks.

Middle Miocene

The Middle Miocene Patut Formation is separated from older stratigraphic units by an argillaceous sandstone and conglomerate sequence belonging to the Nakal Formation. The Nakal Formation, which has not been defined as part of the Radar-Geologic Interpretation, is of Early Miocene age.

The Patut Formation exhibits several facies changes in the Cotabato Basin which indicate variable depositional environments existed during Middle Miocene time. In the northwest, the formation is composed primarily of deep water volcanoclastics, occasional lava flows, and minor intercalations of calcarenites. To the east, in the vicinity of the Kitubod Range, there is a facies change to deep water dark indurated shales which contain no volcanic constituents.

Well data from the central region of the Cotabato Basin indicate a more shallow water environment of deposition during the Middle Miocene consisting of an upper bathyal to outer neritic sequence of mudstone, minor sandstone, and limestone with a basal conglomerate. Outer neritic to lagoonal-shelf

shale, siltstone, and sandstone with minor coals seams of Middle Miocene age have also been identified from cuttings analysis. Sandstones in central Cotabato Basin tend to be medium grained and well bedded. The clastic constituents in this area are usually calcareous, silty or sandy, and tuffaceous. A light colored reefal limestone can also occur at the base of the formation. The Patut Formation varies in thickness from a maximum of 3,770 feet (1,150 m) in the north to 2,950 feet (900 m) in the south.

Middle-Late Miocene

This lithologic unit consists of undifferentiated Middle-Late Miocene clastic rocks.

Late Miocene

The Late Miocene Dinganen Formation is a thick marine sequence consisting of mudstone, claystone, sandstone, siltstone, and conglomerate. In the north, the section is primarily mudstone and claystone and measures 6,560 feet (2,000 m). The section appears to thin towards the south and becomes increasingly non-marine. Southward, the sandstone components become conglomeratic and boulder conglomerates are frequent interbeds in mudstone and siltstone.

Late Miocene-Pliocene

The accumulation of sediments in the Cotabato Basin was continuous through Late Miocene-Pliocene time when the Nicaan Formation was deposited. The lower part of the formation is composed of shallow marine clastic rocks including dark, thin-bedded, tuffaceous sandstone, siltstone, and thin to massive pebble conglomerate. Agglomerates and intercalations of marl and impure limestone are also present in the lower part of the Nicaan Formation. The clastic constituents tend to be coarser toward the top of the formation and vary from conglomeratic, cross-bedded sandstone to marine mudstone

and siltstone. The Nicaan Formation reaches a thickness of 3,900 feet (1,190 m) at its type locality in the north along the Nicaan River. The average thickness for the rest of the study area varies from 960 feet (290 m) to 1,640 feet (500 m).

Pliocene

An unconformity separates Pliocene strata of the Marbel Formation from the underlying Nicaan Formation. The Marbel Formation can be divided into two distinct lithologic facies. The Awang-Table Limestone is stratigraphically lower than the San Mateo Clastics and is described as a light colored, porous, lenticular biohermal limestone with interbedded marl. The San Mateo Clastics often intertongues with the Awang-Table Limestone and is composed of tuffaceous and calcareous mudstone, shale, and sandstone with interbedded marl, limestone, and pebble conglomerate. The total thickness of the Marbel Formation is uncertain, but is estimated between 1,300 feet (400 m) and 1,600 feet (490 m).

Pliocene-Pleistocene

Pliocene-Pleistocene lithologic units in the Cotabato Basin are generally poorly consolidated accumulations of clastic and pyroclastic rocks, volcanic flows, and limestone.

Unconformably overlying the Pliocene Marbel Formation is a thin clastic unit of poorly consolidated fluviatile to shallow lacustrine, ferruginous sandstone and calcareous siltstones with occurrences of tuffaceous sandstone and pebble conglomerate. In some areas, the Pliocene-Pleistocene section consists of soft white chalky coralline limestone.

The Carmen Formation, which covers the slopes of Mount Apo, Mount Parker, and Mount Matutum, is also dated as Pliocene-Pleistocene age and consists predominantly of pyroclastic rocks and volcanic flows with

interbedded clastic material composed largely of detritus from volcanic rocks. The formation contains interbeds of fine- to coarse-grained, poorly consolidated tuffaceous sandstone and clay. Channel deposits of the Carmen Formation are poorly consolidated conglomerates and agglomerates that radiate from volcanic centers.

Pleistocene

The final cycle of marine deposition in the Cotabato Basin is represented by thin accumulations of the Omanay Marl. The formation, with a maximum thickness of only 115 feet (35 m), interfingers with or is conformable over the Carmen Formation. The Omanay Marl is a soft, greenish to cream colored marl and contains perfectly preserved oyster beds and abundant foraminifera. Well developed coralline reefal limestones interbedded with marine mudstones and sandstones have also been included in the Pleistocene stratigraphy.

Quaternary

Quaternary sedimentation in the Cotabato Basin consists of volcanic and alluvial deposits. Lavas, pyroclastics, and poorly consolidated agglomeratic and conglomeratic clastic sediments occur around volcanic centers. Quaternary alluvium consists of unconsolidated stream and valley gravels, low level terrace deposits along present rivers, natural levees, unconsolidated swamp muds, and flood plain sediments.

6.1.3 Hydrocarbon Occurrences and Exploration Activity

According to BED et al. (1987), three oil seeps were reported in the basin. The Kirusoy and Matinaw oil seeps are located in the northernmost part of the basin while the Tiboli oil seep is situated in the southern

portion of the main Cotabato Basin. The Kirusoy oil seep was sampled by PNOC-EC and the Tiboli oil seep was also verified, whereas the Matinaw oil seep is still unconfirmed. The Kirusoy oil seep emanates along a fault plane in overlying fractured basalt of probable Middle Miocene age. The oil reportedly flows at a rate of about one barrel per day and has an API gravity of 23.8°. Recent geochemical analyses indicate that the seep is a biodegraded, originally high gravity (light) oil generated by a probable non-marine algal source at a late maturation stage. Table 6.1 provides pertinent information for the exploratory wells drilled in the Cotabato Basin, and Figure 6.1 shows the approximate locations of these wells.

6.1.4 Reservoir Characteristics

The Cotabato Basin contains a sedimentary section ranging in age from Late Oligocene to Pleistocene. The sequence varies in thickness from 8,300-14,000 feet (2,530-4,268 m). Late Oligocene and Early-Middle Miocene age sandstones are believed to be potential reservoir rocks. Robertson Research International Ltd. (1975) reports that the Roxas-1 well (Table 6.1) encountered porous sandstones and limestones of Early-Middle Miocene age. The Middle Miocene is marked by two distinct facies; a nearshore marine and continental sequence in the northern Cotabato Basin, and an offshore marine sequence to the south. The northern facies is composed of conglomerates, thick bedded graywacke sandstones and a few interbeds of carbonaceous mudstones. The southern facies includes a basal reefal limestone with interbedded siltstone and mudstone. The Late Miocene and Early Pliocene sequence is characterized by marine deposits in the lower sections, becoming non-marine towards the top Late Pliocene to Pleistocene strata. This stratagraphic section includes biohermal limestones, sandstones and conglomerates.

Table 6.1: Exploratory wells and hydrocarbon occurrences – Cotabato Basin, Mindanao. (Modified from BED et al., 1987)

Well Name	Drilling Date	Total Depth m (ft)	Play Type	Defined by	Target	Age of Rock at T.D.	Results	Remarks
Dulawan-1 (Bureau of Public Works)	1916	548.78 (1800)	Drilled as a water well				Dry well	Oil & gas salt water ss at 243.9, 426.8, & 548.8 m
Gansing-1 (MAREMCO - ANGLO)	Jun. 24, 1962	1044.5 (3426)	Anticline	Surf. & seismic mapping	E/M Miocene carb. Late Miocene ss beds	Early Pliocene	Dry well	DST 1 int. 968.3 - 984.8 m Rec: gas & water mud trace Cl: 9,800 ppm. Not a valid test.
Gansing-2 / 2A (MAREMCO - ANGLO)	Sept. 28, 1962	1204.9 (3952)	Anticline	Surf. & Seismic mapping	E/M Miocene carb. Late Miocene ss beds	Pliocene / Pleistocene	Dry well	Gas & water under pressure at 1070.1 m Cl: 18,000 ppm. Not a valid test.
Bambad-1 (MAREMCO - ANGLO)	Dec. 31, 1962	1963.4 (6440)	Unconformity	Seismic	Middle Miocene carb. and ss	Middle Miocene	Dry well	No shows. Not a valid test, target deeper than final T.D.
Tabina-1 (ANGLO)		459.8 (1508)					Dry well	No show
Pedtobo-1 (MAREMCO - ANGLO)	Nov. 14, 1971	1554.9 (5100)				Basement(?)	Dry well	Valid test; missing M/L Miocene sect.
Roxas-1 (SOUTH SEAS OIL)	Sept. 6, 1971	1616.8 (5303)	Anticline	Surf. & seismic mapping		Middle Miocene	Dry well	Tr live oil 1585.4 - 1586.9 m dull brown fluor. (?) M Miocene shale.
Lagao-1 (FIL - AM)	Sept. 27, 1971	1114.9 (3657)	Anticline	Surf. & seismic mapping	E/M Miocene carb. Late Miocene ss beds	Pliocene	Dry well	No sed. older than Pliocene. P & A drilling diff. Not a valid test.
Roxas-2 (SOUTH SEAS OIL)	Jan. 15, 1972	2568.6 (8425)	Anticline	Surf. & seismic mapping		Early Miocene	Dry well	Semi - live oil at 1894.8 m (?) Early - Miocene ss.
Roxas-3 (SOUTH SEAS OIL)	Sept. 5, 1972	2364.3 (7755)	Carbonate build-up	Well data of Roxas-1 and Roxas-2	Middle Miocene reefal carbonates	Early Miocene	Dry well	? dead oil 1402.4 - 1722.6 m. Tr live oil 2100 m - T.D. Thin carb. lenses; non-reefal.

MAREMCO - Maremco Mineral Corporation
ANGLO - Anglo Philippines Oil Corporation
SESMAR - South-East Sierra Madre Resources
FIL-AM - Fil-Am Resources
SOUTH SEAS OIL - Cotabato Basin South Seas Oil

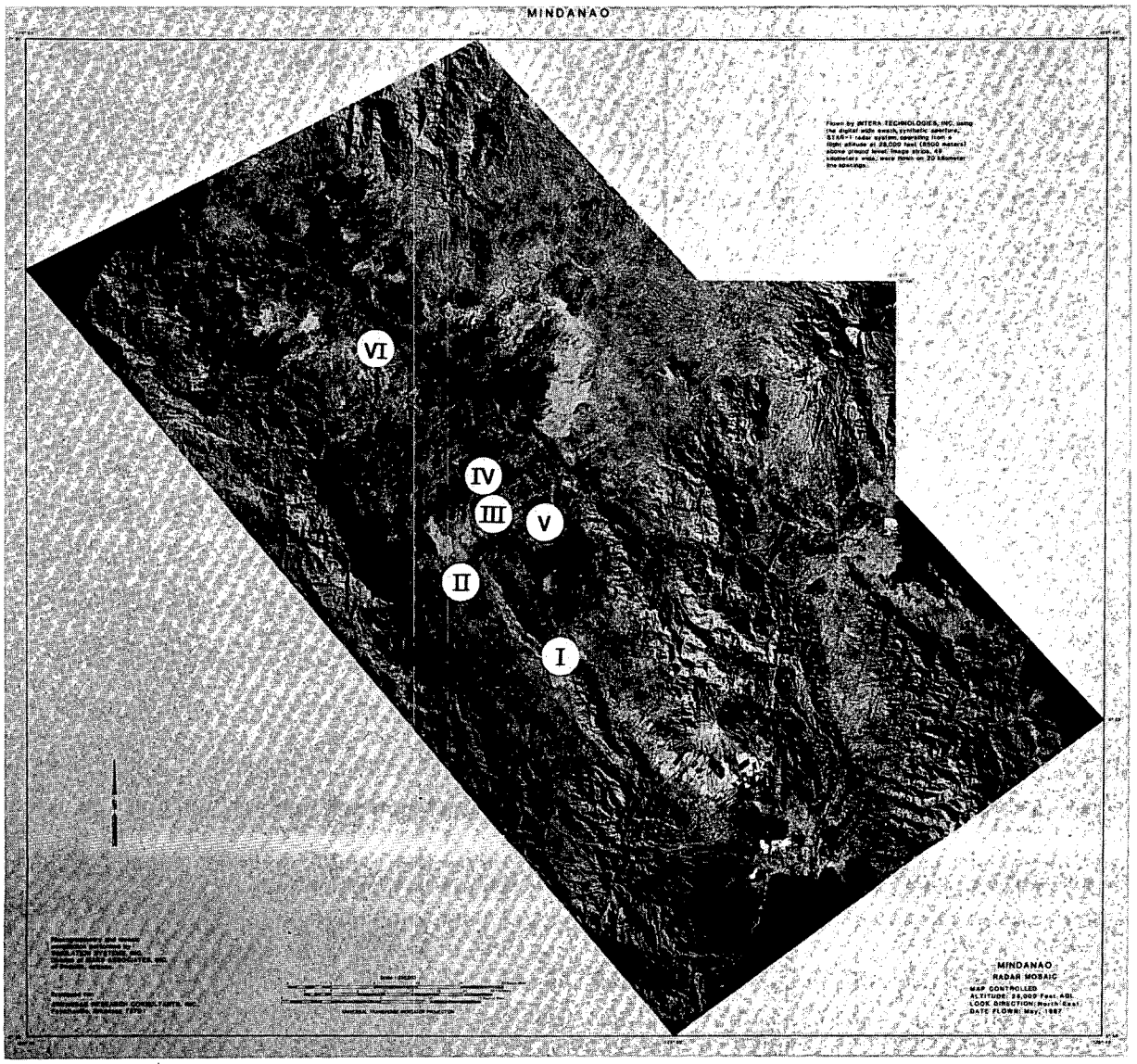

Figure 6.1: Approximate location of petroleum exploration wells. I is Roxas 1-3; II is Bambad-1; III is Gansing 1-2; IV is Lagao-1; V is Pedtobo-1; and VI is Dulawan-1.

Evaluation of reservoir character and properties in the Cotabato Basin is based mainly on lithologic log-reports and outcrop description because of the lack of mechanical logs or petrographic analyses (BED et al., 1987). Nonetheless, reservoir quality rocks can be expected in strata ranging in age from Oligocene to Late Miocene.

6.1.5 Source Rocks

Hydrocarbon source potential of the Cotabato Basin has been evaluated using geochemical analyses of Early Miocene to Pleistocene sediments from the Bambad-1 well (BED et al., 1987). Early Miocene shales are the most likely candidates for potential source rocks and are ranked as middle mature. According to Robertson Research International Ltd. (1975), mature sediments extend downward from depths of approximately 3,000 feet (915 m). In Bambad-1, younger rocks are organically lean, especially the Pleistocene shales. However, the lateral equivalents of these shales in the deepest part of the basin, if mature enough, may provide fair quantities of gas (BED et al., 1987).

6.2 Interpretive Products

6.2.1 Radar-Geologic Map

The Radar-Geologic Map for the Cotabato Basin, Mindanao was developed through the analysis of radar imagery and review of 1985 geological and structural maps of the area provided by BED. The interpretive product contains lithologic boundaries, strike and dip, faults, folds, structural form lines, and geomorphic anomalies.

6.2.1.1 Radar Map Units (Lithology)

The following is a description of the radar appearance of each lithologic unit within the area of interest.

Pre-Oligocene Basement Complex (Bst)

The basement rocks of the Cotabato Basin are extensively exposed in the Daguma Range along the western border of the study area. Other large outcrops are in the southcentral region where in one location, basement rocks form an anticlinal core in the Alip Mountains. This radar map unit occurs as topographic highs that obstruct radar energy from backslope areas and cause large areas of radar shadow. Where the basement forms the cores of anticlines, continuously pointed, symmetrical crestlines separate bright foreslopes from dark radar-shadowed backslopes. The resistant basement unit can be easily distinguished from the adjacent, less resistant sedimentary radar map units.

Late Oligocene Clastics (Tol)

The Maganoy Formation occurs in a limited area in the Kitubod Range located in the northeast corner of the study area. The map unit has been severely faulted and eroded, and any stratigraphic characteristics that may have existed have been replaced by ridges and steep-walled ravines. Ridges and ravine walls oriented more perpendicular to the radar look direction produce the strongest radar returns.

Oligocene-Early Miocene Clastics (Tol-Tme)

The Quezon Mountain Range in southcentral Cotabato Basin is composed primarily of Oligocene-Early Miocene clastic rocks. On radar imagery this unit appears extremely rugged. Uplift, faulting, and erosion has produced a heavily dissected and blocky terrain. Brightest radar tones are produced

from fault scarps and angular ridges that face the incident radar energy. A series of regularly spaced west-trending fault blocks can be easily identified in the central portion of this unit.

Early-Middle Miocene Clastics (Tme-Tmm)

Located in the northwestern corner of the study area, this clastic unit appears on radar imagery as large slabs of gently northeast dipping strata. The surface appears smooth (medium-dark tones) except where poorly consolidated sediments have produced bright image tones. Linear areas of highlight are produced by regularly spaced fault scarps. In certain areas, the boundaries of this radar map unit were difficult to locate and consequently, the interpreters used geologic map data to define unit boundaries.

Middle Miocene Clastics (Tmm)

Middle Miocene clastic rocks are extensively exposed in southeastern Cotabato Basin in the Tangbulan Range and the Kioto Mountains. These rocks also form the core of an anticline in the northern part of the Roxas Range.

In the southeast, this map unit appears on radar imagery as a strongly dissected, high relief, clastic terrain with angular ridges and peaks. These rugged terrain features are distinguished by high intensity radar returns on foreslopes and prominent radar shadow in backslope areas. Stratification is recognizable only in localized areas. The Tmm map unit is easily distinguished from the surrounding less consolidated and low lying radar map units.

As an anticlinal core, this unit displays a prismatic geomorphic appearance which is caused by a pointed symmetrical crest. The crestline is continuous except where it has been displaced by faulting. Brightest

image tones are from fault scarps and crests oriented more perpendicular to the radar look direction. Edges of flatirons that occur on slopes also produce bright tones on the imagery.

Late-Middle Mioene Clastics (Tmm-Tml)

The unit occurs only in a small area in the Roxas Range on the flanks of an anticline. Because of the indistinct radar appearance of this unit, interpreters were forced to rely largely on geologic map data to define unit boundaries.

Late Miocene Clastics (Tml)

Late Miocene clastic rocks occur throughout the Cotabato Basin and exhibit several distinct landforms. In the largest exposure, located in the northcentral region, this unit appears as a broad north-trending area which has been severely dissected by numerous small drainage channels. Consequently, the surface has a uniform rough texture because radar energy reflected from closely spaced channel banks and local fault scarps result in bright tones on the imagery. The topography is of low to moderate relief and consequently, radar shadow is minimal. The escarpments formed by gently dipping clastic strata produce linear bright tones on the imagery. Vertical bedding in the northeastern portion of this area is readily identified on the imagery as a distinct series of parallel highlights and shadows. The Tml map unit in this area is easily distinguished from surrounding map units by abrupt changes in tone, texture, and landform.

In the Roxas Range, the Tml map unit appears as moderately dipping truncated strata on the flanks of anticlines. Again, this unit has been severely affected by drainage channel erosion. Flatirons and fault scarps are common on sloping surfaces. This map unit is easily identified by an apparent change in terrain slope and image texture.

At a third location in southwestern Cotabato Basin, the Tml map unit forms a moderately rugged terrain where angular ridges cause significant areas of highlight and shadow.

Late Miocene–Pliocene Clastics (Tml-Tp)

The Tml-Tp radar map unit occurs mainly in the southeastern region of the study area on the flanks of the Alip, Tangbulan, and Kioto Mountains. Along the Alip Mountain Range these rocks appear as thin, well-bedded, moderately dipping strata. Stratification is evident along the entire length of the north-trending exposure of this map unit.

Along the Tangbulan and Kioto Mountains, the Tml-Tp map unit is poorly distinguished from the adjacent Middle Miocene map unit (Tmm). In both cases, the clastic rocks produce a similar rugged terrain appearance on the radar imagery. Consequently, the interpreters relied largely on geologic map data to define radar map unit boundaries.

Pliocene Limestone Tp(L) and Clastics Tp(C)

The limestone facies of the Pliocene map unit occurs on a northwest-trending, narrow anticline in the northcentral region of the study area. The surface is characterized by intermediate to dark tones except where bright tones are produced by stratification, escarpments, and channel banks. Flatirons surround the structure and are responsible for V-shaped bright tones on the imagery.

The clastic facies of the Pliocene map unit is scattered throughout southcentral Cotabato Basin. This unit has been eroded to small angular ridges and peaks. Stratification cannot be inferred from imagery interpretation.

Pliocene-Pleistocene Limestone Tp-Qp(L) and Clastics Tp-Qp(C)

In northern exposures, the Pliocene-Pleistocene limestone facies appears as broad platforms which have been severely faulted. Groups of parallel trending fault scarps produce linear bright tones on the imagery. The karst topography of this unit is readily identified by a distinctive pitted surface that produces subround small scale areas of radar highlight and shadow. A high degree of stream erosion adds to the overall surface roughness of this map unit.

On the eastern flank of the Alip Mountains, the east dipping surface of the Tp-Qp(L) map unit has been reduced to groups of small scale flatirons. Edges of flatirons that are more perpendicular to the radar look direction cause higher intensity radar returns and consequent bright tones on the imagery. The large number of these features gives this unit an extremely rough appearance.

The Pliocene-Pleistocene clastic facies occurs largely as an elongated north-trending unit on the western flank of the Kioto Mountains. On radar imagery, this map unit appears as a poorly consolidated clastic section which has been strongly dissected by multidirectional stream channels. Erosion has destroyed stratification characteristics that may have existed.

Pliocene-Pliestocene (Tpv-Qpv)

The Pliocene-Pleistocene Tpv-Qpv map unit is located in the vicinity of volcanos or radiates from volcanic centers. This unit is characterized by loosely consolidated pyroclastics which have been deeply incised by drainage channels. Bright linear and curvilinear image tones identify channel banks that face incident radar energy. Drainage density is very high and consequently, laterally continuous surfaces are rare. Small surface areas between drainage channels appear smooth and featureless.

Pleistocene Clastics (Qp)

Pleistocene clastic rocks occur only as the outer most rock unit surrounding the Roxas Range anticlines. The unit possesses a rather subtle image appearance. The distinguishing characteristics used to map this unit were slope changes and a greater surface roughness than surrounding map units. Bright curvilinear image tones produced by stratigraphic escarpments mark the updip truncation of this unit round the anticlinal flanks.

Quaternary Volcanics (Qv)

The Qv map unit occurs as conical-shaped landform deposits of volcanic rocks which radiate from volcanic craters. This unit is somewhat similar in appearance to the Tpv-Qpv map unit except drainage density is less, and the surface materials are significantly more consolidated.

Quaternary Alluvium (Qal)

Alluvial deposits are easily recognized on radar imagery by their flat featureless appearance as well as intermediate to dark gray tones which exhibit a uniform smooth texture. In marshy areas, this characteristic appearance may be disturbed by patches of extremely dark tones caused by pools of water. Vegetation along rivers and streams often causes volume scattering of radar energy which produces sinuous areas of extremely bright image tones.

6.2.1.2 Structure

The Cotabato Basin is characterized by broad areas of topographic relief separated by synclinal basins and plains containing younger sediments. Two major structural provinces, a southcentral province and a northeastern province, display contrasting structural styles.

In the southcentral province, a series of parallel, evenly spaced, symmetrical anticlines are separated by wide synclinal basins. These folds strike parallel to the northwest-trending basin axis. The topographic expression of these structures form the Roxas, Quezon, and Alip mountain ranges. The geologic age of the rock units exposed in the cores of these anticlines becomes increasingly older from west to east.

In the northeastern province, numerous closely spaced folds trend approximately north-south. Rock units exposed in the anticlinal cores range in age from Late Miocene to Pre-Oligocene. Recent uplift in this area has resulted in deflection of the Mindanao River (Rio Grande) to a more southerly course. A geomorphic high has been inferred for the region immediately north of the present river course. Other geomorphic anomalies have been interpreted from the radar imagery based on changes in drainage density and image gray tone.

A single anticline forms the Reina Regente Hills and is located in the northcentral part of the study area. This structure displays the same northwesterly orientation as the folds in the southcentral structural province. This structure, however, has a considerably younger rock unit at the crest (Pliocene age) and appears to represent (1) a less developed, well preserved structural feature from the southcentral structural event, or (2) a younger structure created upon rejuvenation of similar deformational forces that existed during the generation of the southcentral structural province.

Faulting is evident throughout the Cotabato Basin except in areas of thick alluvial cover. The most dramatic faulting occurs near the Daguma Range where fault controlled Pre-Oligocene basement rocks of the Tiruray-Daguma High are in direct contact with Quaternary and Recent alluvial sediments. The uplifted basement high reaches an average elevation

of 984 feet (300 m) and defines the southwestern edge of the main basin. Major faults in southcentral Cotabato are northwest-trending and form horst and graben structures that define the present basin configuration. The Tiruray-Daguma High and the Quezon Mountain Range are the more prominent horst structures in the area.

6.2.2 Radar-Lineament Map

Lineaments in the Cotabato Basin are relatively short in length (3-4 km). This characteristic reflects abrupt truncation by faulting, numerous lateral changes in rock type, and extensive alluvial cover which tends to obscure or segment the surface expression of longer linear features. The principal lineament orientation is northeast, while a lesser number are north- and east-trending.

6.3 Prospect Evaluation

The prioritization sequence and ranking of prospects which follows evolved from the analysis of radar imagery used in conjunction with corroborative data available from sources previously discussed. The study area was subdivided into seven geologic terrain categories which are designated by Roman numerals (Fig. 6.2). The values of the numerals have no prioritization significance, but are provided to aid in discussing the significant geologic aspects of the Cotabato Basin. The letters (A-E) indicate prospects with potential for hydrocarbon accumulation and entrapment.

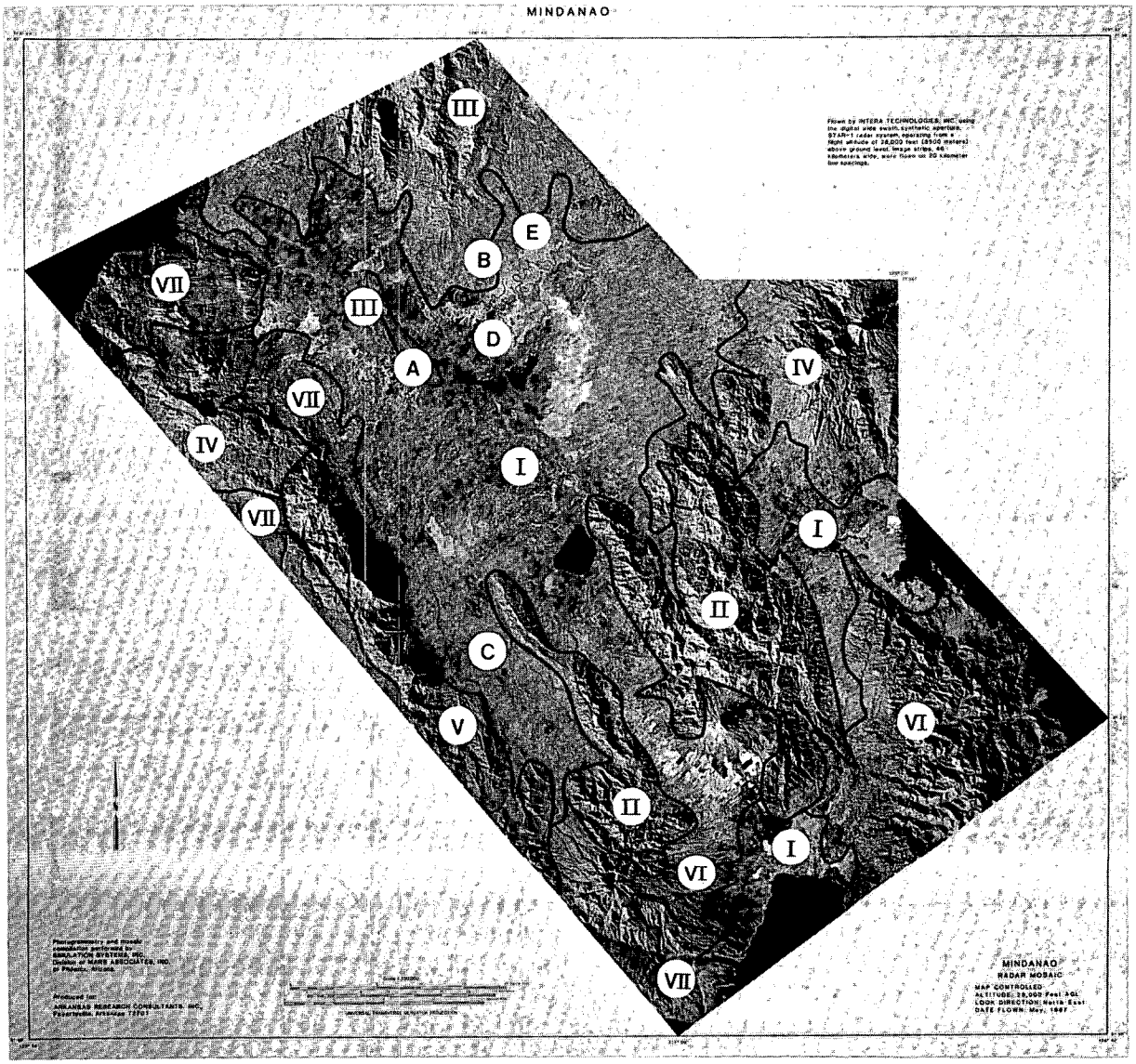

Figure 6.2: Terrain categories (I-VII) and prospects (A-E).

6.3.1 Geologic Terrain Category Criteria

AREA I

* Cotabato Basin alluvial deposits.

AREA II

* Southern Cotabato Basin structural province.

AREA III

* Northeastern Cotabato Basin structural province.

AREA IV

* Cotabato Basin geothermal/volcanic regions.

AREA V

* Cotabato Basin Basement Complex.

AREA VI

* Southeastern Cotabato Basin mountain ranges.

AREA VII

* Areas lacking structural features considered potential sites for hydrocarbon accumulation.

6.3.2 Prospects and Selection Criteria

Based on the following negative criteria, five areas have been excluded as having potential for hydrocarbon accumulation.

AREA II

* Extensive surface exposure of Middle Miocene and older stratigraphic units indicates lack of suitable subsurface sedimentary sequence.

AREA IV

* Area of recent volcanic activity.

AREA V

* Surface stratigraphic unit is the Basement Complex; lack of subsurface sedimentary sequence.

AREA VI

* Extensive surface exposure of Middle Miocene stratigraphic unit indicates lack of suitable subsurface sedimentary sequence.

* Poorly expressed structural features.

AREA VII

* No surface expression of structural features considered favorable for hydrocarbon accumulation.

The areas considered to be the most potentially important as sites for hydrocarbon exploration are I and III. The following is a list of prospects with the selection criteria for each potential site.

Prospect A Anticlinal Crest (6°59'N, 124°33'30"E)

* Two directions of plunge, creating potential for complete closure.

* Pliocene stratigraphic unit at the surface indicates sufficient subsurface sedimentary section.

* Prospect is in an area which has not been tested for hydrocarbon accumulation.

* Presence of secondary structures (faults) located down dip from crest; potential for additional entrapment feature and/or fracture porosity.

* Well expressed on radar imagery.

* Faults transverse anticlinal axis which may provide additional structural entrapment.

Prospect B Anticlinal Crest (7°8'45"N, 124°39'30"E)

* Two directions of plunge, creating potential for complete closure.

* Presence of secondary structures (faults) located down dip from crest; potential for additional entrapment feature and/or fracture porosity.

* Prospect is in an area which has not been tested for hydrocarbon accumulation.

* Well expressed on radar imagery

* Severely faulted crest, which may be indicative of additional structural entrapment.

Prospect C Inferred Anticlinal Crest (6°31'N, 124°39'57"E)

* Nearby well (Bambad-1) indicates a thick sedimentary section in this area.

* Located along trend with structural features considered favorable for hydrocarbon accumulation.

* Identified on radar imagery by analysis of drainage patterns and regional structural trends.

Prospect D Geomorphic High (7°00'N, 124°38'E)

* Possible subsurface structural feature considered favorable for hydrocarbon potential.

* Quaternary alluvium at surface indicates potential for complete subsurface stratigraphic sequence.

* Prospect is in an area which has not been tested for hydrocarbon accumulation.

* Located along trend with structural features considered favorable for hydrocarbon accumulation.

* Identified on radar imagery by analysis of drainage patterns and regional structural trends.

* Well expressed on radar imagery.

Prospect E Geomorphic High (7°11'N, 124°45'E)

* Possible subsurface structural feature considered favorable for hydrocarbon potential.

* Quaternary alluvium at surface indicates potential for complete subsurface stratigraphic sequence.

* Prospect is an area which has not been tested for hydrocarbon accumulation.

* Located along trend with structural features considered favorable for hydrocarbon potential.

* Identified on radar imagery by analysis of drainage patterns and regional structural trends.

* Moderately expressed on radar imagery.

6.4 Estimated Hydrocarbon Resources

According to BED et al. (1987), the Cotabato Basin is ranked as Class IV, which includes those assessed with poor to fair oil potential. Average field size should be in the range of 5-20 MMBBLS of oil.

6.5 Recommendations

The most obvious prospects are anticlines mapped at the surface; however, according to BED et al. (1987), most of the folding in the Cotabato Basin is thrust-fault related. Consequently, the mapped axial positions of the radar-inferred structures may not coincide with their subsurface locations. In order to refine the prospects obtained from interpretation of the radar data, it is therefore recommended that:

* geophysical data be acquired and interpreted to confirm subsurface closure of prospects,

* the approximate thickness of the subsurface sedimentary section be inferred from the seismic data.

7 RADAR–GEOLOGIC INTERPRETATION – MINDORO ISLAND

The island of Mindoro is located south of Luzon and is considered to be the northeastern part of the North Palawan-Mindoro Basin. For the purposes of flight line planning, the Mindoro radar mosaic includes approximately 11,500 km^2 of land/water coverage (see Mindoro Radar Mosaic which is an enclosure with this report).

7.1 Background and Petroleum Exploration Activities

The North Palawan-Mindoro Basin is the largest sedimentary basin in the Philippines, and contains all of the country's commercially producing oil fields. The basin represents the oldest and most stable terrain in the Archipelago, having a metamorphic basement complex of Paleozoic age. Prior to radar interpretation, the Geologic Map of Mindoro (PNOC EC, 1986) was provided to familiarize radar image interpreters with the regional geologic framework. PNOC EC has conducted intensive geological mapping and geophysical surveys for a large area of Mindoro (Fig. 7.1). During the interpretation effort, a 20-page Executive Summary (PNOC EC, 1987a) **Petroleum Potential on Mindoro, Philippines** was provided and used to brief image analysts on the important geologic aspects of Mindoro. After completion of the radar-geologic map, additional geological and geophysical data were provided by both PNOC EC and BED to aid in refining prospects and preparing this final report.

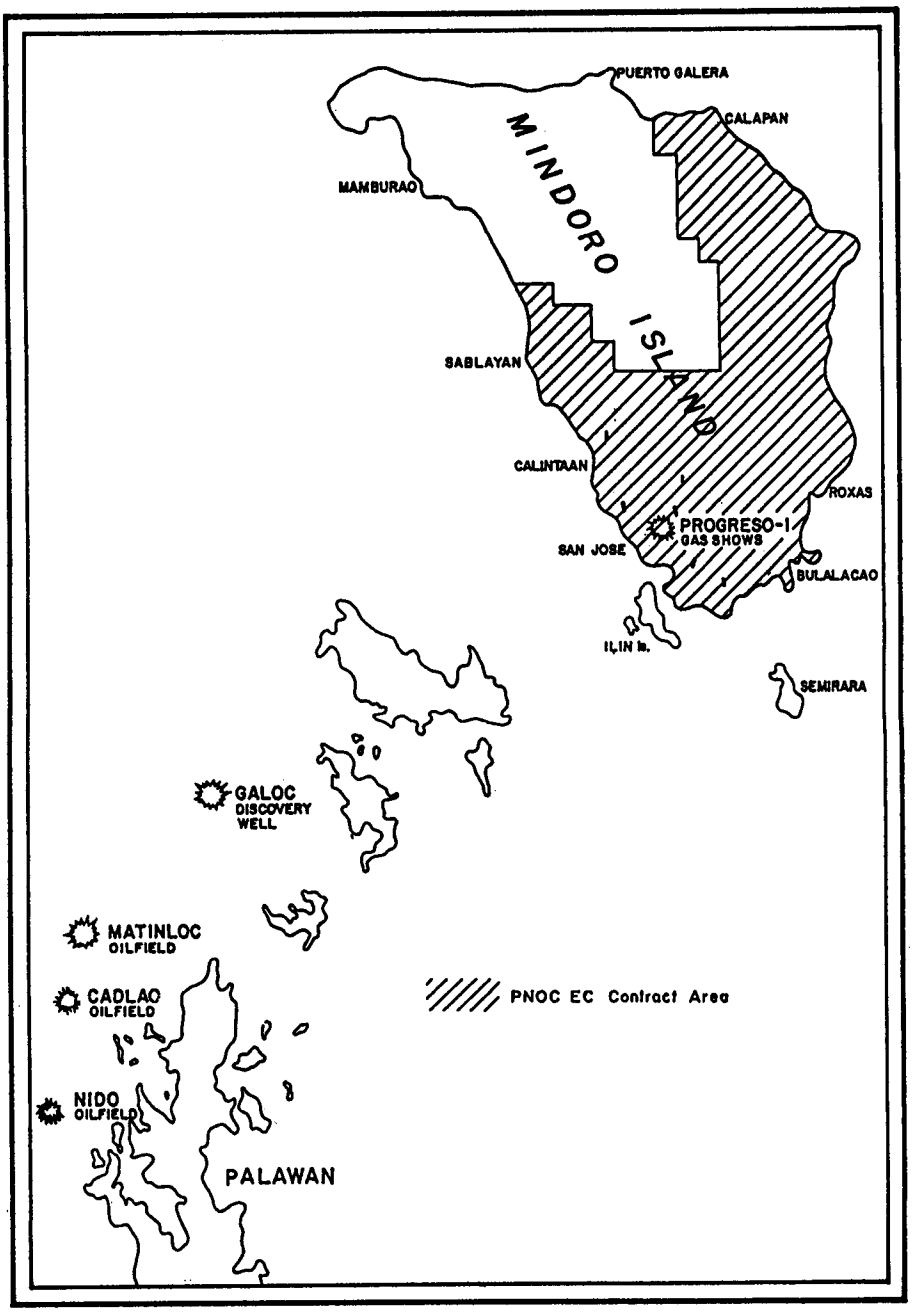

Figure 7.1: Mindoro Island and vicinity. Map shows the contract area for geologic and geophysical studies. (After PNOC EC, 1987b.)

7.1.1 Structure

Since the first commercial oil discovery in 1976 off the northwest coast of Palawan, extensive geologic exploration has been conducted in the Mindoro Island region. PNOC EC (1987) reports that this effort has resulted in formulation of two significant geologic concepts concerning the origin of Palawan and Mindoro: 1) they are similar continental crustal blocks that rifted-off from a zone of spreading on the Asian continental margin in Early Oligocene time during evolution of the South China Sea, and 2) they evolved from contiguous areas of sedimentation, which makes their hydrocarbon potentials very closely related or equivalent. The continental fragments migrated southward until they collided with the Philippines magmatic arc during the Middle to Late Miocene. Consequently, even though Palawan and Mindoro are part of the present-day Philippines Archipelago, they have distinctly separate origins and geologic histories from the Philippines Island-arc system (Holloway, 1982).

Two major tectonic styles are recognized in the region (PNOC EC, 1987). One is related to extensional deformation which created rift depression basins as the continental fragments moved away from the Asian continental margin. The other is compressional deformation which occurred during the convergence of the fragments with the Philippines arc, resulting in a zone of thrust-fold structures (Figure 7.2).

7.1.2 Stratigraphy

The Mindoro Island stratigraphic column consists of a variety of rock types ranging in age from Carboniferous to Pleistocene. The stratigraphy of the Mindoro Island has been described by BED et al. (1987), PNOC EC

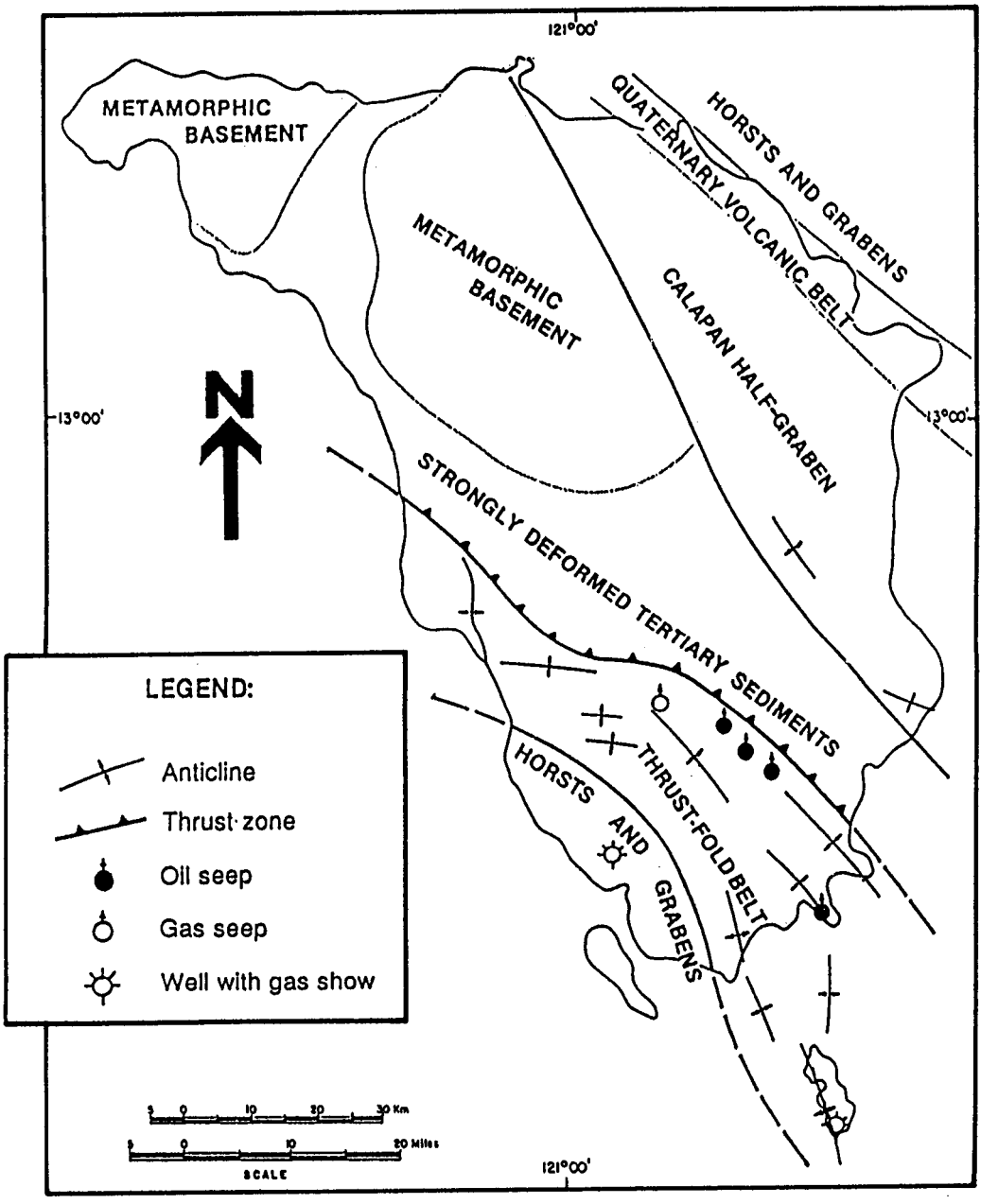

Figure 7.2: Major structural features of Mindoro. (After PNOC EC, 1987a.)

(1987), Holloway (1982), and the Philippines Bureau of Mines and Geo-Sciences (1981). The following stratigraphic discussion is a synthesis of these reports.

The successive stratigraphic descriptions include only those stratigraphic units that have been mapped on the Radar-Geologic Interpretation of Mindoro Island which accompanies this report. Stratigraphic units were selected from the 1986 Geologic Map of Mindoro.

Upper Paleozoic-Mesozoic

Metamorphic rocks of the Mindoro Metamorphics are the oldest exposed stratigraphic unit in the Mindoro Island study area. An upper Paleozoic section exposed along the Bongabon River consists of schist, phyllite, gneiss, and marble. Upper Paleozoic intrusions of metaquartz diorite, hornblende diorite, and quartz monzonite occur within this sequence. Age determination for this section is from a Carboniferous cyatopsid coral found within a clast of highly indurated mudstone.

Semischists, spilitic basalt, and metaconglomerate unconformably overlie Paleozoic rocks. Fossils in the metaconglomerate suggest a Late Triassic age for this section.

Eocene

The Eocene Batangan formation, which attains an estimated thickness of 14,000 feet (4260 m) in the Batangan Creek area, can be divided into two distinct lithologic facies. A lower, thick clastic facies is mostly quartz-rich arkosic sandstone, shelfal calcarenites, and thick dark shale with thin carbonate and carbonaceous siltstone beds deposited in a shallow marine environment. Claystone and minor cross-bedded quartz arenite are

also present. In the upper portion of this clastic sequence is a sandstone unit which varies in composition from hard foraminiferal sandstone to coarse porous quartz-feldspathic sandstone with metamorphic lithic grains.

The remainder of the Eocene section is composed of a biohermal orbitoidal limestone and interbedded shale facies. The limestones are generally banded, hard, and in part micritic to calcarenitic.

Oligocene

The Oligocene stratigraphy is represented by a group of dissimilar rock types. Altered pillow basalts and bathyal red argillites occupy a large central portion of the study area and occur as scattered outcrops to the north. The Anahawin Formation attains maximum thickness of 10,000 feet (300 m) and consists of a thin-bedded open marine detrital limestone facies and a clastic facies of shallow water argillaceous sandstone and claystone. Small areas of undifferentiated ultramafic rocks are also part of the Oligocene stratigraphy.

Miocene

Early Miocene strata are composed of marine clastics and limestone. The Mompong Turbidites are clastic turbidites, interbedded carbonaceous shale and sandstone, and hypabyssal micrites. The Bulalacao Limestone is a group of undifferentiated carbonate rocks.

A Middle Miocene limestone unit, the Tusk Peak Limestone, is a section of thick-bedded lagoonal and shelfal carbonates and patch reefs.

Late Miocene sedimentation is represented by the non-marine Punso Conglomerates. This unit is an accumulation of conglomerates with poorly consolidated arkose and terrigenous calcarenite.

Late Miocene–Pliocene

The Late Miocene-Pliocene section in the Mindoro Island study area includes a transgressive shelfal limestone of the Bongabong Limestones and a polymictic conglomeratic unit called the Bansud Conglomerates. Surface exposures of these two units are confined to a narrow strip of land that trends parallel to the eastern coast.

Pliocene

A shallow marine depositional environment appears to have existed during Pliocene time. A thick section of reefal and shallow water detrital limestone, belonging to the Pliocene Paclolo Limestones, crops out in the southcentral region and also forms the Ilin and Ambulong Islands. Pliocene clastic rocks occur throughout the southcentral and southwestern Mindoro Basin area and are composed of a basal planktonic calcisiltite unit and a poorly consolidated quartzose sandstone and siltstone sequence with coal seams.

Pleistocene

The Pleistocene stratigraphic section in the Mindoro Island study area is represented by the Central Conglomerate and the Sumagui Pyroclastics. The Central Conglomerate occurs as scattered outcrops in the southwestern region and consists of semi-consolidated conglomerates of terrace gravel and carbonate rubble. The Sumagui Pyroclastics occur in the northwest in the general vicinity of the Mount Dumali volcano.

Quaternary

Quaternary calk-alkali volcanic rocks occur only as a small outcrop in southcentral Mindoro Island. Quaternary alluvium is widespread along the coastal areas of the island and consists mainly of clay, silt, sand, and gravel deposits along streams and rivers and in flood plains.

7.1.3 Hydrocarbon Occurrences and Exploration Activity

According to the geologic information available, only three wells have been drilled to test the sedimentary area of Mindoro that is included in the radar mosaic coverage. Table 7.1 provides pertinent information for the exploratory wells drilled on Mindoro, and Figure 7.3 shows the approximate locations of these wells. The Progreso-1X well (Figures 7.1 and 7.2), which was abandoned as a dry hole in 1982, had significant shows of methane gas while drilling through Eocene sandstones.

Table 7.1: Exploratory wells and hydrocarbon occurrences - South Mindoro
(Modified from BED et al., 1987)

Well Name	Drilling Date	Total Depth m (ft)	Play Type	Defined by	Target	Age of Rock at T.D.	Results	Remarks
Central-1 (REDECO)	1962	1915.9 (6286)	Anticline	Seismic and gravity	Eocene quartz sand	Not known	Dry	Valid Test
Mindoro-1 (BP / INTER-PORT)	1979	1523.9 (5000)	Anticline	Outcrop mapping	Eplog Anticline Omega Struct.	Eocene (?) Jurassic (?)	Dry	Objective section missed. Not valid test.
Progreso-1X (SEDCO)	1982	1594 (5230)	Anticline	Seismic	Miocene clastic	L. Eocene	Dry	Valid test

REDECO - Republic Resources and Development Corporation
SEDCO - South East Exploration Company

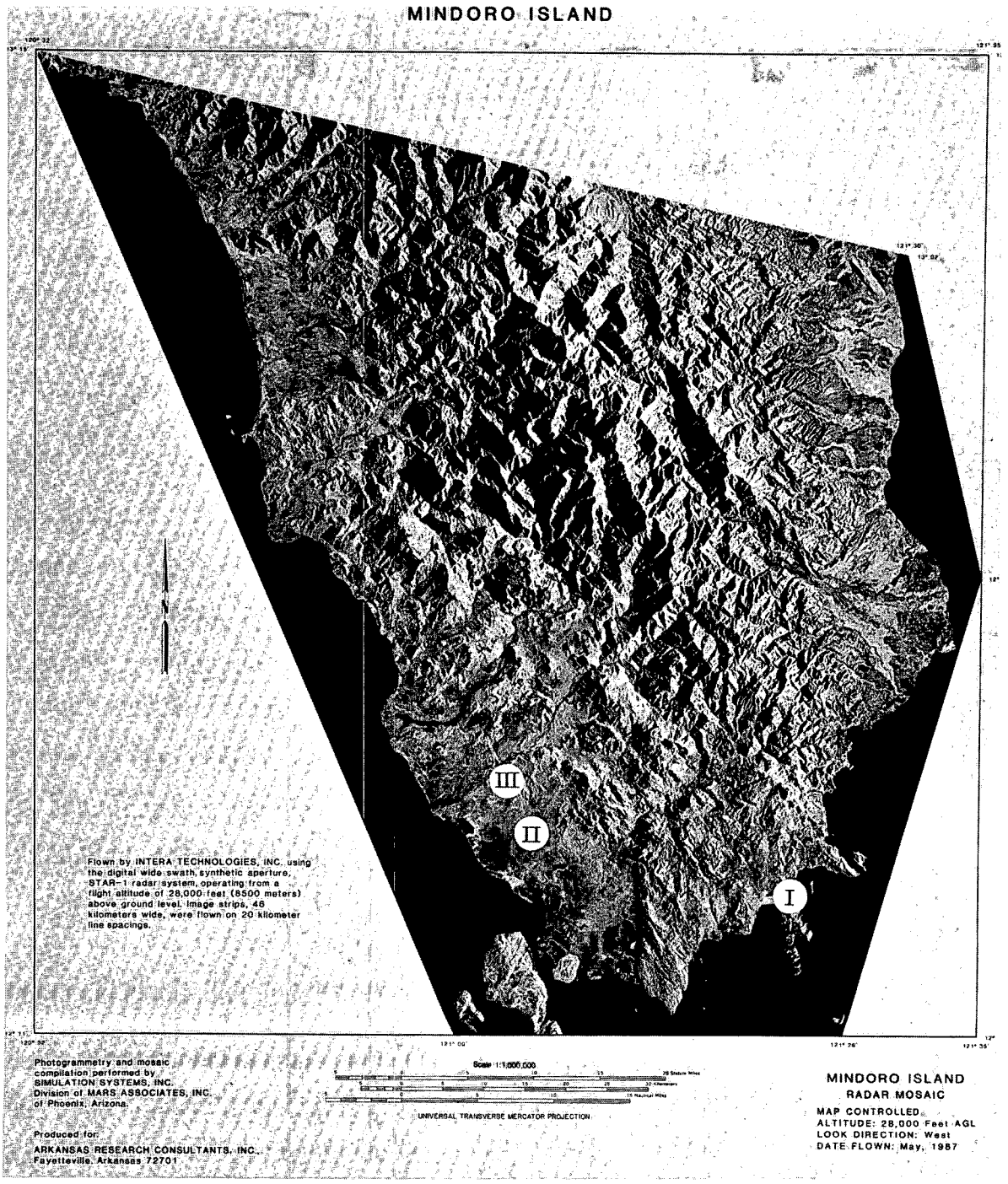

Figure 7.3: Approximate locations of petroleum exploration wells. I is Mindoro-1; II is Progresso-1X; and III is Central-1.

7.1.4 Reservoir Characteristics

Reservoir strata have been identified in Eocene to Oligocene sections, as well as in the Lower Miocene sequence. The quartz arenites and arkoses with calcareous cement that comprise the uppermost Eocene-transitional Oligocene sequence are considered to be the most attractive reservoirs. Oligocene to Miocene carbonate strata which are known to be oil reservoirs in the Nido, Cadlao, and Matinloc North Palawan oil fields may be present on Mindoro. The lower section of the Eocene sandstone sequence and the Middle Miocene carbonates also provide rocks with favorable reservoir characteristics. Turbidite sandstone sections that overlie Oligocene to Lower Miocene Carbonates on Mindoro may be correlatable with the oil-producing turbidites in the Galoc-1 well of North Palawan (Figure 7.1), thus could provide potential reservoir rock.

7.1.5 Source Rocks

Rocks capable of generating hydrocarbons have been identified from the Eocene and Oligocene to Lower Miocene sections. Fully mature Eocene source rocks consist of dark-colored carbonaceous siltstones, silty claystones, and occasional coaly lenses. Marginally mature Oligocene and Lower Miocene strata consist of carbonaceus mudstones and claystones. Source rocks in the Miocene-Pliocene horizon, although generally immature, show oil generation potential.

7.2 Interpretive Products

7.2.1 Radar-Geologic Map

The Radar-Geologic Map for the Mindoro Island study area was developed through analysis of radar imagery and review of the Geologic Map of

Mindoro (PNOC EC, 1986). The interpretive product contains lithologic boundaries, stratigraphic strikes and dips, faults, folds, structural form lines, and geomorphic anomalies.

7.2.1.1 Radar Map Units (Lithology)

The following is a description of the radar appearance of each lithologic unit within the area of interest.

Paleozoic-Mesozoic Metamorphics (Bst)

The Mindoro Metamorphic Formation forms the stable core of Mindoro Island. The strongly dissected metamorphic terrain is composed of high relief angular ridges that distinguish it from the lower relief and rounded appearance of the surrounding sedimentary terrain. The relatively high relief of this unit results in bright image tones on foreslopes, and large areas of radar shadow on backslope regions.

Eocene Limestone Btn (L) and Clastics Btn (C)

The limestone facies of the Eocene Batangan Formation occurs as large outcrops in the southwestern Mindoro region that are easily differentiated from the adjacent metamorphic terrain. This unit commonly forms large mound-like topographic highs. The surface of these features appears extremely rugged which is typical of carbonate terrain in humid environments. The karst landforms produce small scale, subround areas of highlight and shadow on the radar imagery.

The clastic facies of the Batangan Formation occupies a large portion of southcentral Mindoro. The terrain is rugged and consists of subangular landforms of moderate relief. This unit is distinguished from the adjacent metamorphic complex by its lower relief, less rugged, more rounded peaks

and ridges. The surface of the Btn (C) map unit displays a rough grainy texture composed of intermediate to bright image tones. The terrain is heavily dissected, and stratification characteristics are not recognizable.

Oligocene Ultramafics (Umf)

Oligocene ultramafic rocks are scattered throughout northcentral and northeastern Mindoro. The massive, well consolidated appearance of this unit was the distinguishing characteristic used to define the boundaries of this radar map unit.

Oligocene Metavolcanics (Mv)

The Oligocene metavolcanics map unit (Mv) occurs in close proximity to the Mindoro Metamorphic Formation. Because the metavolcanics have a radar appearance that is similar to the adjacent metamorphic unit, map boundaries for the metavolcanics were obtained from the geologic map of Mindoro.

Oligocene Limestone Anw (L) and Clastics Anw (C)

The Oligocene Anahawin Formation limestone facies appears on radar imagery as a massive coarse-textured unit. In smaller exposures, the unit is reduced to groups of coarse-textured subangular peaks and ridges that produce isolated high intensity radar returns.

The clastic facies is distinguished as a thinly-bedded sequence with a smooth to moderately rough surface. Stratification is well developed and easily identified on the imagery by linear bright tones from radar-facing escarpments. Largest exposures of this map unit occur in the westcentral region of the study area near Tusk Peak and Mount Tallulah.

Early Miocene Clastics (Mpo)

The Mompong Turbidites are easily defined as a radar map unit in the westcentral portion of Mindoro Island. The rocks of this unit form distinct groups of moderate relief, narrow ridges that have been severely segmented and eroded. Sloping surfaces produced by dipping strata are heavily dissected and cause bright image tones from drainage channels and fault scarps. Truncation of strata has produced escarpments that are identified by linear areas of image highlight and shadow.

Early Miocene Limestone (Bll)

The Bll map unit represents an Early Miocene carbonate unit belonging to the Bulalacao Limestone. The unit is found mainly in southeastern Mindoro near the town of Bulalacao and on the slopes of Knob Peak. Morphological differences from surrounding map units were used to define the boundaries of the Bll radar map unit. The rocks of this unit form broad areas of elevated terrain. The unit appears partly massive, but remnants of stratification are present in the form of segmented subangular ridges. The surface of this unit produces intermediate and bright image tones typical of a rough pitted carbonate surface.

Middle Miocene Limestone (Tpl)

The thick carbonate beds of the Tusk Peak Limestone form the topographic highs of Mount Tallulah and Tusk Peak. In both locations, thick resistant stratification is clearly expressed on radar imagery. Surface texture is difficult to determine since the stratigraphic escarpments produce large areas of image highlight and shadow. The rocks of Mount Tallulah form a large mound-like geomorphic expression.

Late Miocene Clastics (Pso)

The Late Miocene Punso Conglomerates map unit (Pso) appears as a thick bedded sedimentary section that forms distinctive curvilinear ridges. The unit generally displays significant stratigraphic dip with flatirons present on sloping surfaces. In smaller outcrops, the ridges have been reduced to isolated triangular or cone-shaped peaks. Bright image tones identify stratigraphic escarpments and peaks.

Late Miocene-Pliocene Limestone (Bnb)

The Bongabong Limestones have a radar image appearance characteristic of extreme surface roughness. The terrain is composed of relatively small scale rectangular blocks which have formed through faulting, dissection by drainage channels, and solutioning of carbonate constituents. This unit is limited to the eastern Mindoro Island coast in the vicinity of Bongabong town.

Late Miocene-Pliocene Clastics (Bsd)

Parallel, rectangular-shaped, northeast-trending ridges of moderate relief characterize this Late Miocene-Pliocene map unit. The unit has an overall coarse surface texture on radar imagery and appears less affected by weathering than the surrounding map units. The Bsd map unit occurs exclusively along the eastern coast of Mindoro near the town of Bansud.

Pliocene Clastics (Hno)

The Hinago Calcisiltites, in the southeastern region of Mindoro, appear on radar imagery as flat, low lying areas with very rough surfaces. The boundaries of this unit are easily identified from adjacent areas of high relief, and the featureless, smooth-textured alluvial deposits.

Pliocene Limestone (Pcl)

Large carbonate platforms of the Paclolo Limestones form the Ilin and Ambulong Islands in the southwest, and the highlands of southcentral Mindoro. On the islands, this map unit displays well developed bedding. Circular to semi-circular bright tones define the edges of successive rock layers. The surface appears uniformly rough and produces bright image tones. The southcentral exposure is characterized by a distinctive pitted surface which is characteristic of carbonate terrain in humid environments. Karst surfaces produce alternating light and dark subround image tones.

Pliocene Clastics (Cwc)

The clastic rocks of this Pliocene map unit (Cwc) form a featureless rolling terrain. The surface area appears smooth and is characterized by intermediate gray tones on the imagery. The Cwc map unit occurs only in southeastern to southcentral Mindoro, and is easily distinguished from the more rugged topography of surrounding radar map units.

Pleistocene Pyroclastics (Smg)

The Pleistocene Sumagui Pyroclastics occupy a significant portion of the coastal region in northeastern Mindoro. The volcanic constituents appear to be poorly consolidated in that the entire surface area of this map unit has been heavily dissected by subparallel drainage channels. Alternating light and dark linear to curvilinear image tones correspond to radar-facing channel banks and radar-shadowed channel floors respectively.

Pleistocene Clastics (Ctr)

The Central Conglomerate map unit (Ctr) exhibits an extremely rough surface appearance on radar imagery. Angular and subround light tones saturate the map unit area. The Central Conglomerate is located exclusively on the northwestern to southwestern region of the study area.

Quaternary Volcanics (Qv)

Large areas of Quaternary volcanic rocks are outside the current area of interest near the Dumali volcano in northeast Mindoro. The only occurrence of these rocks in the study area is in southcentral Mindoro. The boundaries of this map unit are poorly expressed on the radar imagery. Consequently, the interpreters relied largely on the Mindoro geologic map to define map unit boundaries.

Quaternary Alluvium (Qal)

Quaternary alluvial deposits occur in broad areas near coastlines and in depressions between highlands. Alluvial deposits are easily recognized on radar imagery by their flat featureless appearance and uniform intermediate to dark tones. In marshy areas and near river floodplains, this characteristic appearance may be disturbed by patches of extremely dark tones from pools of water and mud. Vegetation along drainage channels often causes volume scattering of incident radar energy which is characterized by sinuous patterns of extremely bright image tones.

7.2.1.2 Structure

Numerous folds, faults, and geomorphic anomalies were inferred from the radar imagery of Mindoro Island. These features, along with strike and dip directions and estimations of dip angles, appear on the Radar-Geologic Interpretation (an enclosure with this report).

The Mindoro Island structural style is characterized by a broad central Paleozoic-Mesozoic metamorphic basement that is separated from peripheral deformed Tertiary sedimentary sections by major northwest-trending faults. The central basement complex and eastern sedimentary units have no surface expression of fold structures.

Folds in the Mindoro Island study area have a subtle surface expression and generally extend less than 4 miles (6.4 km) in the axial direction. Folded strata have been severely affected by faulting and erosion, and consequently, surficial structural characteristics are difficult to identify. The best preserved structures commonly occur within the boundaries of the Mompong Turbidites radar map unit (Mpo).

Faults are prevalent throughout the study area particularly within the sedimentary radar map units. However, large alluvial deposits tend to obscure the surface expression of faults in low lying coastal areas. Two principal strike directions, northwest- and northeast-trending, can be observed. As previously mentioned, major northwest-trending faults define general boundaries between metamorphic basement rocks and adjacent sedimentary sections on the east and west. Other major faults are oriented northeast or nearly perpendicular to this group. Two conspicuous north-trending parallel faults in the southcentral region isolate the Pliocene Paclolo Limestones from surrounding sedimentary units.

7.2.2 Radar-Lineament Map

Lineaments in the Mindoro Island study area are evenly distributed among radar map units, and have two principal orientations; northwest- and northeast-trending. Small-scale lineaments, which have a surface expression of approximately 5 miles (8 km), may be related to faults which are inherent only to a particular radar map unit, or are regionally

extensive but have limited surficial expression. Small-scale lineaments within the boundaries of the metamorphic basement may represent local areas of fractures or joints.

7.3 Prospect Evaluation

The prioritization sequence and ranking of prospects which follows evolved from the analysis of radar imagery used in conjunction with corroborative data available from sources previously discussed. The study area was subdivided into three geologic terrain categories which are designated by Roman numerals (Fig. 7.4). The values of the numerals have no prioritization significance, but are provided to aid discussing the significant radar-geologic aspects of Mindoro. The letters (A - G) indicate prospects with potential for hydrocarbon accumulation and entrapment.

7.3.1 Geologic Terrain Category Criteria

Area I

* Western Mindoro sedimentary section.

* Youngest stratigraphic unit in the study area appears at the surface indicating the possibility for a relatively thick subsurface sedimentary section.

* Contains several structural features that may provide potential prospects for hydrocarbon accumulation.

Area II

* Paleozoic and Mesozoic metamorphic rocks constitute the majority of the surface area.

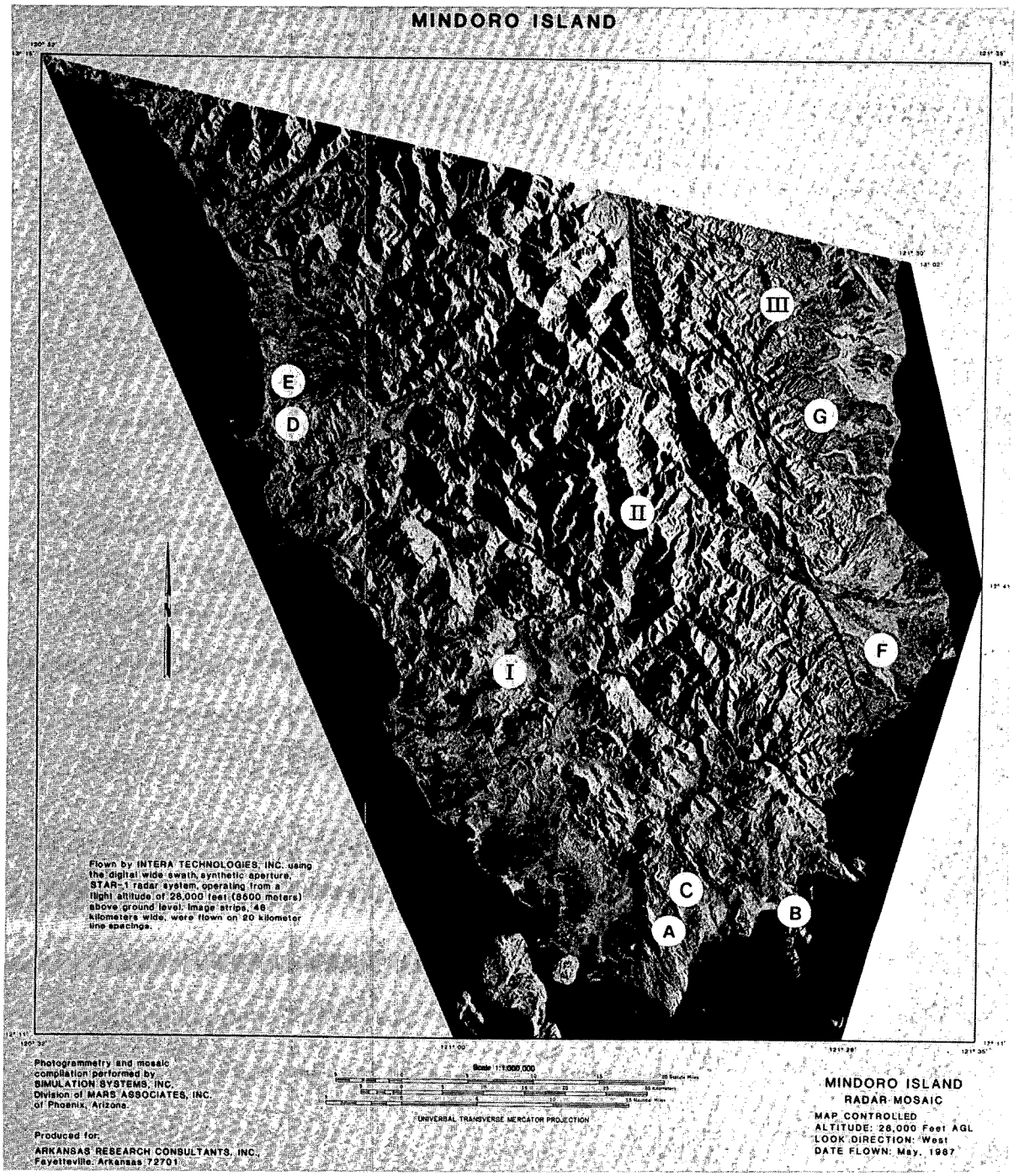

Figure 7.4: Terrain categories (I–III) and prospects (A–G).

* Youngest stratigraphic unit at the surface is Oligocene age indicating lack of suitable subsurface sedimentary sequence.

Area III

* Eastern Mindoro sedimentary section.

* Youngest stratigraphic unit in the study area appears at the surface indicating the possibility for sufficient subsurface sedimentary section.

7.3.2 Prospects and Selection Criteria

Based on negative criteria, Area II has been excluded from prospect consideration. The areas considered potentially important as sites for hydrocarbon exploration are Areas I and III.

Prospect A Anticlinal Crest (12°19'50"N, 121°13'50"E)

* Two directions of plunge, creating potential for complete subsurface closure.

* Anticline is regionally extensive, extending more than 6 miles (9.6 km) in the axial direction.

* Presence of secondary structures (faults) located down dip from crest; potential for additional entrapment feature and/or fracture porosity.

* Moderately expressed on radar imagery.

* Breached anticlinal crest indicates some loss of near-surface structural closure.

Prospect B Inferred Anticlinal Crest (12°19'20"N, 121° 22'20"E)

* Probable structural feature considered favorable for hydrocarbon accumulation.

* Secondary structures (faults) located down dip from crest; potential entrapment features and/or fracture porosity.

* Prospect is located up dip from an area which has demonstrated the presence of hydrocarbons.

* Faulted crest which may provide additional structural entrapment.

* Identified by geomorphic expression and scattered structural dip angles.

Prospect C Anticlinal Crest (12°21'30"N, 121°15'15"E)

* Secondary structures (faults) located down dip from crest; potential entrapment features and/or fracture porosity.

* Moderately expressed on radar imagery.

* Location appears to coincide with a seismically defined structure, East Paclolo Prospect (PNOC EC, 1987a).

Prospect D Anticlinal Crest (12°51'30"N, 120°48'50"E)

* Numerous secondary structures (faults); potential for entrapment feature and/or fracture porosity.

* Apparent breached anticlinal crest indicates some loss of near-surface structural closure.

* Subtle expression on radar imagery.

Prospect E Geomorphic Anomaly (12°55'00"N, 120°48'45"E)

* Possible subsurface structural feature.

* Quaternary stratigraphic unit at the surface indicates sufficient subsurface sedimentary section.

* Moderately expressed on radar imagery.

* Identified on radar imagery by drainage pattern analysis.

Area III

Prospect Area F Onshore Deltaic Sediments (12°32'00" - 12°45'00"N, 121°28'00" - 121°33'00"E)

* Large area of fluvio-deltaic sedimentation; potential for a well sorted, high porosity subsurface section.

* No structural features expressed at the surface.

* Onshore and offshore plays need to be defined with geophysical data.

Prospect Area G

* Fault patterns may aid in refining seismically defined half-graben plays.

* Area is within the Calapan half-graben structural element (Fig. 7.2). Although folds are not apparent on the radar imagery, radar-inferred fault patterns may aid in refining seismically defined half-graben plays.

7.4 Estimated Hydrocarbon Resources

According to BED et al. (1987), the Mindoro region is ranked as Class III, having fair to good potential for predominantly gas plays. Average field size should be in the range of 5-50 MMBBLS of oil, or 50-500 BCF of gas.

7.5 Recommendations

With sufficient seismic coverage, anticlinal fold structures whose subsurface axial positions may have been displaced by wrench or thrust faulting can usually be accurately delineated. In order to refine the prospects obtained from interpretation of the radar data, it is therefore recommended that:

* geophysical data be acquired and interpreted to confirm subsurface closure of prospects,

* the approximate thickness of the subsurface sedimentary section be inferred from the seismic data.

It is further recommended that:

* the anticlinal prospects referred to as prospects "A" and "B" be confirmed with field and seismic investigations,

* since prospect "C" appears to coincide with a seismically-defined PNOC EC prospect, an attempt should be made to correlate the surface structure with additional seismic interpretation,

* prospects "D" and "E", which are subtly expressed on the radar imagery, be confirmed with seismic investigations,

* fault traps within area "G" should be defined using seismic data in conjunction with radar imagery-defined fault zones.

It is also noted that:

* prospect area "F" includes a large area of fluvio-deltaic sedimentation,

* onshore and offshore plays need to be defined with geophysical data.

This page is intentionally left blank.

8 RADAR–GEOLOGIC INTERPRETATION – CEBU ISLAND

Cebu is a long narrow island with its major axis trending slightly east of north, located within the Visayan Basin in the Central Philippines between the islands of Negros on the west, and Leyte and Bohol to the east. For the purposes of radar flight planning, the Cebu radar mosaic includes approximately 7,525 km^2 of land/water coverage (see Cebu Radar Mosaic which is an enclosure with this report).

8.1 Background and Petroleum Exploration Activities

Prior to radar interpretation, the 1985 Geologic Map of Cebu (1:250,000) was provided by PNOC EC. The PNOC EC technical staff has conducted detailed geological and geophysical studies in southern Cebu to develop tectonic models and upgrade petroleum prospects (Fig. 8.1). During the interpretation effort, a draft copy of a report "Hydrocarbon Potential of the Cebu Basin Philippines" (PNOC EC, 1987c), and the following additional maps were made available:

* 1:60,000 Map set for southern Cebu including Geologic Map of Ginatilan Area, Geologic Map of Alegria Area, and Geologic Map of Mompeller Badian Area
* 1:125,000 Structure Map in Time of Eocene Horizon Southwestern Cebu (Sub-Thrust/Extensional Zone)
* 1:125,000 Structure Map in Time of Eocene Horizon - Southwestern Cebu (Thrust - Fold Zone).

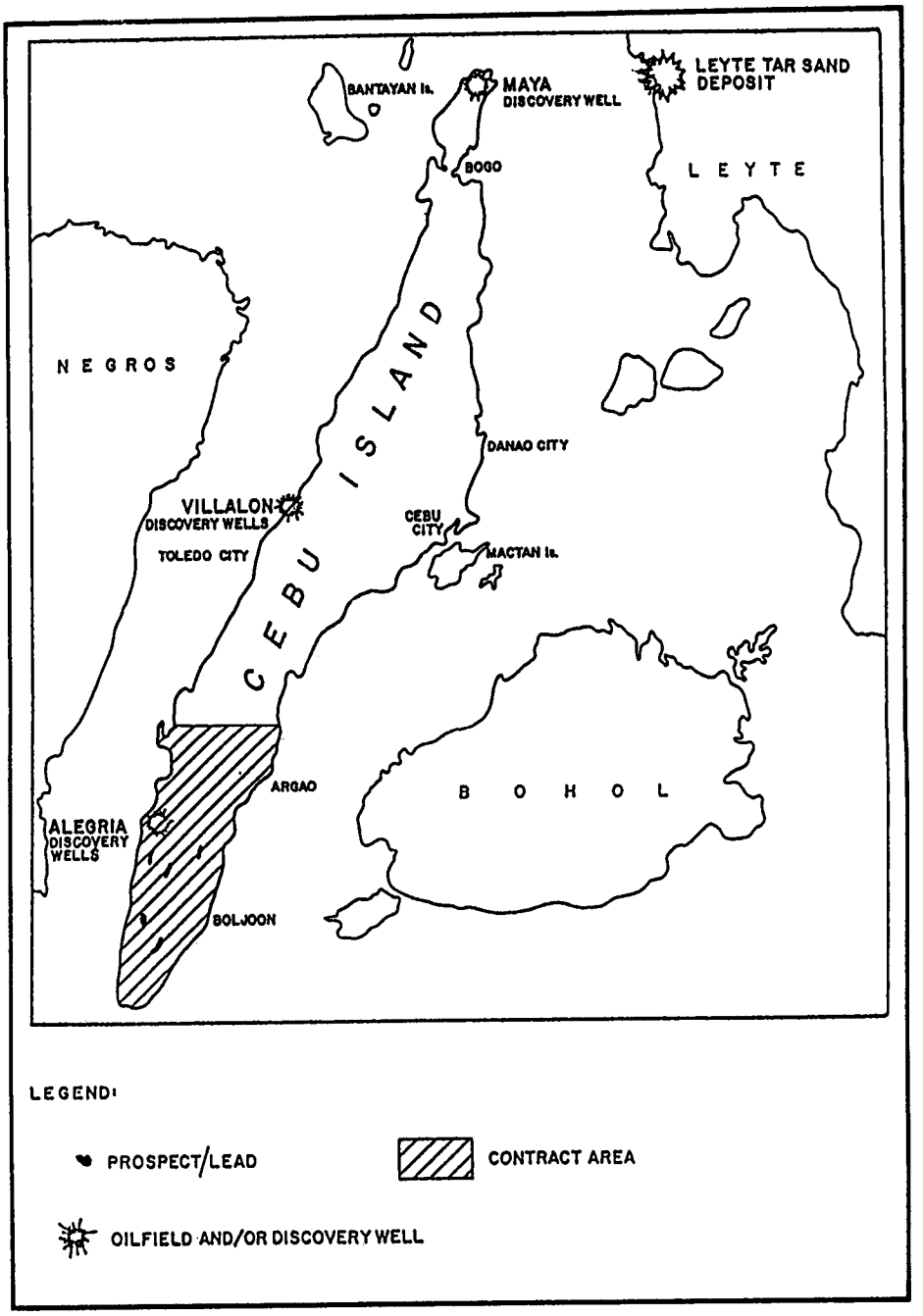

Figure 8.1: Contract area for detailed geological and geophysical studies. (After PNOC EC, 1987b).

After completion of the radar-geologic map, additional geological and geophysical data were provided by both PNOC EC and BED to aid in refining prospects and preparing this final report.

8.1.1 Structure

The entire island of Cebu has been described as a sigmoidal, north-northeast oriented fault block (BED et al., 1987). The dominant faults are reported to be north to north-northeast-trending in the north and south, and northeast oriented in central Cebu. According to PNOC EC (1987c), two parallel fold belts are mappable over long distances on the southwestern and south-central portion of the island, and are referred to as the Alegria-Malabuyoc fold belt and the Cebu anticlinorium, respectively. A third eastern fold belt has been identified in the subsurface from seismic data. The Alegria-Malabuyoc fold belt extends from Aloguisan on the north (9°48'N, 123°22'E), to Ginatilan on the south (9°34'N, 123°20'E). The southern Cebu anticlinorium consists of a narrow (3.5 to 7.0 km-wide) fold belt that extends southward from the central Cebu highland.

8.1.2 Stratigraphy

The Cebu Island stratigraphic column is composed of a pre-Cretaceous basement complex consisting of metamorphic, intrusive, and volcanic rocks overlain by a succession of Oligocene to Pliocene-Pleistocene sedimentary rocks. The stratigraphy of Cebu Island has been described in detail by BED et al. (1987), PNOC EC (1987c) , the Philippines Bureau of Mines and Geo-Sciences (1981), and Corby et al. (1951). The following stratigraphic discussion is a synthesis of these reports, and the stratigraphic descriptions include only those stratigraphic units that have been mapped on the

Radar-Geologic Interpretation of Cebu Island which accompanies this report. Stratigraphic units were selected from the 1985 Geological Map of Cebu Island.

Pre-Cretaceous (?)

The basement complex consists mostly of metamorphic rocks overlain by volcanic and clastic sections. The Tunlob Schist is the oldest identified formation on the island. This unit is Cretaceous in age or younger and consists mainly of chlorite-amphibolite schist and partly of phyllites and slates.

The Cansi and Pandan Formations are included as part of the basement complex on the Radar-Geologic Map but are undifferentiated. The Early Cretaceous Cansi Formation, often referred to as the Cansi Volcanics, is a sequence of basaltic to andesitic lava flows and agglomerates with interbeds of limestone and volcanic breccia. Massive extrusive rocks and pillow lavas have also been identified. Early Cretaceous Orbitolina fossils in shale and limestone fragments from the Cansi Formation have been found near the Managa River.

The Pandan Formation consists of an indurated sequence of limestones, shales, sandstones, and conglomerates with occasional coal stringers. Globotruncana fossils in the limestone are a Late Cretaceous marker.

Middle-Late Oligocene

The Calagasan Formation of southern Cebu is composed of conglomerate, fine to coarse-grained tuffaceous sandstone, and carbonaceous shale with interbedded limestone and coal seams.

Late Oligocene

The Cebu Limestone Member of the Cebu Formation is hard, white, pure limestone which locally may contain gray or brown shale stringers. Orbitoid Lepidocyclina fossils are present throughout this unit and become more abundant near the base. The Cebu Limestone varies in thickness from 250 feet (75 m) to 330 feet (100 m).

Early Miocene

The Early Miocene Malubog Formation is composed essentially of shale and sandstone with lesser amounts of conglomerate, limestone, and coal. The clastic section is highly variable and exhibits rapid horizontal and vertical lithologic and facies changes. The lower portion consists mainly of shale, mudstone, and siltstone with thin sandstone interbeds. Foraminifera are present which suggests an upper to middle bathyal environment. This fine clastic sequence coarsens upward to a section of siltstone, tuffaceous sandstone, and conglomerate with interbedded coal. Stratigraphic and lithologic evidence points to a fluvial-deltaic depositional environment. Dark gray claystone, carbonaceous shale and siltstone with frequent interbeds of sandstone occur towards the top of the formation. Locally, the upper part of this sequence contains limestone composed of branching corals in a calcareous sand matrix. The presence of benthonic foraminifera suggests a middle neritic environment of deposition. The total thickness of the Malubog Formation ranges from 1640 feet (500 m) to 4920 feet (1500 m).

Middle Miocene

The Middle Miocene depositional record, as preserved by the Toledo Formation, indicates a time of intense tectonic activity. The formation is predominantly thick tuffaceous shale with sandstone interbeds and occasional lenses of clastic limestone. Andesitic breccias, tuffs, tuffaceous marls,

bentonites, and a striking white bentonitic shale occur as basal units. Abundant foraminifera and scarce megafossils indicate that the Toledo Formation was probably deposited in an upper to middle bathyal environment. Formational thickness ranges from 660 feet (200 m) to 820 feet (250 m).

Middle–Late Miocene

A basal white reefal limestone belonging to the Maingit Formation has been interpreted to represent a progressive lowering of sea level during the late Middle Miocene. The limestone contains numerous corals but few microfossils and is usually less than 165 feet (50 m) in thickness.

The remainder of the Maingit Formation is composed of conglomerate, coarse carbonaceous sandstones, and shale with coal stringers and occasional thin beds of limestone. The conglomeratic section is around 1880 feet (575 m) thick and contains boulders of conglomerate in a sandstone matrix which are as large as 15 centimeters in diameter. The total thickness of the Maingit Formation is estimated at 3850 feet (1175 m).

Late Miocene–Pliocene

Late Miocene to Pliocene sedimentation on Cebu Island is represented by the Barili Formation which unconformably overlies the Maingit Formation. The formation is divided into two members; a lower limestone, and an upper marl.

The Barili Limestone, which has a thickness of 660 feet (200 m) to 1150 feet (350 m), is widespread in the southern half of Cebu. Lithologically, this unit is composed of dense, white, deep water, micritic limestone and minor porous coralline limestone. The limestone is occasionally light brown and marly.

The Barili Marl is generally a brown, poorly bedded, slightly sandy marl with occasional thin stringers of limestone. Basal sections contain dark gray to blue, carbonaceous shale and thin, poorly bedded, lenticular sandstone and conglomerate. The Barili Marl ranges in thickness from 660 feet (200 m) to 1640 feet (500 m).

Pliocene-Pleistocene

The Pliocene-Pleistocene Carcar Formation is a porous coralline transgressive-type limestone that is poorly bedded to massive. Occasionally, the limestone grades into limestone rubble or conglomerate and may contain thick beds of marl. The Carcar Formation lies unconformably on the Barili Formation and is widespread throughout the study area especially along coastal areas.

Quaternary

Quaternary alluvial deposits occur predominantly along coastal margins.

8.1.3 Hydrocarbon Occurrences and Exploration Activity

Surface seepages of oil have been known in the southwestern part of Cebu, and the first recorded show of oil in a well occurred in 1896 when Smith, Bell and Co. drilled two wells in the Toledo area (Corby et al., 1951). Considerable exploration has continued to the present date; however, in spite of some significant oil and gas flows on drillstem tests or hydrocarbon shows during drilling, Cebu has no commercial oil or gas production. Table 8.1 provides pertinent information for some of the more significant exploratory wells drilled on Cebu Island, and Figure 8.2 shows the approximate location of these wells. Data for most of the exploratory wells are listed (chronologically) in Appendix A.

Table 8.1: Significant exploratory wells and hydrocarbon occurrences - Cebu (Modified from BED et al., 1987)

Well Name	Drilling Date	Total Depth m (ft)	Play Type	Defined by	Target	Age of Rock at T.D.	Results	Remarks
Cebu-3 (PODCO)	1949	2336.3 (7663)	Anticline	Surface mapping seismic	No data	Base-ment	Total of 9 MMCFGPD in 113 days; Barili ls	Valid test
Libertad-11 (ACOJE)	1958	217.1 (712)	No data	No data	No data	Late Miocene (Barili ls)	250 MCFGPD from Barili ls Retested 280 MCFGPD	
Libertad-13 (ACOJE)	1958	175.3 (575)	No data	No data	No data	Not known	250 MCFGPD from Barili ls Retested 650 MCFGPD in 1974	Indeterm-inate
Reina Regente-1A (REDECO)	1959	407.0 (1335)	No data	No data	No data	Early Miocene (Malu-bog Fm.)	3-6 bbl oil; Malubog Fm. Retested 29.4 BOPD in 1974	?Valid test
Reina Regente-1AX (REDECO)	1959	1833.8 (6015)	No data	No data	No data	Metam. base-ment	250 BOPD; Malubog Fm. Retested max 42 BOPD in 1960	?Valid test
Malolos-1 (HIXBAR / ACOJE)	1960	2749.1 (9017)	No data	No data	No data	Malubog Fm	Tested some 39° API oil at 2185.6 - 2252.1 m	Indeterm-inate
Maya-11 (MST-11) (AAOC)	1961	87.2 (286)	Anticline	Recon geology gravity and sono probe	No Data	L. Mio-cene	450 bbls oil in 203 hrs; Maingit clastics	?Valid test
Villalon-4 (PODCO / REDECO)	1962	564.0 (1850)	No Data	No Data	No Data	Not known	168 bbl oil in 4 days; Malubog Fm	Blew out; swabbed at 10 bbls / hr valid test
Lumpan-1 (JOSE TIONG-1) (PODCO / REDECO)	1964	206.7 (678)	Anticline	Surface geology	M. Mio-cene ss	Middle Miocene	1964; 605 bbl oil (44° API) 1970; 255 bbl oil in 40 hrs. 1974; 301 bbl oil in 72 hrs.	Valid test but drilled off structure

Table 8.1 (cont.)

Well Name	Drilling Date	Total Depth m (ft)	Play Type	Defined by	Target	Age of Rock at T.D.	Results	Remarks
Lumpan-2 (PODCO / REDECO)	1964	204.3 (670)	Anticline	Surface geology	M. Miocene ss	Maingit Fm.	1964 tested 218 bbl oil, 1973 tested 93 bbl oil (35.4°API) in 42 hrs.	Valid test but drilled off structure
CMB-2 (AAOC / PIONEER / CPC)	1972	967.4 (3173)	Anticline	Surface geology, other well data, seismic and gravity surveys	L. Miocene ls E. Miocene ls ss L. Oligocene ls	Argillite Metam. Basement (Cretaceous)	70 - 100 MCFGD (478 - 486 m) & 106 BOPD- M. Miocene ss prod. rapidly declined	Valid test but drilled off structure
CMB-4 (AAOC / PIONEER / CPC)	1972	787.2 (2582)	Anticline ss lenses	Seismic gravity drilling data	Early Miocene sand lenses ls stringers	Late Oligocene	Total of 5.6 bbl of oil- Malubog Fm. in 36 days	Valid test
CPR-1 (REDECO / CPC / PIONEER)	1974	1588.4 (5210)	Anticline	Surface geology other well data	Late Miocene ss	Late Miocene (Maingit Fm.)	Max 424 MCFGPD & some oil- Maingit clastics	Valid test
CPR-2 (REDECO / CPC / PIONEER)	1975	2045.7 (6710)	Anticline fault trap	Surface geology other well data	Late Miocene ss	Early Miocene (Malubog Fm.)	Max 212 MCFGPD & 16.2 BOPD- Maingit clastics	Valid test

PODCO - Philippines Oil Development Company
ACOJE - Acoje Oil Exploration & Drilling Co., Inc.
REDECO - Republic Resources & Development Corporation
HIXBAR - Hixbar Mining Co., Inc.
AAOC - American-Asiatic Oil Corporation
CPC - Chinese Petroleum Corporation

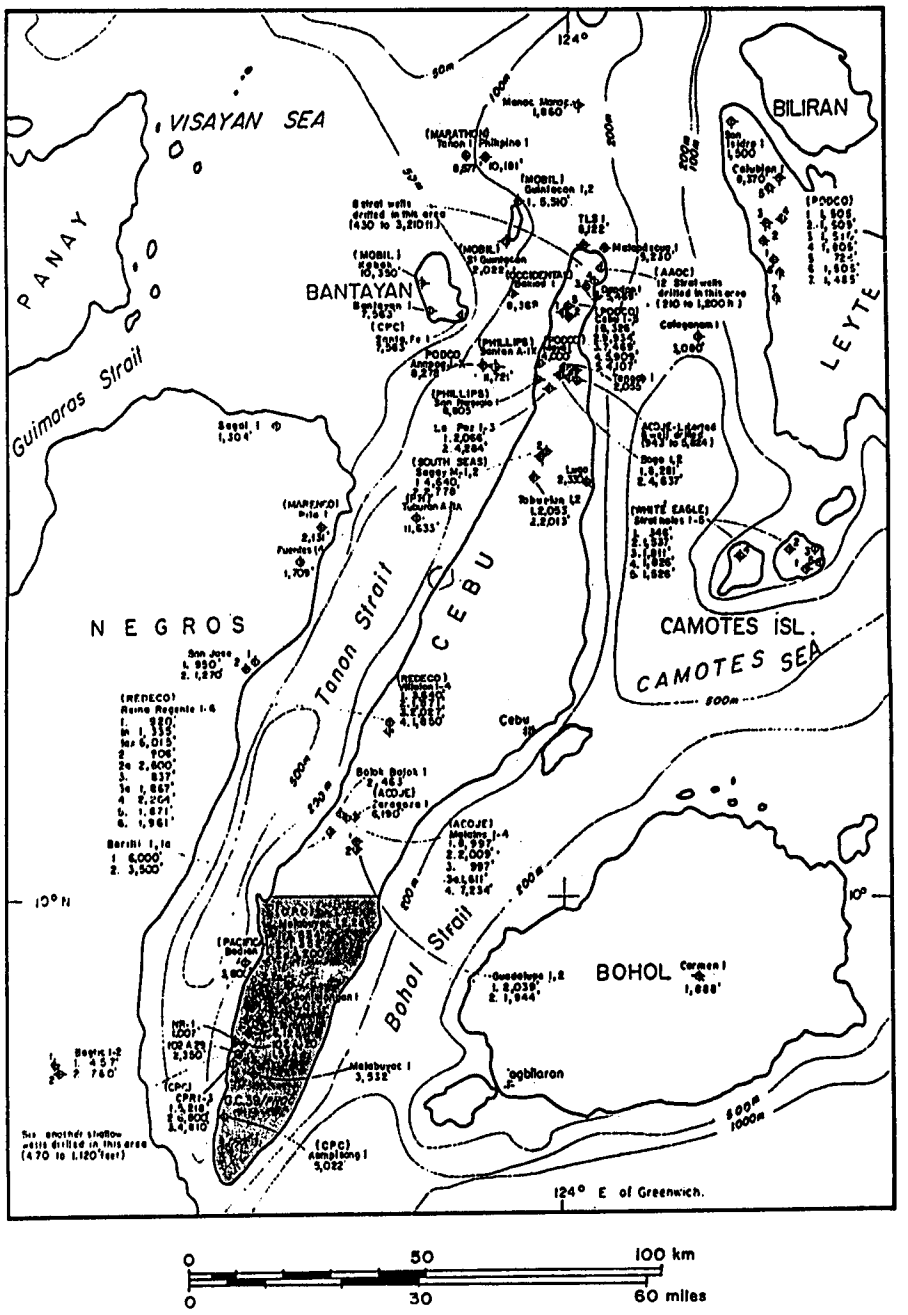

Figure 8.2: Approximate locations of petroleum exploration wells. (After Petroconsultants, 1986).

8.1.4 Reservoir Characteristics

According to PNOC EC (1987c) and BED et al. (1987), exploration in southern Cebu has defined the existence of potential reservoir horizons, both clastics and carbonates in the Oligocene to Pliocene succession. However, the primary reservoirs include: 1) Upper Miocene sandstones of the Maingit Formation, 2) Middle Miocene carbonates of the Maingit Formation, and 3) Upper Oligocene to Lower Miocene sandstones of the Malubog Formation. The Tertiary depositional environments include bathyl clastics, shallow beach sands, and coral patch reefs, all of which have reservoir potential.

8.1.5 Source Rocks

Source rock potential occurs throughout the Oligocene-Miocene succession, primarily because of the organically rich sediments. For example, analysis of samples obtained from the Malubog Formation indicated that 70% contained a total organic carbon content ranging from 1 to 5% (PNOC EC, 1987c). This is in excess of the 0.5% considered to be a minimum requirement for a rock to have a source potential. Other geochemical studies have indicated that the fine grained clastics of the Middle Miocene Toledo Formation, and Upper Miocene Maingit Formation also have hydrocarbon source potential.

8.2 Interpretive Products

8.2.1 Radar-Geologic Map

The Radar-Geologic Map for the Cebu Island study area was developed through analysis of radar imagery and review of geological and structural

maps provided by PNOC EC. The interpretive product contains lithologic boundaries, strikes and dips, faults, folds, structural form lines, and geomorphic anomalies.

8.2.1.1 Radar Map Units (Lithology)

The following is a description of the radar appearance of each lithologic unit within the area of interest.

Pre-Cretaceous Metamorphics, Volcanics, Clastics (Bst)

Rocks of the basement complex are widespread throughout central Cebu where they form dissected ridges of high relief. The steep ridge faces cause high intensity radar returns and are identified on the imagery by linear or angular bright tones. Radar shadow is prominent in backslope areas. The clastic units frequently exhibit well defined stratification.

Middle-Late Oligocene Clastics (Tocgs)

The Calagasan Formation map unit (Tocgs) is located in central and southcentral Cebu, and occurs as low lying terrain between adjacent areas of higher elevation. On radar imagery, this unit produces uniform bright tones which are indicative of a continuously rough surface. Low relief ridges which have been severely dissected are common throughout the exposures.

Late Oligocene Limestone (Tmcl)

The Cebu Limestone Member of the Cebu Formation has a comparatively small surface exposure. The limestone forms narrow, conspicuous, highly resistant, steep ridges which are recognized on the imagery as curvilinear, bright tones.

Early Miocene Clastics (Tme)

Widespread occurrences of the Malubog Formation map unit (Tme) are in central Cebu. Typically, the unit forms smooth rolling hills and valleys of moderate relief. Radar image tones are predominantly intermediate on the gray scale which indicates a relatively smooth surface.

Middle Miocene Clastics (Tmm)

The boundaries of the Tmm map unit are difficult to locate due to limited surface expression and indistinct image appearance. The unit forms low relief terrain, without obvious stratification. Geologic map data aided the interpreters in defining the Tmm map unit boundaries.

Middle-Late Miocene Limestone and Clastics (Tmmgt)

The Middle-Late Miocene map unit (Tmmgt) occurs predominantly in west central Cebu. On radar imagery, this unit appears thick bedded and very well stratified. The strata dip to the west at moderate to steep angles. Bright linear image tones result from updip, ridge-forming escarpments. Ridges have been reduced to individual angular peaks where escarpments have been heavily dissected by faults.

Late Miocene-Pliocene Limestone (Tpbl)

The Barili Limestone (Tpbl) is one of the most widespread formations in the southern half of Cebu. The map unit exhibits a karst topographic surface which is easily identified on radar imagery by a distinctive pitted surface. Small scale, subrounded, bright tones mark pit and groove edges which strongly reflect the incident radar imagery.

Late Miocene-Pliocene Clastics (Tpbm)

The Barili Marl (Tpbm) covers a comparatively large surface area in southwestern Cebu. The unit is characterized by uniform intermediate image tones which exhibit a smooth image texture. Escarpments which are associated with steeply dipping strata appear on the imagery as sinuous and linear bright tones.

Pliocene-Pleistocene Limestone (Tpcl)

The Carcar Limestone map unit (Tpcl) is the most widespread of all formations on the island of Cebu. It occupies nearly the entire coastal area and is continuous across the island in the north. A distinctive pitted surface (karstic) permits easy delineation of map unit boundaries throughout most of the outcrop area. The unit extends outward from the center of the island. Sharp, angular escarpments with near vertical faces cause high intensity radar returns.

Quaternary Alluvium (Qal)

Quaternary alluvial deposits occur mainly along coastal margins and are easily recognized on radar imagery by their flat and featureless appearance. Image tones are intermediate to dark except where heavy vegetation cover causes volume scattering of incident radar energy, resulting in bright image tones.

8.2.1.2 Structure

Numerous folds and faults were highlighted on the radar imagery. The Cebu Island structural style is characterized by two distinct fold groups. Broad, oval-shaped, breached anticlines are oriented parallel to the local trend of the island and are generally centered between adjacent coastlines. These folds are regionally expressed and have axial lengths

that vary from 7-15 miles (11-24 km). A second group of smaller, lower amplitude, more narrow folds is located along the southwest, northwest, and northern coastlines, and also near the limbs of the major central anticlines.

Faults are prevalent throughout the entire study area. Major faults generally have a strike direction that is near parallel to coastlines. These faults are recognized on the radar imagery by abrupt textural differences between radar map units on opposite sides of the faults. Local or minor faults occur with high frequency in the Pliocene-Pleistocene Carcar Limestone. The faults in this group generally intersect at 45° angles and strike northeast or northwest.

8.2.2 Radar-Lineament Map

Lineaments mapped on Cebu Island have at least two general orientations. One major group is northwest-trending, whereas a second less significant group is northeast-trending. The majority of the lineaments in these two groups is located along coastal regions within exposures of the Pliocene-Pleistocene Carcar Limestone. These linear features may correspond to zones of structural weakness in the limestone.

Other lineaments have a more north-south orientation and are commonly parallel to local coastlines. These lineaments may represent contacts between stratigraphic units that dip seaward from the center of the island, or poorly expressed faults which are present in the dipping strata.

8.3 Prospect Evaluation

The prioritization sequence and ranking of prospects which follows evolved from the analysis of radar imagery used in conjunction with

corroborative data available from sources previously discussed. The study area was subdivided into two geologic terrain categories which are designated by Roman numerals (Fig. 8.3). The values of the numerals have no prioritization significance, but are provided to aid discussing the significant geologic aspects of Cebu Island. The letters (A - J) indicate prospects with potential for hydrocarbon accumulation and entrapment.

8.3.1 Geologic Terrain Category Criteria

Area I

* Youngest stratigraphic formation of the area is widespread at the surface indicating the possibility for sufficient subsurface sedimentary section.

* Contains several structural features that may provide potential sites for hydrocarbon accumulation.

Area II

* Youngest stratigraphic unit at the surface is Middle-Late Miocene age indicating lack of suitable subsurface sedimentary section.

* Pre-Cretaceous basement metamorphic rocks constitute a large percentage of the surface area.

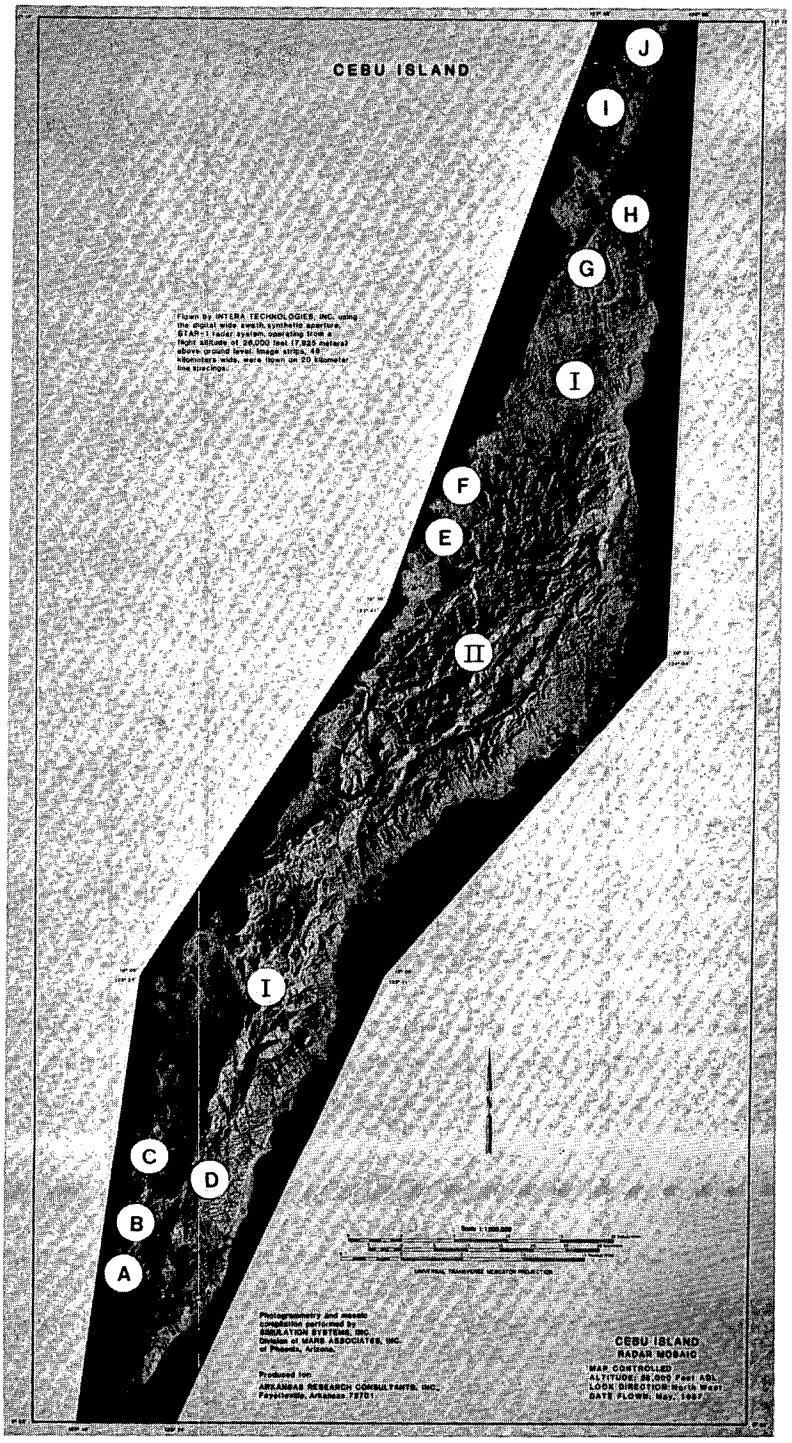

Figure 8.3: Terrain categories (I–II) and prospects (A–J).

8.3.2 Prospects and Selection Criteria

Based on negative criteria, Area II has been excluded as having potential for hydrocarbon accumulation. Area I has several distinct anticlinal features that have been inferred from radar imagery analysis.

Prospect A Anticlinal Crests (9°37'40"N, 123°20'30"E), (9°36'40"N, 123°20'15"E)

* Two directions of plunge; creating potential for complete closure.
* Secondary structures (faults) located down dip from crest; potential for additional entrapment feature and/or fracture porosity.
* Prospect area is adjacent to regions which have demonstrated the presence of hydrocarbons.
* Location appears to coincide with a seismically defined structure, the Ginatilan North Prospect (PNOC EC, 1987b).
* Faults transverse crest which may provide additional structural entrapment.

Prospect B Anticlinal Crest (9°40'N, 123°20'30"E)

* Late Miocene-Pliocene strata at the surface indicates suitable subsurface sedimentary section.
* Two directions of plunge; creating potential for complete closure.
* Surface exposure of Late Oligocene stratigraphic unit near the prospect indicates faulting which may provide additional structural entrapment.
* Structure is well expressed on radar imagery.
* Location appears to coincide with a seismically defined structure, the Malabuyoc Prospect (PNOC EC, 1987b).

Prospect C Anticlinal Crest (9°42'55"N, 123°21'50"E)

* Two directions of plunge; creating potential for complete closure.

* Surface exposure of Late Oligocene stratigraphic unit near the prospect indicates faulting which may provide additional structural entrapment.

* Numerous wells in the prospect area have demonstrated the presence of hydrocarbons.

* Structure is well expressed on radar imagery.

* Prospect appears to coincide with seismically defined prospects; the Lumpan and Alegria Prospects (PNOC EC, 1987b).

Prospect Area D Anticlinal Crests (9°42'15"N, 123°26'20"E), (9°43'30"N, 123°26'30"E)

* Late Miocene-Pliocene stratigraphic units at the surface indicate suitable subsurface sedimentary section.

* Secondary structures (faults) located down dip from crest; potential for structural entrapment features and/or fracture porosity.

* Prospect Area appears to be in proximity to a seismically defined structure, the Central Anticline East Prospect (PNOC EC, 1987b).

Prospect E Anticlinal Crest (10°35'20"N, 123°45'20"E)

* Two directions of plunge, creating potential for complete closure.

* Secondary structures (faults) located down dip from crest; potential for additional entrapment features and/or fracture porosity.

* Structure is regionally expressed, extending over 5 miles (8 km) in the axial direction.

* Structure is well expressed on radar imagery.

* Faults occur near the crest which may provide additional structural entrapment.

Prospect F Anticlinal Crest (10°39'45"N, 123°47'20"E)

* Two directions of plunge, creating potential for complete closure.

* Secondary structures (faults) located down dip from crest; potential for additional entrapment features and/or fracture porosity.

* Structure is regionally expressed extending over 5 miles (8 km) in the axial direction.

* Structure is well expressed on radar imagery.

* Severely faulted crest which may provide additional structural entrapment.

Prospect G Anticlinal Crest (10°56'40"N, 123°58'00"E)

* Structure is regionally expressed, extending over 9 miles (14.4 km) in the axial direction.

* Secondary structures (faults) located down dip from crest; potential for entrapment features and/or fracture porosity.

* Breached anticlinal crest indicates some loss of near-surface structural closure.

* Severely faulted crest which may provide additional structural entrapment.

Prospect H Anticlinal Crest (11°01'30"N, 124°01'30"E)

* Moderately expressed on radar imagery.

* Prospect is located near an area which has demonstrated the absence of hydrocarbons; however, these wells were drilled off structure.

* Severely faulted crest which may provide additional structural entrapment.

Prospect I Anticlinal Crest (11°10'N, 123°59'E)

* Late Miocene-Pliocene stratigraphic formation at the surface indicates suitable subsurface sedimentary section.

* Secondary structures (faults) located down dip from crest; potential for structural entrapment features and/or fracture porosity.

* Structure is regionally expressed, extending over 6 miles (9.6 km) in the axial direction.

* Several wells in the area have demonstrated the presence of hydrocarbons.

* Prospect is considered a structural lead on the Play Map of the Visayan Basin, Plate No. III A. H. 20 (BED et al., 1987).

* Breached anticlinal crest indicates some loss of near-surface structural closure.

Prospect J Anticlinal Crest (11°15'10"N, 124°02'20"E)

* Pleistocene stratigraphic formation at the crest indicates suitable subsurface sedimentary section.

* Severely faulted crest which may provide additional structural entrapment features and/or fracture porosity.

* Nearby wells demonstrated the presence of hydrocarbons.

* Moderately expressed on radar imagery.

8.4 Estimated Hydrocarbon Resources

According to BED et al. (1987), the Visayan Basin which includes Cebu Island is ranked as Class II, having good potential for both oil and gas. Average field size should range from 5-50 MMBBLS of oil, or 50-500 BCF of gas.

8.5 Recommendations

The anticlinal prospects referred to as prospects "A", "B", "C" and "D" (described in Section 8.3.2) appear to be in proximity to seismically-defined structures. In order to refine the prospects obtained from interpretation of the radar data, it is therefore recommended that:

* geophysical data be acquired and interpreted to confirm subsurface closure of prospects,

* the approximate thickness of the subsurface sedimentary section be inferred from the seismic data.

It is specifically recommended that:

* detailed field studies be conducted to determine the precise locations of surface features "A", "B", "C" and "D", and then compared with subsurface structural data,

* prospects which do not coincide with seismically-defined PNOC EC plays should be refined with additional seismic interpretation,

* more subtle structural targets, such as fault traps, should receive exploration attention using seismic data to confirm the radar imagery-defined fault zones.

9 SUMMARY AND RECOMMENDATIONS

The Philippines Archipelago is not well endowed with hydrocarbon reserves, and the Government of the Philippines is anxious to spur more petroleum exploration. For both the Philippine National Oil Company Exploration Corporation (PNOC EC) and Bureau of Energy Development (BED), it has been an important goal to upgrade available geological information on various sedimentary basins in the interest of attracting foreign firms to invest or explore for hydrocarbons. The Government of the Republic of the Philippines has invited new bids from international companies to explore for oil and gas in onshore and offshore sedimentary basins. To assist the private oil industry in the evaluation of the petroleum potential of these basins, the Government, with the assistance of a loan from the World Bank, has completed a nation-wide basin evaluation program.[4]

The collection and interpretation of radar imagery was designed to augment and complement the existing data base prepared by PNOC EC and BED. The primary objective of the project was to further the goals of international energy development by aiding the Republic of the Philippines in the assessment of potential petroleum prospects within the areas imaged. Secondary goals were to assist the Republic of the Philippines in utilizing state-of-the-art radar remote sensing technology for resource exploration, and to train key Philippines scientists in the use of imaging radar data.

---

4 BED, 1987, **Sedimentary Basins of the Philippines - Their Geology and Hydrocarbon Potential**, Bureau of Energy Development, Manila, The Republic of the Philippines.

9.1 Radar's Value

Because a radar provides its own source of illumination, radar images can be produced that preferentially highlight geologic structure and surface detail. Radar images so constructed provide unique information about the local geology which may not be available from other sources. Such information is needed in the Republic of the Philippines because although the region has been extensively mapped via conventional techniques, large uncertainties in the petroleum resource potential of the area still exist.

Radar's unique capabilities include:

* All weather, day-night operation
* Control of look direction and look angle for improved geological interpretation
* Wide areal coverage-synoptic view
* High resolution comparable with most remote sensing systems
* Stereo capability allows rapid formulation of geologic models
* Sensitivity to vegetation at shorter wavelengths
* Terrain texture discrimination in non-vegetated regions
* Digital capability for image enhancement and multi-sensor integration
* Radar mosaic provides an accurate base map

9.2 Data Acquired

Radar imagery covering roughly 60,000 km^2 was acquired. These data were collected by Intera Technology, Inc., under subcontract from ARCI. ARCI provided mission planning and quality assurance for the program.

Complete stereo coverage of five different regions was acquired. Within these five sites, the following four different sets of data were collected for hydrocarbon interpretation.

Hydrocarbon Sites

* Bondoc Peninsula
* Cotabato Basin, Mindanao
* Mindoro Island
* Cebu Island

9.3 Data Produced

The final data products were (1) negative film and positive prints of each of 34 flight line strips, (2) computer compatible tapes (CCT) of each image strip, and (3) negative film and positive prints of radar mosaics of four petroleum sites at 1:250,000 scale. The Intera STAR-1 imaging radar system used to acquire these data operated at X-band with the linear HH-polarization, and produced data representing 12 m resolution. The final data set represents one of the best examples of radar imagery for resource exploration available anywhere.

Interpretive data products produced include (1) geologic maps, (2) lineament maps, and (3) prospect evaluations. Development of geologic maps and prospect evaluations included extensive use of surface and subsurface data furnished by BED and PNOC EC. Thus, the final evaluation is a synthesis of all data available rather than simply that obtainable from the radar imagery itself. This is perhaps the most significant aspect of the program in that it demonstrates the use of radar as a sensor in an

integrated program for hydrocarbon and geothermal exploration. The imagery acquired is an excellent source of data that may be used to refine exploration strategy and define areas for more detailed investigation by ground survey and seismic data acquisition. The image analysis shows numerous areas of agreement with prospects developed from other data sources such as field and geophysical surveys. In addition, a considerable number of structures and prospects were discovered, particularly in areas where other data sources were unavailable.

9.4 Summary

This synthesis of all available data shows radar imagery to be an excellent survey tool in an integrated multilevel exploration. The radar by itself may be used to guide acquisition of more detailed data and develop a general exploration strategy. Where other survey data such as photography or LANDSAT are available, the unique response and illumination enhancement of surface structure obtainable with radar is seen to provide additional data complementary to other survey imagery.

Important new prospects and prospect areas have been identified which will provide a focus for further follow-up field and geophysical studies.

Especially for the Bondoc Peninsula and Cotabato Basin, Mindanao, radar imagery interpretation has provided an increase in the structural information by several orders of magnitude over existing data, and the fault and lineament patterns reveal structural complexity not previously recognized.

Hydrocarbon Prospects

* **Bondoc Peninsula** - Seven prime hydrocarbon prospects have been identified. It is recommended that these potential plays be refined with seismic data. The region is considered to have good potential for both oil and gas. Average field size should range from 5-50 MMBBLS of oil, and 50-500 BCF of gas.

* **Cotabato Basin** - Five prime hydrocarbon prospects have been identified. Two of these plays are in the central part of the basin where relatively large reserves are possible. The region is considered to have poor to fair oil potential. Average field size should be in the range of 5-20 MMBBLS of oil.

* **Mindoro Island** - Only the coastal margins on the southern two-thirds of Mindoro Island are considered favorable for hydrocarbon accumulation. Five prime hydrocarbon prospects and two additional prospect areas have been identified. Although the geologic maps provided by PNOC EC are of good quality for delineating fold patterns, the structural complexity of fault and lineament patterns has been revealed for the first time on the radar imagery. The Mindoro region is considered to have fair to good potential for predominantly gas plays. Average field size should be in the range of 5-50 MMBBLS of oil, or 50-500 BCF of gas.

* **Cebu Island** - Southern Cebu has received considerable seismic exploration effort; however, the northern half of the island has not been mapped in detail. Ten prime hydrocarbon prospects have been identified with more than half of them being located in the poorly explored northern portion part of the island. Cebu is considered to have good potential for both oil and gas. Average field size should range from 5-50 MMBBLS of oil, or 50-500 BCF of gas.

9.5 Highlights

* The radar geologic maps produced, while important by themselves, can be used to complement existing geoscience data and can provide new map products tailored to support exploration activities.

* An important aspect of radar investigations is that reconnaissance radar images facilitate field work in remote and impassable areas.

* The radar data will significantly improve the existing knowledge of stratigraphy and structure, and in many cases update existing geologic maps.

* Because of the significant number of new onshore prospects identified in this project, new seismic investigations are warranted. Prospects and prospect areas have been defined which will provide a focus for further follow-up field and geophysical studies.

* With the base line survey provided by radar, it is possible to upgrade and extend the interpretation using a large-scale (1:100,000 or 1:50,000) image format in conjunction with field surveys.

* A training course on radar interpretation has been provided to Philippines geoscientists, and they have been made aware of the importance of using radar imagery in other application areas such as land cover mapping, land use mapping, hydrology, and ground-water exploration.

* Radar imagery has provided significant new geologic information that could complement the existing petroleum potential data set used to attract foreign energy investment.

9.6 Recommendations

* Detailed field studies should be conducted to determine the precise locations of prime prospects and then correlate with all available subsurface data. Prospects that do not have supporting surface or subsurface data should be refined with seismic interpretation. More subtle structural targets, such as fault traps and geomorphic anomalies should receive exploration attention using seismic data to confirm the radar imagery-defined plays.

* Additional radar imagery should be acquired over a much larger region of the Philippines, especially within those sedimentary basins where radar can contribute significant data to the development of an integrated exploration strategy for hydrocarbons.

This page is intentionally left blank.

10 REFERENCES

BED, Robertson Research Australia, Pty. Ltd., and Flower, Doery and Bucham, Pty. Ltd., 1987, **Sedimentary Basins of the Philippines - Their Geology and Hydrocarbon Potential**.

BED, 1985, ***Geologic Map of the Bicol Shelf - Lamon Bay - and South east Luzon Basins, Scale 1:500,000***, Philippine Bureau of Energy Development, Manila.

Blom, R., and M. Daily, 1982, ***Radar Image Processing for Rock Type Discrimination***, **IEEE Trans. Geo. Rem. Sens.**, Vol. GE-20, pp. 343-351.

Canoba, C. A., 1983, ***SIR-A and Landsat Imagery Interpretation of Sierra Velazco, La Rioja Province, Argentina***, **ITC Journal**, pp. 332-337.

Corby, G. W. et al., 1951, ***Geology and Oil Possibilities of the Philippines***, Rep. Philippine Dept. Agric. and Nat. Resources Tech. Bull. 21.

Curlis, J. D., V. S. Frost, and L. F. Dellwig, 1986, ***Geologic Mapping Potential of Computer-Enhanced Images from the Shuttle Imaging Radar: Lisbon Valley Anticline, Utah***, **Photogrammetric Engineering and Remote Sensing**, Vol. 52, No. 4, pp. 525-532.

Daily, M., C. Elachi, and T. Farr, 1978, ***Discrimination of Geologic Units in Death Valley Using Dual Frequency and Polarization Imaging Radar Data***, **Geophysical Research Letters**, Vol. 5, No. 10, pp. 889-892.

Elachi, C., R. Blom, M. Daily, T. Farr, and R. S. Saunders, 1980, ***Radar Imaging of Volcanic Fields and Sand Dune Fields: Implications for VOIR***, in Radar Geology Workshop Report, Snowmass, Colorado, JPL Publ., 80-61, pp. 114-150.

Ford, J., and Others, 1980, ***Seasat Views North America, the Caribbean and Western Europe with Imaging Radar***, JPL Publication 80-67, Pasadena, California, pp. 141.

Holloway, H. H., 1982, ***North Palawan Block, Philippines - Its Relation to Asian Mainland and Role in Evolution of South China Sea, Amer. Assoc. Petroleum Geologists Bulletin***, Vol. 66, No. 9, pp. 1355-1383.

Kaupp, V. H., W. P. Waite, and H. C. MacDonald, 1982, ***Incidence Angle Considerations for Spacecraft Imaging Radar***, IEEE Trans, on Geoscience and Remote Sensing Vol. GE-20, No. 3, pp. 384-390.

Longoria, J. F., and O. H. Jimenez, 1985, ***Spaceborne Radar Imagery in Regional Geologic Mapping of the Sierra Madre Oriental, Northeastern Mexico: The Use of Morphostratigraphic Units in Mapping by Remote Sensing***, Fourth Thematic Conference - Remote Sensing for Exploration Geology, San Francisco, CA., pp. 437-446.

MacDonald, H. C., 1980, ***Historical Sketch - Radar Geology***, in Proc. Radar Geology Workshop, Snowmass, Colorado, JPL Rept. 80-61, Pasadena, California, pp. 23-37.

O'Leary, D. W., J. D. Friedman, and H. A. Pohn, 1976, ***Lineaments, Linear, Lineation - Some Proposed New Standards for Old Terms***, Geological Society of America Bulletin, Vol. 87, pp. 1463-1469.

Petroconsultants, 1986, ***Foreign Scouting Service, Far East***, October 1986, Map Scale 1:2,000,000, Geneva, Switzerland.

Petroconsultants, 1988, ***Philippine Exploration Activity***, International Oil Letter, Vol. 4, No. 19, Houston, Texas.

Philippine Bureau of Mines and Geo-sciences, 1981, ***Geology and Mineral Resources of the Philippines***, Vol. 1, Ministry of Natural Resources, Manila, 406 p.

Philippine Mineral Fuels Division, 1976, ***A Review of Oil Exploration and Stratigraphy of Sedimentary Basins of the Philippines***, United Nations ESCAP, CCOP Technical Bulletin, Vol. 10, pp. 55-72.

Philippine Oil Development Co., 1978, ***Geology of Bondoc Peninsula***, unpublished report.

PNOC EC, 1986, ***Geologic Map of Mindoro***, Scale 1:250,000, Philippine National Oil Company Exploration Corporation, Manila.

PNOC EC, 1987a, ***Petroleum Potential on Mindoro, Philippines***, Executive Summary, Philippine National Oil Company Exploration Corporation, Manila, 20 p.

PNOC EC, 1987b, **Petroleum Exploration in Cebu and Mindoro Philippines - An Invitation to a Joint Venture**, 10 p.

PNOC EC, 1987c, **Hydrocarbon Potential of the Cebu Basin Philippines**, 33 p.

Podwysocki, M. H., M. S. Power, and M. H. Kovolow, 1985, ***Use of Multi-Frequency Radar Images for Botanical and Lithologic Mapping in an Arid Terrain***, Thematic Conference, Remote Sensing for Exploration Geology, San Francisco, CA., p. 555.

Pravdo, S. H., B. Huneycutt, B. M. Holt, and D. N. Held, 1983, ***Seasat Synthetic-Aperture Radar Data User's Manual***, JPL Publ. 82-90, Pasadena, California, 52 p.

Rebillard, P., and D. Evans, 1983, ***Analysis of Co-Registered Landsat, Seasat, and SIR-A Images of Varied Terrain Types***, Geophysical Research Letters, Vol. 10, No. 4, pp. 277-280.

Robertson Research International Ltd., 1975, ***The Regional Geology and Hydrocarbon Potential of the Philippines***, Vol. 1, 108 p.

Santiago, Sigfredo, 1968, ***The Geology and Oil Possibilities of Bondoc Peninsula, Quezon, Province***, White Eagle Oil Company, unpublished report.

Wadge, B., and Dixon, T. H., 1984, ***A Geological Interpretation of Seasat-SAR Imagery of Jamaica***, **Journal of Geology**, Vol. 92, pp. 561-581.

Appendix A – CEBU WELL HISTORY

The following table contains a listing of the known historical exploratory wells drilled on Cebu.

Table A.1: Significant exploratory wells and hydrocarbon occurrences – Cebu. (Modified from BED et al., 1987)

Well Name	Drilling Date	Total Depth m (ft)	Play Type	Defined by	Target	Age of Rock at T.D.	Results	Remarks
Toledo-1 (SMITH, BELL & CO)	1896	268.3 (880)	No data	Oil seeps	No data	Malubog	Oil shows	Indeterminate
Toledo-2 (SMITH, BELL & CO)	1896	405.5 (1330)	No data	Oil seeps	No data	Malubog	Oil shows	Indeterminate
Toledo-3 (SMITH, BELL & CO)	1936	152.4 (500)	No data	Oil seeps	No data	Malubog	Oil shows	No data
Barili-1 (NAT'L DEV'T CO)	1941	623.5 (2045)	Anticline	Surface geology	No data	Miocene	Oil shows	No data
Barili-1A (NAT'L DEV'T CO)	1941	1067.1 (3500)	Anticline	Surface geology	No data	Not known	Oil shows	No data
Cebu-1 (PODCO / FAR EAST OIL)	1942	2538.4 (8326)	Anticline	Surface mapping	No data	L. Oligo-cene(?) (Malu-bog Fm.)	Oil shows in the Mal-ubog Fm.	Well and equipment demolished at start of WWII
Cebu-2 (PODCO)	1947	3033.5 (9950)	Anticline	Surface mapping	No data	Metam. base-ment	Good oil and gas shows in Malubog Fm.	Valid test
Cebu-3 (PODCO)	1949	2336.3 (7663)	Anticline	Surface mapping seismic	No data	Base-ment	Tested a total of 9 MMCFGPD in 113 days from Barili s	Valid test
Cebu-4 (PODCO)	1950	1801.5 (5909)	Anticline	Surface mapping seismic	No data	Base-ment	Gas shows	?valid test

Table A.1 (cont.)

Well Name	Drilling Date	Total Depth m (ft)	Play Type	Defined by	Target	Age of Rock at T.D.	Results	Remarks
Palanas-1 (ACOJE)	1956	236.9 (777)	No data	No data	No data	Not known	Dry	Indeterminate
Palanas-2 (ACOJE)	1956	68.3 (224)	No data	No data	No data	Not known	Dry	Indeterminate
Palanas-3 (ACOJE)	1956	61.0 (200)	No data	No data	No data	Not known	Dry	Indeterminate
Libertad-1 (ACOJE)	1958	1775.6 (5824)	Anticline	Surface geology	No data	Malubog Fm. (?)	Gas shows	?Valid test
Libertad-2 (ACOJE)	1958	186.6 (612)	Anticline	Surface geology	Dingle ls	Not known	Dry	?Valid test
Libertad-3 (ACOJE)	1958	197.2 (647)	Anticline	Surface geology	Dingle ls	Not known	Dry	?Valid test
Libertad-4 (ACOJE)	1958	221.0 (725)	Anticline	Surface geology	Dingle ls	Not known	Dry	?Valid test
Libertad-5 (ACOJE)	1958	260.7 (855)	Anticline	Surface geology	Dingle ls	Not known	Dry	?Valid test
Libertad-6 (ACOJE)	1958	259.1 (850)	No data	No data	No data	Not known	Dry	?Valid test
Libertad-7 (ACOJE)	1958	249.7 (819)	No data	No data	No data	Not known	Dry	Indeterminate
Libertad-8 (ACOJE)	1958	268.3 (880)	No data	No data	No data	Not known	Dry	Indeterminate
Libertad-9 (ACOJE)	1958	230.2 (755)	No data	No data	No data	Not known	Dry	Indeterminate
Libertad-10 (ACOJE)	1958	229.6 (753)	No data	No data	No data	Not known	Subcom-mercial gas from Barili ls	Indeterminate
Libertad-11 (ACOJE)	1958	217.1 (712)	No data	No data	No data	Late Miocene (Barili ls)	Tested about 250 MCFGPD from Barili ls Retested 280 MCFGPD	
Libertad-12 (ACOJE)	1958	42.7 (140)	No data	No data	No data	Plio - Pleisto-cene(?) Carcar ls	Dry	Indeterminate
Libertad-13 (ACOJE)	1958	175.3 (575)	No data	No data	No data	Not known	Tested about 250 MCFGPD from Barili ls Retested 650 MCFGPD in 1974	Indeterminate

Table A.1 (cont.)

Well Name	Drilling Date	Total Depth m (ft)	Play Type	Defined by	Target	Age of Rock at T.D.	Results	Remarks
Reina Regente-1 (REDECO)	1958	277.4 (910) 583.5 (1914)	No data	No data	No data	Early Miocene	Good oil shows at 437.5 - 447.3m	Indeterminate
Libertad-14 (ACOJE)	1958	220.4 (723)	No data	No data	No data	Not known	Dry	Indeterminate
Reina Regente-2 (REDECO)	1959	276.2 (906)	No data	No data	No data	Early Miocene	Oil shows	Indeterminate
Reina Regente-3 (REDCO)	1958	255.2 (837)	No data	No data	No data	Early Miocene	Oil and gas shows	Indeterminate
Bolokbolok-1 (HIXBAR / ACOJE)	1959	750.9 (2463)	No data	No data	No data	Not known	Dry	Indeterminate
Libertad-16 (ACOJE)	1959	333.2 (1093)	No data	No data	No data	Not known	Dry	Indeterminate
Libertad-20 (ACOJE)	1959	287.5 (943)	No data	No data	No data	Not known	Dry	Indeterminate
Libertad-21 (ACOJE)	1959	458.2 (1503)	No data	No data	No data	Not known	Dry	Indeterminate
LaPaz-1 (ACOJE)	1959	629.9 (2066)	No data	No data	No data	Not known	Minor oil and gas shows	Indeterminate
Bogo-1 (ACOJE)	1959	2524.7 (8281)	Anticline	Surface geology Gravity	Middle Miocene and older carbonates and clastics	Early Miocene (?)	Minor gas shows	Valid test
Tangob-1 (ACOJE)	1959	626.5 (2055)	No data	No data	No data	Not known	Dry	Indeterminate
Reina Regente-1A (REDECO)	1959	407.0 (1335)	No data	No data	No data	Early Miocene (Malubog Fm.)	Tested 3 - 6 bbl oil from Malubog Fm. Retested 29.4 BOPD in 1974	?Valid test
Reina Regente-1A X (REDECO)	1959	1833.8 (6015)	No data	No data	No data	Metam. basement	Tested 250 BOPD from Malubog Fm. Retested a maximum of 42 BOPD in 1960	?Valid test
LaPaz-3 (ACOJE)	1959	1306.1 (4284)	No data	No data	No data	Not known	Minor oil and gas shows	Indeterminate

Table A.1 (cont.)

Well Name	Drilling Date	Total Depth m (ft)	Play Type	Defined by	Target	Age of Rock at T.D.	Results	Remarks
Manta-longon-1 (ACOJE)	1959	633.2 (2077)	No data	No data	No data	Not known	Dry	Indeterminate
Libertad-18 (ACOJE)	1959	No data	No data	No data	No data	Not known	Dry	Indeterminate
Libertad-19 (ACOJE)	1959	No data	No data	No data	No data	Not known	Dry	Indeterminate
Villalon-1 (PODCO / REDECO)	1960	1109.7 (3640)	Anticline	Surface geology	No data	Not known	Dry	Indeterminate
Parahinog-1 (PODCO / REDECO)	1960	607.9 (1994)	No data	No data	No data	Not known	Dry	Indeterminate
Malolos-1 (HIXBAR / ACOJE)	1960	2749.1 (9017)	No data	No data	No data	Malubog Fm	Tested some 39° API oil at 2155.6 - 2252.1 m	Indeterminate
Maya-2 (MST-2) (AAOC)	1961	173.8 (570)	Anticline	Recon geology gravity and sono probe	?Maingit Fm	Maingit Fm	Dry	Indeterminate
Guadalupe-1 (ACOJE / HIXBAR)	1961	621.6 (2039)	No data	No data	?Maingit Fm	Maingit Fm	Oil shows	Indeterminate
Daanban-tayan-A (PODCO)	1961	978.6 (3210)	No data	No data	No data	Not known	Dry	Indeterminate
Guadalupe-2 (ACOJE / HIXBAR)	1961	592.7 (1944)	No data	No data	?Maingit Fm	Maingit Fm	Dry	Indeterminate
Maya-7 (MST-7) (AAOC)	1961	30.5 (100)	Anticline	Recon geology gravity and sono probe	?Maingit Fm	Maingit Fm	Dry	Indeterminate
Malolos-4 (ACOJE / HIXBAR)	1961	2205.8 (7235)	No Data	No Data	No Data	Malubog Fm	Oil shows	Indeterminate
Maya-10 (MST-10) (AAOC)	1961	64.0 (210)	Anticline	Recon geology gravity and sono probe	?Maingit Fm	Maingit Fm	Dry	Indeterminate

Table A.1 (cont.)

Well Name	Drilling Date	Total Depth m (ft)	Play Type	Defined by	Target	Age of Rock at T.D.	Results	Remarks
Maya-11 (MST-11) (AAOC)	1961	87.2 (286)	Anticline	Recon geology gravity and sono probe	No Data	L. Miocene	Produced 450 bbls oil in 203 hrs from Maingit clastics	?Valid test
Reina Regente-4 (REDECO)	1961	690.2 (2264)	No Data	No Data	No Data	Not known	Oil shows	Indeterminate
Maya-13 (MST-13) (AAOC)	1961	232.0 (761)	Anticline	Recon geology gravity and sono probe	No Data	Not known	Dry	Indeterminate
Daanban-tayan-B (PODCO)	1961	153.3 (503)	No Data	No Data	No Data	Not known	Dry	Indeterminate
Reina Regente-5 (REDECO)	1961	570.4 (1871)	No Data	No Data	No Data	Not known	Dry	Indeterminate
Daanban-tayan-C (PODCO)	1961	518.0 (1699)	No Data	No Data	No Data	Not known	Dry	Indeterminate
Maya-14 (MST-14) (AAOC)	1961	114.9 (377)	Anticline	Recon geology gravity and sono probe	No Data	Not known	Dry	Indeterminate
Reina Regente-1B (REDECO)	1961	533.5 (1750)	No data	No data	No data	Not known	Subcommercial oil from Malubog Fm.	?Valid test
Maya-15 (MST 15) (AAOC)	1961	204.9 (672)	Anticline	Recon geology gravity and sono probe	No data	Not known	Dry	Indeterminate
Cebu-5 (PODCO)	1961	1252.7 (4109)	No data	No data	No data	L. Miocene (Barili Marl)	Dry	Indeterminate
Maya 16 (MST 16) (AAOC)	1961	268.3 (880)	Anticline	Recon geology gravity and sono probe	No data	Not known	Dry	Indeterminate
Reina Regente-6 (REDECO)	1961	597.9 (1961)	No data	No data	No data	Not known	Subcommercial oil from Malubog Fm.	?Valid test

Table A.1 (cont.)

Well Name	Drilling Date	Total Depth m (ft)	Play Type	Defined by	Target	Age of Rock at T.D.	Results	Remarks
Zaragosa-1 (ACOJE / HIXBAR)	1962	1880.0 (6169)	No data	No data	No data	Not known	Dry	Indeterminate
Maya-17 (MST 17) (AAOC)	1962	364.9 (1197)	Anticline	Recon geology gravity and sono probe	No data	Not known	Dry	Indeterminate
Maya-18 (MST 18) (AAOC)	1962	134.4 (441)	Anticline	Recon geology gravity and sono probe	No data	L. Miocene (Maingit Fm.)	Dry	Indeterminate
Villalon-3 (PODCO / REDECO)	1962	618.0 (2027)	No Data	No Data	No Data	Not known	Dry	Indeterminate
Dapdap-1 (PCRC (PHILEX))	1962	206.1 (676)	No Data	No Data	No Data	Not known	Dry	Indeterminate
Villalon-4 (PODCO / REDECO)	1962	564.0 (1850)	No Data	No Data	No Data	Not known	Tested 168 bbl of oil in 4 days from Malubog Fm	Hole blew out while perforating casing and was swabbed at 10 bbls / hr valid test
Hobot-1 (PCRC (PHILEX))	1962	176.8 (580)	No Data	No Data	No Data	Not known	Minor gas shows	Indeterminate
Maya-19 (MST 19) (AAOC)	1962	453.3 (1487)	No Data	No Data	No Data	Not known	Gas shows	DP stuck, shut in pressure of 1045 psi incomplete test
Daanban-tayan-1 (PCRC (PHILEX))	1962	138.1 (453)	No data	No data	No data	Not known	Dry	Indeterminate
Talisay-1 (PCRC (PHILEX))	1962	244.2 (801)	No data	No data	No data	Not known	Minor gas shows	Indeterminate
Maya-20 (Mst 20) (AAOC)	1962	109.7 (360)	No data	No data	No data	Not known	Dry	Indeterminate
Lugo-1 (ACOJE)	1962	710.3 (2330)	Reefal ls	Surface geology	No data	Not known	Gas shows	Valid test
Lanao-1 (PCRC (PHILEX))	1962	131.1 (430)	No data	No data	No data	Not known	Dry	Indeterminate

Table A.1 (cont.)

Well Name	Drilling Date	Total Depth m (ft)	Play Type	Defined by	Target	Age of Rock at T.D.	Results	Remarks
Maya-21 (MST 21) (AAOC)	1962	457.3 (1500)	Anticline	Recon geology gravity and sono probe	No data	Not known	Dry	Indeterminate
Maya-22 (MST 22) (AAOC)	1962	152.4 (500)	Anticline	Recon geology gravity and sono probe	No data	Not known	Dry	Indeterminate
Tabuelan-1 (AAOC / MOBIL / VIS.EXPL.)	1962	613.7 (2013)	No data	No data	No data	Middle Miocene	Dry	Indeterminate
Tabuelan-2 (AAOC / MOBIL / VIS.EXPL.)	1962	619.8 (2033)	No data	No data	No data	Maingit ls	Dry	Indeterminate
Bulalaqui Pt. (AAOC / MOBIL / VIS. EXPL.)	1963	523.2 (1716)	No data	No data	No data	Not known	Dry	Indeterminate
ST-26	1964	604.6 (1983)	No data	No data	No data	L. Miocene (Maingit ls)	Gas shows	Indeterminate
Alegria-1 (PODCO / REDECO / VIS. EXPL.)	1964	755.2 (2477)	No data	No data	No data	Not known	Dry	Indeterminate
Lumpan-1 (JOSE TIONG-1) (PODCO / REDECO)	1964	206.7 (678)	Anticline	Surface geology	M. Miocene ss	Middle Miocene	1964 tested 605 bbl oil (44° API) 1970 tested 255 bbl oil in 40 hrs. in 1974 tested 301 bbl oil in 72 hrs.	Valid test but drilled off structure
Lumpan-2 (PODCO / REDECO)	1964	204.3 (670)	Anticline	Surface geology	M. Miocene ss	Maingit Fm.	1964 tested 218 bbl oil. in 1973 tested 93 bbl oil (35.4°API)in 42 hrs.	Valid test but drilled off structure
Lumpan-3 (PODCO / REDECO)	1964	306.7 (1006)	Anticline	Surface geology	M. Miocene ss	Not known	Oil shows	Valid test but drilled off structure
Lumpan-4 (PODCO / REDECO)	1964	365.8 (1200)	Anticline	Surface geology	M. Miocene ss	Not known	Oil shows	Valid test but drilled off structure

Table A.1 (cont.)

Well Name	Drilling Date	Total Depth m (ft)	Play Type	Defined by	Target	Age of Rock at T.D.	Results	Remarks
Lumpan-5 (PODCO / REDECO)	1964	116.1 (381)	Anticline	Surface geology	M. Miocene ss	Not known	Dry	Valid test but drilled off strucutre
Lumpan-5a (PODCO / REDECO)	1964	385.1 (1263)	Anticline	Surface geology	M. Miocene ss	Not known	Oil shows	Valid test but drilled off strucutre
Alegria-2	1964	702.4 (2304)	Anticline	Surface geology	M. Miocene ss	Not known	Dry	Valid test but drilled off structure
Cletom-102 A-16 (PODCO / REDECO / CLETOM)	1964	533.5 (1750)	Anticline	Surface geology	M. Miocene ss and ls	Middle Miocene	Oil shows at 372.6 - 390.2 m and 449.0 - 463.4 m	Indeterminate
Cletom-102 A-21 (PODCO / REDECO / CLETOM)	1971	574.1 (1883)	Anticline	Surface geology	Middle Miocene ss / ls	Middle Miocene (Uling ls)	Gas shows	Valid test but drilled off structure
Badian-1 (PACIFIC / IMPERIAL)	1971	1211.6 (3974)	Anticline	Surface geology	L. and M. Miocene ss	L. Miocene (Maingit Fm.)	Gas shows from Maingit ss	Valid test
Cletom-102 A-20 (PODCO / REDECO)	1971	470.7 (1544)	Anticline	Surface geology	Middle Miocene ss / ls	M. Miocene (Toledo Fm.)	Gas and oil shows	Valid test. Encountered 13.4 m of hydrocarbon bearing sand at bottom that flowed 13 bbls of light oil in 8 min with pressure of 650 psi. Later testing no oil.
Cletom-102 A-29 (AAOC / PIONEER / ACOJE / CLETOM)	1972	716.5 (2350)	Anticline	Surface geology	Middle Miocene ss / ls	Toledo Fm.	Gas and oil shows	Valid test. Drilled 2 gas horizons 554.9 - 590.0. Produced gas with intermittent oil flow. Drilled off structure.
CMB-1 (AAOC / PIONEER / CPC)	1972	1018.3 (3340)	Anticline	Surface geology, surrounding well data	Oligocene L. Miocene ls / ss	Argillite Metam. Basement (Cretaceous)	Tested negligible amounts of oil and gas from L. Miocene ls	Valid test

Table A.1 (cont.)

Well Name	Drilling Date	Total Depth m (ft)	Play Type	Defined by	Target	Age of Rock at T.D.	Results	Remarks
CMB-2 (AAOC / PIONEER / CPC)	1972	967.4 (3173)	Anticline	Surface geology, other well data, seismic and gravity surveys	L. Miocene ls E. Miocene ls/ss L. Oligocene ls	Argillite Metam. Basement (Cretaceous)	Tested 70 - 100 MCFGD (478 - 486 m) & 106 BOPD from M. Miocene ss production rapidly declined	Valid test but drilled off structure
Cletom-102 A-33 (REDECO / PODCO / CLETOM)	1972	961.3 (3153)	Anticline	Surface geology	Middle Miocene ss / ls	Maingit Fm.(?)	Oil and gas shows	Suspended due to stuck pipe
CMB-3 (AAOC / PIONEER / CPC)	1972	1140.2 (3740)	Anticline ss lenses	Seismic gravity drilling data	E. Miocene sand lenses ls stringers	L. Oligocene (Cebu ls)	Dry	Valid test
CMB-4 (AAOC / PIONEER / CPC)	1972	787.2 (2582)	Anticline ss lenses	Seismic gravity drilling data	E. Miocene sand lenses ls stringers	L. Oligocene	Tested total of 8.6 bbl of oil from Malubog Fm. in 36 days	Valid test
DAB-1 (AAOC / PIONEER / CPC)	1973	2404.0 (7888)	Anticline stratigraphic trap	Gravity other well data	Late and Middle Miocene ss lenses and ls and Late Oligocene ls	L. Oligocene (Cebu ls)	Dry	Valid test
TLS-1 (AAOC / PIONEER / CPC)	1973	1866.5 (6122)	Anticline stratigraphic traps	Seismic gravity other well data surface geology	Late Miocene ss and Early Miocene ss and ls	E. Miocene (Malubog Fm.)	Dry	Valid test
NR-1 (REDECO / PODCO)	1973	307.0 (1007)	Anticline	Surface geology other well data	Late Miocene ss	L. Miocence (Maingit Fm.)	Tested 26.2 bbl oil (39.4° API) in 3.5 hrs from Maingit Fm. In 1974, tested max of 12 BOPD	Valid test. Drilled 2 oil bearing zones (287.8 - 298.0 m and 300.3 - 306.4 m). Drilled off structure.
Sagay-M-2 (ACOJE / SOUTH SEAS)	1973	843.9 (2768)	No data	No data	No data	Barili Ls (L. Miocene)	Dry	Not valid test. Severe loss circulation in Barili Ls
Sagay-M-1 (ACOJE / SOUTH SEAS)	1974	1417.1 (4648)	No data	No data	No data	E. Miocene? (Malubog Fm.)	Oil shows	Not valid test due to formation sloughing

Table A.1 (cont.)

Well Name	Drilling Date	Total Depth m (ft)	Play Type	Defined by	Target	Age of Rock at T.D.	Results	Remarks
CPR-1 (REDECO / CPC / PIONEER)	1974	1588.4 (5210)	Anticline	Surface geology other well data	L. Miocene ss	L. Miocene (Maingit Fm.)	Tested max 424 MCFGPD and some oil from Maingit clastics	Valid test
CPR-2 (REDECO / CPC / PIONEER)	1975	2045.7 (6710)	Anticline fault trap	Surface geology other well data	L. Miocene ss	E. Miocene (Malubog Fm.)	Tested max 212 MCFGPD and 16.2 BOPD from Maingit clastics	Valid test
CPR-3 (REDECO / CPC / PIONEER)	1975	1468.6 (4817)	Anticline	Surface geology other well data	E. Miocene ss and ls	E. Miocene (Malubog Fm.)	Dry	Valid test on structure
Malabuyoc-1 (CPRS-1) (CPC)	1977	1077.4 (3534)	Anticline	Well data	L. Miocene ss	L. Miocene (Maingit Ls)	Dry	Valid test on structure
San Remigio-1 (PODCO)	1977	2593.9 (8508)	Carbonate buildup	Seismic	E. to M. Miocene reef	E. Miocene (Toledo Fm.)	Dry	No reefs. Not valid test
Kampisong-1 (CPC)	1978	1531.4 (5023)	Anticline	Surface geology seismic other well data	M. to L. Miocene ss and ls	E. Miocene (Malubog Fm.)	Dry	Valid test on structure
Malabuyoc-2 (CPRS-3) (CPC)	1979	1250.5 (4200)	Anticline	Surface geology and other well data	L. Miocene ss	L. Miocene (Maingit Ls.)	Tested max 106 MCFGPD from Maingit clastics	Valid test on structure
Bogo-2 (PODCO)	1979	1413.7 (4637)	Reefal Carbonate	Seismic	L. Miocene reef	L. Miocene (Barili Fm.)	Dry	Valid test. Encountered reef
Mayo-1 (PODCO)	1979	1219 (4000)	Reef	Seismic	L. Miocene reef	L. Miocene (Maingit clastics)	Dry	

NAT'L DEV'T CO - National Development Company
PODCO - Philippine Oil Development Company
ACOJE - Acoje Oil Exploration & Drilling Co., Inc.
REDECO - Republic Resources & Development Corporation
HIXBAR - Hixbar Mining Co., Inc.
VIS EXPL - Visayan Exploration
AAOC - American-Asiatic Oil Corporation
MOBIL - Mobil Philippines Exploration, Inc.
CLETOM - Cletom International Exploration Corporation
PACIFICA - Pacifica Richfield Corporation
IMPERIAL - Imperial Resources, Inc.
CPC - Chinese Petroleum Corporation

Appendix B – TRAINING COURSE

A training course in the methods of interpreting SLAR images, the relative merits of SLAR vs other forms of images, and the results of the interpretation of images used for this project was prepared. The training course, of one week duration, was conducted for key Philippine geoscientists during May, 1988.

In the following sections are shown an outline of the course and a very brief description of some of the more significant points concerning the use of radar images for geoscience applications. The details of the treatment are contained in the notes[5] distributed to the training course participants.

B.1 Training Course Outline

The following topics were covered in the training course. The fundamental theoretical concepts are contained within this document, but the enhanced treatment beyond basic principles will be presented during the course.

I. Radar theory.
- **i.** Real aperture systems.
- **ii.** Synthetic aperture systems.
- **iii.** Stereo radar concepts.

II. Interpretation concepts.
- **i.** Principles of interpretation.
- **ii.** Radar image interpretation keys.
- **iii.** Laboratory exercises.

---

5 ARCI, 1988, ***SAR Technology and Interpretation***, ARCI TR 8701-104, Arkansas Research Consultants, Inc., Fayetteville.

III. **Multi-parameter concept.**
   - **i.** Frequency.
   - **ii.** Polarization.
   - **iii.** Techniques and exercises.

IV. **Enhancement Techniques**
   - **i.** Resolution vs coherent noise.
   - **ii.** Dynamic range, mapping, and information content.
   - **iii.** Image quality.
   - **iv.** Mission planning.
   - **v.** Digital image exploitation.

V. **Advanced Concepts**
   - **i.** Automated digital stereo.
   - **ii.** Interferometry techniques.
   - **iii.** Automated image rectification.
   - **iv.** Commercial imaging systems.
   - **v.** Future radar sensors and space programs.

B.2 Background

B.2.1 Introduction

Radar is generally described as a mapping device although the direct product is not a map but a visual output, called imagery, from which maps can be constructed. Although the resolutions of most side looking airborne radar (SLAR) systems do not match those of high resolution photography (but exceed resolutions of systems such as LANDSAT MSS - multi-spectral scanners), these same systems have the unique ability to delineate physical characteristics of the Earth's surface providing an image of *photographic* quality independent of visibility or weather conditions. This operational advantage is related to the wavelength region of radars, which can penetrate clouds, smoke, fog, and most precipitation. Radar mapping surveys can thus be conducted at virtually any time, day or night.

A task shared by almost every nation in the world today is the identification, development, and conservation of natural resources. From the geologist's point of view, it is essential that older exploration methods be improved, and newer exploration techniques be developed. The unique operational capabilities and information content available in radar remote sensing establishes it as a prime candidate for continued evaluation and development as an exploration tool.

Microwave sensing shows two distinct areas of sensor utilization; active and passive. The active systems, which will be explained in detail in other sections, have been employed to generate radar images for a variety of geoscience studies for which cameras were exclusively used in the past. In contrast, passive systems have not yet proven to be practical for most geologic exploration investigations. The passive microwave radiometer, for example, when directed toward the ground, provides composite signals resulting in a brightness temperature of the terrain. Applicability of passive systems appears to have value for sea state determination, sea ice identification, soil moisture studies and basic investigations for microwave-terrain interaction mechanisms.

The design of imaging radars for geological investigations requires an interdisciplinary effort which includes both a theoretical (provided by the radar engineer) and applications-oriented (provided by the geologist or other geoscientists) understanding of the sensor's operation. Certainly the geologist utilizing the imagery need not be capable of system design; however, certain fundamentals of radar operation should be understood in order to provide optimum data retrieval for the interpretation.

B.2.2 Radar Operation Frequencies

Conventional radars utilize the frequency range from 230 to 40,000 MHz although neither end of this range is truly definitive of the frequency limitation for radar operation. A letter code of frequency-wavelength bands, *K*, *X*, *L*, etc., was arbitrarily selected for military security in the early developmental stages of radar and has continued in remote sensing for convenience. Table B.1 lists these bands. The military has reassigned the wavelength bands, but the older band designations are still popularly used.

Table B.1: Radar wavelength bands.

BAND	WAVELENGTH (cm)	FREQUENCY RANGE (MHz)
K	2.4 - .83	12,500 - 36,000
X	5.5 - 2.4	5,200 - 12,500
C	7.7 - 4.8	3,900 - 6,200
S	19. - 5.8	1,550 - 5,200
L	77. - 19.	390 - 1,550
P	133 - 77.	220 - 390

B.2.3 Radar Geology before Side-Looking Radar

In the early 1900's the United States and several European countries independently developed Plan Position Indicator (PPI) radar for military applications. These circularly scanning devices provided a terrain format radiating in a circular fashion from beneath the aircraft. During World War II, radar operational techniques were developed to a high degree; after the war, however, the development of radar technology was somewhat decelerated. Dunlap (1946) was among the first authors to provide high-quality PPI radar scope photographs in the open literature after the war. These relatively high resolution images of New York City, Washington, D.C., and Nantucket Island off the Massachusetts coast provided an early indication of non-military uses for radar. Lt. H. P. Smith (1948) compared PPI presentations with existing charts of northwestern Greenland and noted that the radar-derived data far exceeded the terrain information from available maps. He submitted his report to the U.S. Geological Survey and subsequently other government agencies began to consider the potential of radar imagery for displaying terrain information (Scheps 1962).

Among the first unclassified reports and open literature articles suggesting the use of radar images (PPI) for terrain-geologic studies were those of Hoffman (1954, 1958, 1960) and Feder (1957, 1959, 1960a). Hoffman's work related mostly to development of radar imagery interpretation keys, parallel to the recognition elements used in photo interpretation. Feder stressed the potential qualitative and quantitative uses of radar, and suggested that textures of surficial materials as well as subsurface soil and rock composition might be determined through image interpretation. Feder (1960b) completed an M. S. thesis, "Radar Geology," at the University

of Buffalo, and although his initial research embraced only images from low resolution PPI systems, he was one of the primary advocates of the potential application of radar interpretation to geologic investigations. Coincident with the declassification of PPI radar images in the early 1950's was the development of complex navigational radars and sophisticated components required for the tracking of missiles and satellites. Although the concept of side-looking airborne radar (SLAR) systems had been known in the late 1940's, it was not until the 1950's that system components became available.

B.2.4 Side-Looking Radar Operation

Side-looking airborne radars (SLAR) produce imagery of the terrain on one or both sides of the aircraft flight path. SLAR differs from other scanning radar systems in that the antenna is fixed to the aircraft and its radiation pattern is directed perpendicular to the ground track. Scanning is accomplished by the movement of the aircraft in flight.

Side-Looking Airborne Radar (SLAR)
Side-looking airborne radars often produce imagery of the terrain on one or both sides of the aircraft flight path. SLAR differs from other scanning radar systems in that the antenna is fixed to the aircraft and its radiation pattern is directed perpendicular to the ground track. Scanning is accomplished by the movement of the aircraft in flight.

B.2.4.1 Real Aperture vs Synthetic Aperture

There are two primary methods of SLAR operation: (1) real aperture (brute force) and (2) synthetic aperture. Advantages of one mode of operation over the other are related to achieving improved azimuth resolution (along track).

There are two primary methods of SLAR operation
Real aperture radar (RAR)
Real aperture radar systems employ long antennas to achieve their resolution. The longer the antenna, compared to the wavelength of the transmitted electromagnetic signal, the finer the resolution. Practical antenna sizes limit resolution achievable via this technique.
Synthetic aperture radar (SAR)
Synthetic aperture radar systems use signal processing theory to synthesize the effect of a long antenna from a short one thereby achieving fine resolution. The smaller the antenna, compared to the transmitted wavelength, the finer the resolution achievable via synthetic aperture techniques.

Figure B.1(a) shows an area being imaged by a typical real aperture SLAR system where the antenna (A) is repositioned laterally at the velocity of the aircraft (V_a). Each radar pulse transmitted (B) returns signals from the targets within the beamwidth. These target returns are converted to

a time/amplitude video signal (C) which is imaged as a signal line (E) on photographic film (F). Returns from subsequently transmitted pulses are displayed on the CRT at the same position (D) as the previous scan lines. By moving the photographic film past the CRT display line at a velocity (V_f) proportional to the velocity of the aircraft (V_a), an image of the terrain is recorded on the film (F) as a continuous strip map.

B.2.4.2 Terrain-Signal Interaction

Radar return is that portion of the transmitted radar energy returned to the receiver. The appearance of radar imagery can be understood by considering some of the characteristics microwave energy shares with light waves. When electromagnetic waves strike a boundary or surface, some of the energy is transmitted into the new material with the remainder reflected. Waves striking a boundary are reflected specularly (similar to light reflection from a mirror) or diffusely (scattered in all directions). The significant difference between light waves and microwave energy is the respective wavelength involved (visible light is 0.4-0.7 micrometers, radar is 1 mm to several meters).

Radar signals are normally returned from the terrain to the receiver by a scattering process (backscatter). The signal strength (or intensity of this terrain return) received at the antenna determines the relative degree or brightness (tone) on the imagery. The fundamental parameters which affect radar return are: angle of incidence, surface roughness, frequency/wavelength, polarization, and complex dielectric constant.

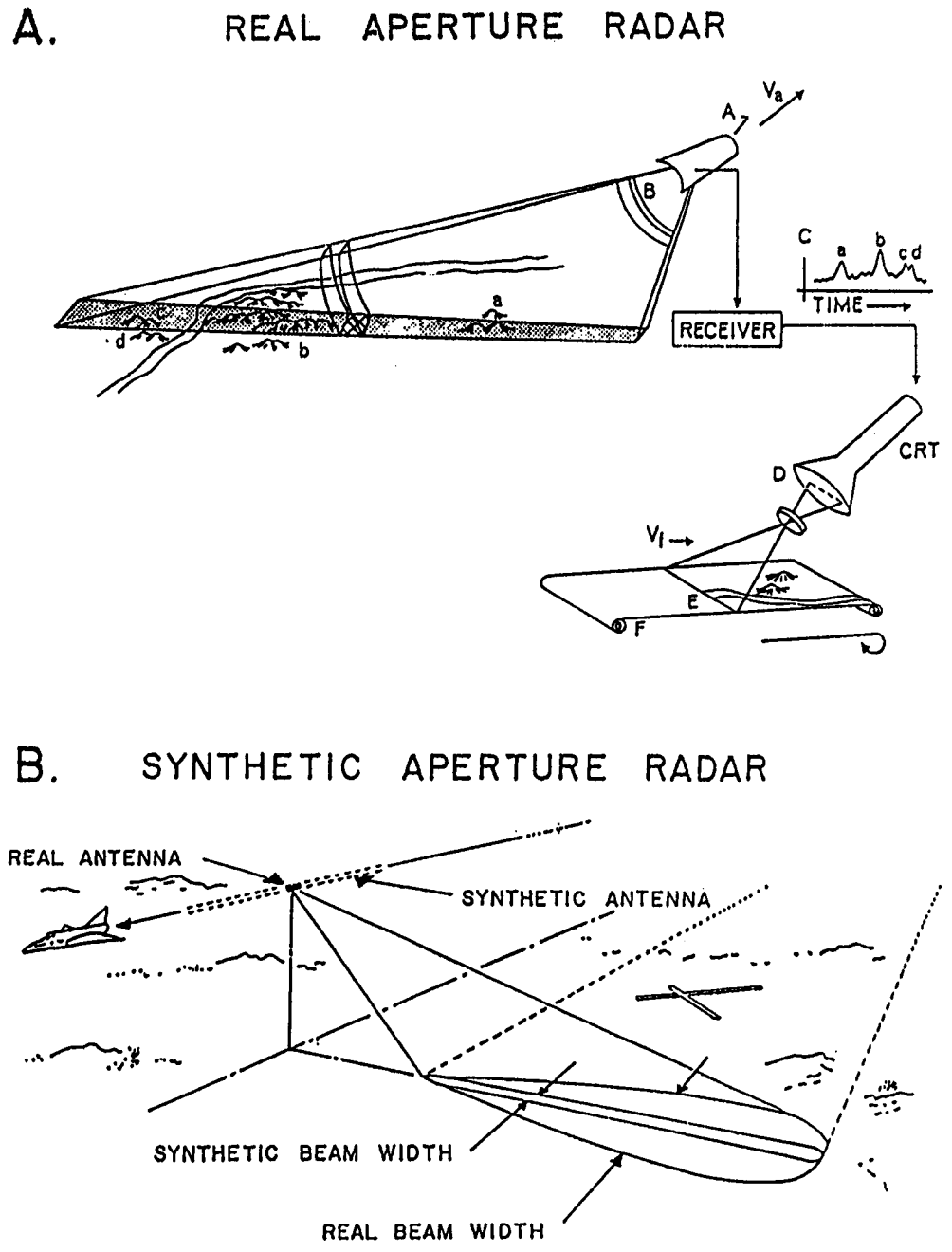

Figure B.1: Radar imaging system illustrations. (a) Real aperture system. (b) Synthetic aperture system.

The fundamental parameters which influence radar return
Angle of Incidence
Surface Roughness
Frequency/Wavelength
Polarization
Complex Dielectric

B.2.4.2.1 Angle of Incidence

The angle of incidence θ (often referred to as radar look angle) is the angle formed by an impinging beam of radar energy and a perpendicular to the incident surface at the point of incidence (Figure B.2 (a) and (b)). The angle between a line from the transmitter to a point on the terrain, and a horizontal plane passing through the transmitter is the depression angle.

The geometric parameters of SLAR imaging systems are such that along the swath of an area imaged (near to far range) there is a continuous change in the angle of incidence (Figure B.2 (a) and (b)). When imaging homogeneous flat terrain for any constant depression angle along the flight path, the angle of incidence will remain constant. Under more typical natural terrain conditions, however, local variations in terrain slope can change the effective angle of incidence (called the local angle of incidence). The consequence of terrain slope on both the local incidence angle and aspect angle (complement of incidence angle), at a constant depression angle, is shown in Fig. B.2c. Note in Fig. B.2(c) that if the terrain is flat,

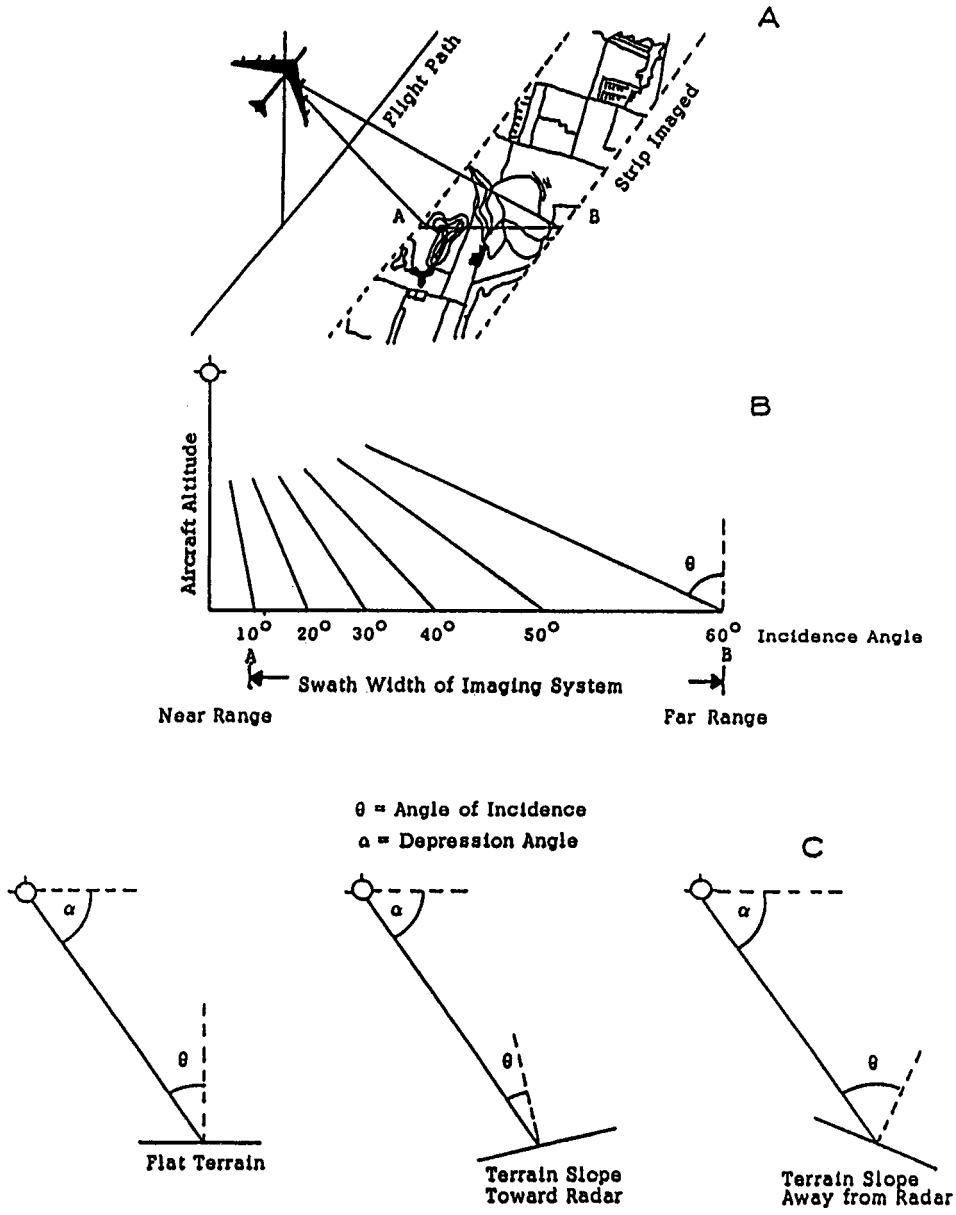

Figure B.2: SLAR ground swath. (a) Ground coverage. (b) Swath width for flat terraain, change in incidence and depression angles near to far range. (c) Effect of terrain slope (with constant depresssion angle) on incidence and aspect angle.

the aspect angle equals the depression angle and the local incidence angle equals the incidence angle. However, if terrain slopes are oriented at an angle toward the imaging radar, the effective angle of incidence decreases (with increasing terrain slope angle) to a point where the aspect angle equals 90° and the local angle of incidence is 0° (vertical incidence) and maximum reradiation results. Conversely, if terrain slopes are oriented away from the imaging radar, the angle of incidence increases (with increasing terrain slope angle) to a point where grazing (minimum reradiation) results.

Local Angle of Incidence
The angle formed by an impinging beam of radar energy and a perpendicular to the incident surface at the point of incidence.
Look Angle or Angle Of Incidence
The angle formed by an impinging beam of radar energy and a perpendicular drawn at nadir.
Depression Angle
The angle between a line from the antenna to a point on the terrain, and a horizontal line passing through the antennna.
Aspect Angle
The angle between a line from the antenna to a point on the terrain and a line parallel to the incident surface.

B.2.4.2.2 Surface Roughness

Surface roughness, a geometric property of the terrain, generally has the most important influence upon the return signal (image tone). Terrain surfaces may be divided into two major categories according to the degree of surface roughness; smooth or rough. In general, smooth surfaces appear dark in an image and rough surfaces appear bright. If the root-mean-square (rms) surface roughness is much less than a wavelength ($rms \leq \lambda/10$), the surface appears "smooth". If the rms surface roughness is of the order of a wavelength or more ($rms \geq \lambda$) the surface appears "rough". Terrain surfaces therefore can be classed according to roughness. On the one extreme is a very smooth surface acting like a perfect specular reflector, where backscatter exists only near vertical incidence. At the other extreme is a very rough surface acting like a perfect diffuse or isotropic scatterer, where the scattering coefficient is independent of the angle of incidence.

Surface Roughness
Geometric property of the terrain at a wavelength scale. Generally surface roughness is the most important influence upon radar return. In general, smooth surfaces appear dark in an image and rough surfaces appear bright. Signal surface roughness is not an absolute roughness, but the relative roughness expressed in wavelength units.

B.2.4.2.3 Frequency/Wavelength

The variations attributable to frequency are directly related to two parameters; surface roughness and complex dielectric constant. In general, the rougher the surface in terms of wavelength, the more diffuse the return. Consequently, a given surface will normally appear rougher at a higher frequency (shorter wavelength) than at a lower frequency. Varying the frequency of the wave incident upon a natural terrain surface of any roughness produces an effect similar to variations in surface roughness.

Frequency/Wavelength
Varying the frequency of the radar energy upon a natural terrain surface produces an effect similar to variations in surface roughness.

B.2.4.2.4 Polarization

The polarization of an electromagnetic wave describes the orientation of the electric field strength vector at a given point in space during one period of oscillation. With traditional single polarization SLAR configurations, a horizontal electric field vector is radiated and upon striking the terrain some of the energy is returned to the antenna with the same polarization as the transmitted pulse. Thus, only the horizontal component of the return signal from the terrain will be displayed on the imagery; however, independent of the transmitted polarization, the return signals can also contain a depolarized component, i.e., energy depolarized by the terrain surface and vibrating in various directions. Depolarization refers to the

change in polarization that an electromagnetic wave undergoes as a consequence of interaction with the terrain. Radar systems which provide traditional horizontally polarized antenna and an additional vertically polarized antenna allow simultaneous display of return signals of both polarizations. The HH (transmit and receive horizontal electric-field vector) is known as the co-polarized return; the HV (receive vertical electric-field vector) return is known as the cross-polarized return.

Polarization
In traditional SAR configurations the electromagnetic signal is radiated and received with the electric vector oriented so that it is horizontal to the Earth at grazing incidence. This is known as horizontal co-polarization. Vertical co-polarization and both cross-polarizations can also be transmitted and received.
Independent of the transmitted polarization, the return signal will be depolarized as a function of certain terrain parameters. The cross-polarized return can be displayed simultaneously with the like-polarized signal, if the SAR system is capable of receiving both polarizations.

B.2.4.2.5 Complex Dielectric

The complex dielectric constant (the electrical properties of the surface) will influence reflectivity of the radar return from terrain surfaces. As a function of the dielectric constant, observed changes in reflectivity from natural surfaces are primarily due to changes in the moisture content of either the vegetation or soil surface. In the microwave region of the

spectrum, the dielectric constant of most naturally occurring materials, when dry, is in the range of 3 to 8. Here, the radar energy would travel through a relatively large volume of material and reflectivity would be comparatively low. However, in the same frequency region, the dielectric constant of water may be near 80. An increase in the dielectric constant increases the reflectivity of a surface and the radar energy would be reflected back without significant travel through the material. The effect of water content on the return from a dense volume of foilage has been observed where variations in return were attributable principally to the moisture content of the vegetation itself.

We may also see that the loss or attenuation of the microwave energy is a function of the conductivity of the material and the frequency of the energy. In general, the higher the frequency, the greater is the attenuation in the material and hence the effective penetration is less. This may have a marked effect on the return from vegetated surfaces. At the higher frequencies, the return is essentially from the top of the vegetation canopy. At lower frequencies, with greater penetration capability, the return may be primarily a volume return contributed by leaves, branches, trunks, and, perhaps, even the ground. The complex dielectric constant varies almost linearly in response to the moisture per unit volume contained, and penetration of microwave energy is greatest and reflection least with low moisture contents. Conversely, penetration is least and reflection is greatest when moisture contents are high.

Complex Dielectric
Relates to the electrical properties of the surface. At radar frequencies, the dielectric constant of most Earth materials, when dry, are very similar. However, significant changes in dielectric properties of natural materials usually result from changes in moisture content.

REPUBLIC OF THE PHILIPPINES

Bondoc Peninsula

N

Transverse Mercator 1/250,000

Statute Miles
0 5 10 15 20

0 5 10 15 20 25 30
Kilometers

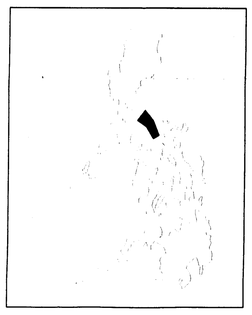

Radar-Lineament Interpretation

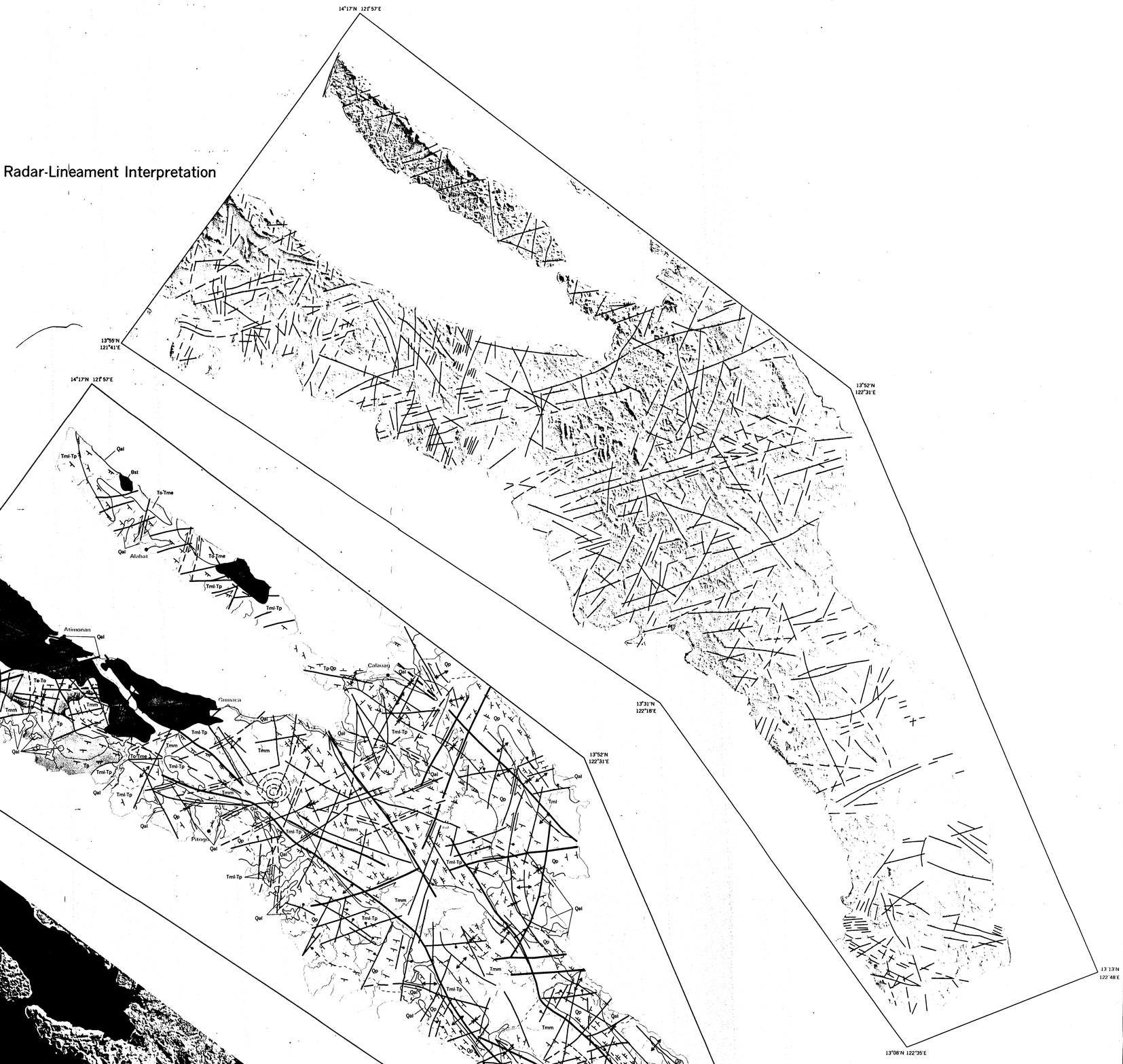

Radar-Geologic Interpretation

Radar Mosaic

Altitude: 28,000 feet AGL
Look Direction: South-West
Date Flown: May 1987

Qal	Quaternary alluvium.
Qp	Pleistocene limestone. Malumbang Fm.
Tp-Qp	Pliocene - Pleistocene clastics; interbedded sandstone and shale with gravelly limestone lenses. Vinas Fm.
Tp	Pliocene clastics; interbedded siltstone , shale, calcareous sandstone. Hondagua Fm.
Tml-Tp	Late Miocene - Pliocene clastics; sandstone and siltstone. Upper Canguinsa Fm.
Tml	Late Miocene clastics; predominantly sandstone with interbedded siltstone, shale, mudstone, local basal conglomerate. Lower Canguinsa Fm.
Tmm	Middle Miocene clastics; mostly shale with interbedded sandstone, limestone lenses. Vigo Fm.
To-Tme	Oligocene - Early Miocene limestone. Panaon Fm.
	Eocene - Oligocene volcanics; porphyritic andesite, amygdaloidal basalt, tuffaceous sandstone and conglomerate. Unisan Volcanics.
	Cretaceous metamorphics/intrusives; amphibolites, gneiss and splitic rock groups, pillow lavas, graywacke, chert. Basement Complex.

Lithologic boundary
Faults (dashed where inferred); ↑ on downthrown side, ⇌ strike-slip
Anticline (dashed where inferred)
Syncline (dashed where inferred)
Dip group less than 15 degrees
Dip group 15 to 45 degrees
Dip group greater than 45 degrees
Structural form lines

ARCI

REPUBLIC OF THE PHILIPPINES

Cotabato Basin, Mindanao
Radar-Geologic Interpretation

N

Transverse Mercator 1/250,000

Statute Miles
0 5 10 15 20

0 5 10 15 20 25 30
Kilometers

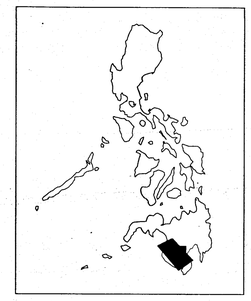

7°30'N 124°40'E — 124°30'E — 124°45'E — 124°15'E — 7°15'N — Cotabato — 124°00'E — 125°00'E — 7°07'N 123°55'E — 7°06'N 125°02'E — 125°15'E — 7°06'N 125°22'E — 7°00'N — 124°00'E 7°00'N — 6°45'N — 124°15'E — 6°30'N — 124°30'E — 6°15'N — 125°30'E — 6°45'N 125°22'E — 6°30'N — 6°22'N 125°42'E — 6°15'N — 125°30'E — 124°45'E — General Santos — 125°15'E — 6°00'N — 5°50'N 125°00'E

HIGH — LOW — Korondal

Qal — Quaternary alluvium.

Qv — Quaternary volcanics; pyroclastics and lava flows, alternating tuffaceous shale or mudstone, tuffaceous sandstone and conglomerate.

Qp — Pleistocene clastics; reefal limestone interbedded with marine mudstone and sandstone; Omanay Marl; well preserved oyster beds.

Tpv-Qpv — Pliocene-Pleistocene volcanics; interbedded silty tuffaceous shale, tuffaceous sandstone, pyroclastics, volcanic flows. Carmen Fm.

Tp-Qp (C) — Pliocene-Pleistocene limestone/clastics; (L) limestone facies; (C) clastic facies; interbedded tuffaceous sandstone, poorly consolidated ferruginous sandstone, calcareous siltstone.

Tp (L) Tp (C) — Pliocene limestone/clastics; Marbel Fm.; (L) Awang-Table Limestone; biohermal limestone with interbedded marl; (C) San Mateo Clastics; tuffaceous mudstone, marl, limestone, tuffaceous sandstone, pebble conglomerate.

Tml-Tp — Late Miocene-Pliocene clastics; conglomerate, sandstone, marine mudstone, siltstone. Nicaan Fm.

Tml — Late Miocene clastics; mudstone, claystone, sandstone, conglomerate, siltstone. Dinganen Fm.

Tmm-Tml — Middle-Late Miocene clastics; undifferentiated.

Tmm — Middle Miocene clastics; thick sequence of shale, siltstone, carbonaceous mudstone with interbedded sandstone and basal limestone. Patut Fm.

Tme-Tmm — Early-Middle Miocene clastics; undifferentiated.

Tol-Tme — Oligocene-Early Miocene clastics; undifferentiated.

Late Oligocene clastics; primarily limestone with conglomerate, interbedded sandstone, and occasional coal seams. Maganoy Fm.

Pre-Oligocene metamorphics/volcanics/intrusives; schist, quartzite, slates, marbles, metavolcanics, porphyritic andesite, basalt, peridotites, gabbro, diorites. Basement Complex.

- Lithologic boundary
- Faults (dashed where inferred); ↑ on downthrown side, ⇌ strike-slip
- Anticline (dashed where inferred)
- Syncline (dashed where inferred)
- Dip group less than 15 degrees
- Dip group 15 to 45 degrees
- Dip group greater than 45 degrees
- Vertical beds
- Structural form lines
- (?) Geomorphic anomaly

ARCI

REPUBLIC OF THE PHILIPPINES

Cotabato Basin, Mindanao
Radar Mosaic

N

Transverse Mercator 1/250,000

Statute Miles
0 5 10 15 20

0 5 10 15 20 25 30
Kilometers

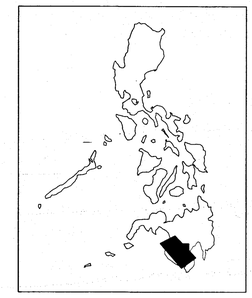

7°30'N 124°40'E

7°07'N 123°55'E

7°06'N 125°02'E

7°06'N 125°22'E

6°45'N 125°22'E

6°22'N 125°42'E

5°50'N 125°00'E

Altitude: 28,000 feet AGL
Look Direction: North-East
Date Flown: May 1987

ARCI

REPUBLIC OF THE PHILIPPINES

Cotabato Basin, Mindanao
Radar-Lineament Interpretation

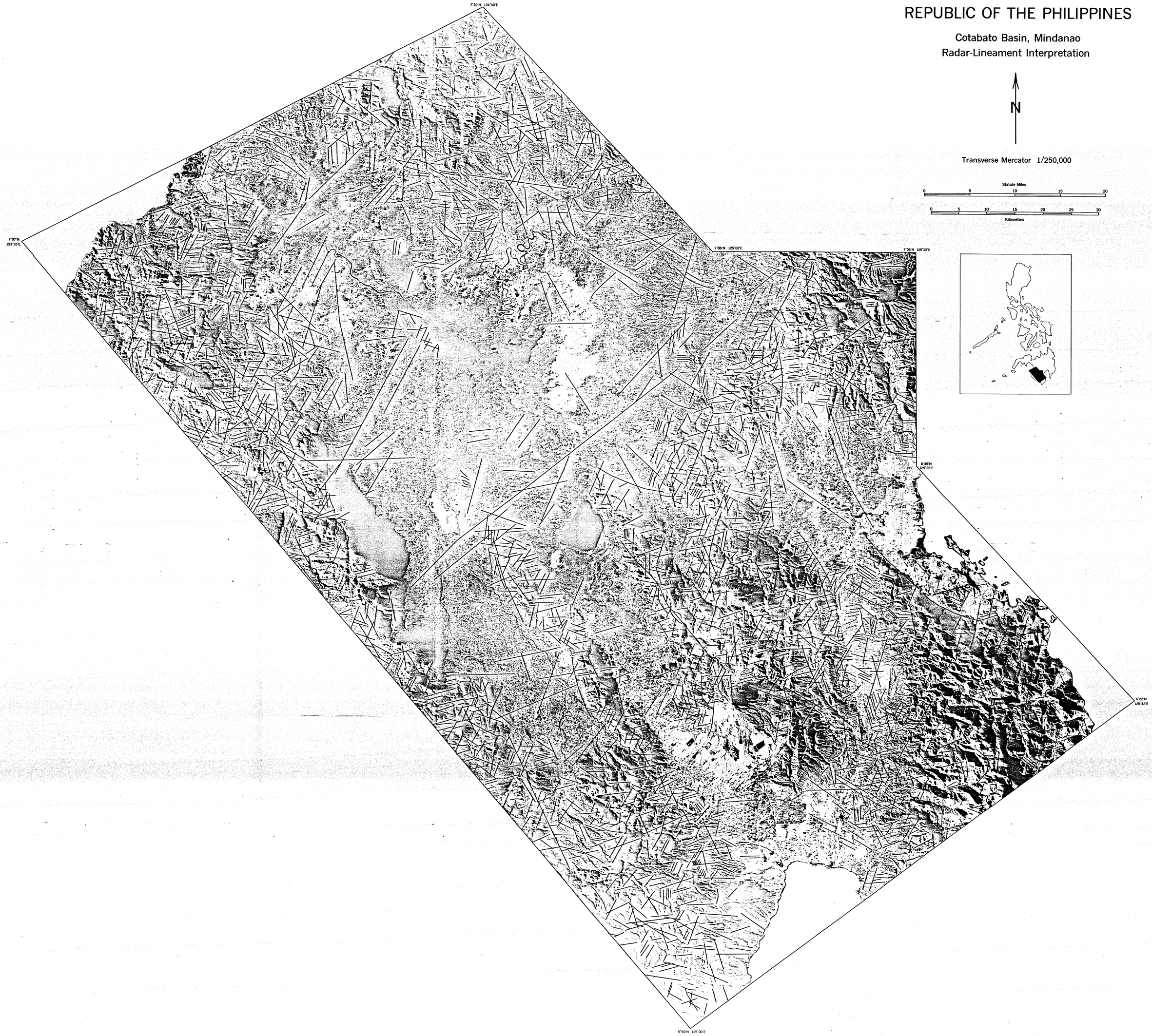

N

Transverse Mercator 1/250,000

Statute Miles
0 5 10 15 20

0 5 10 15 20 25 30
Kilometers

ARCI

REPUBLIC OF THE PHILIPPINES

Cebu Island

N

Transverse Mercator 1/250,000

Statute Miles
0 5 10 15 20

0 5 10 15 20 25 30
Kilometers

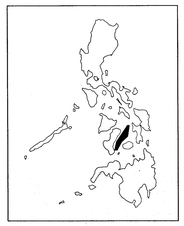

Radar Mosaic

Altitude: 26,000 feet AGL
Look Direction: North-West
Date Flown: May 1987

Radar-Geologic Interpretation

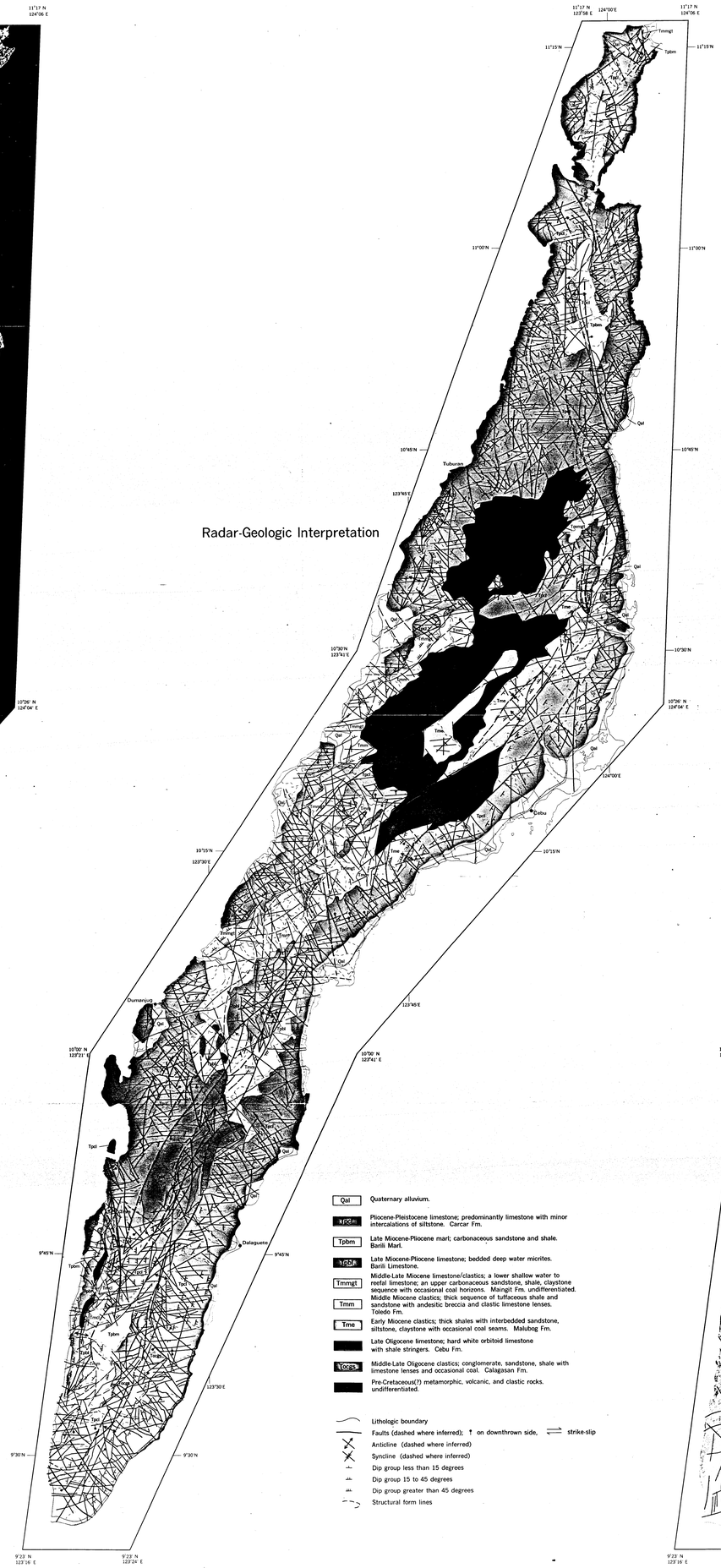

Qal	Quaternary alluvium.
Tpd	Pliocene-Pleistocene limestone; predominantly limestone with minor intercalations of siltstone. Carcar Fm.
Tpbm	Late Miocene-Pliocene marl; carbonaceous sandstone and shale. Barili Marl.
Tpbl	Late Miocene-Pliocene limestone; bedded deep water micrites. Barili Limestone.
Tmmgt	Middle-Late Miocene limestone/clastics; a lower shallow water to reefal limestone; an upper carbonaceous sandstone, shale, claystone sequence with occasional coal horizons. Maingit Fm. undifferentiated.
Tmm	Middle Miocene clastics; thick sequence of tuffaceous shale and sandstone with andesitic breccia and clastic limestone lenses. Toledo Fm.
Tme	Early Miocene clastics; thick shales with interbedded sandstone, siltstone, claystone with occasional coal seams. Malubog Fm.
	Late Oligocene limestone; hard white orbitoid limestone with shale stringers. Cebu Fm.
Tocgs	Middle-Late Oligocene clastics; conglomerate, sandstone, shale with limestone lenses and occasional coal. Calagasan Fm.
	Pre-Cretaceous(?) metamorphic, volcanic, and clastic rocks, undifferentiated.

- Lithologic boundary
- Faults (dashed where inferred); ↑ on downthrown side, ⇌ strike-slip
- Anticline (dashed where inferred)
- Syncline (dashed where inferred)
- Dip group less than 15 degrees
- Dip group 15 to 45 degrees
- Dip group greater than 45 degrees
- Structural form lines

Radar-Lineament Interpretation

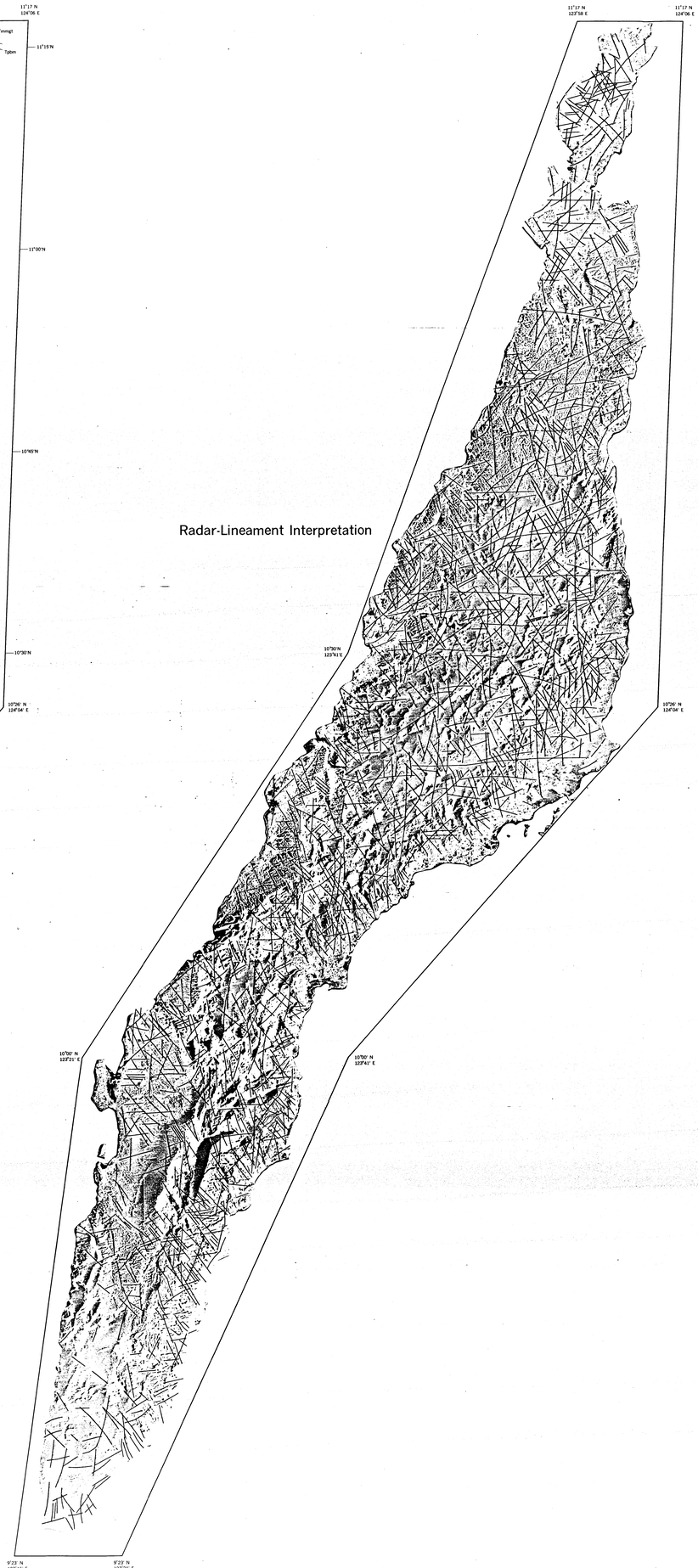

ARCI

REPUBLIC OF THE PHILIPPINES

Mindoro Island

N

Transverse Mercator 1/250,000

Statute Miles
0 5 10 15 20

Kilometers
0 5 10 15 20 25 30

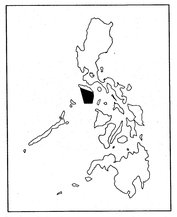

Radar Mosaic

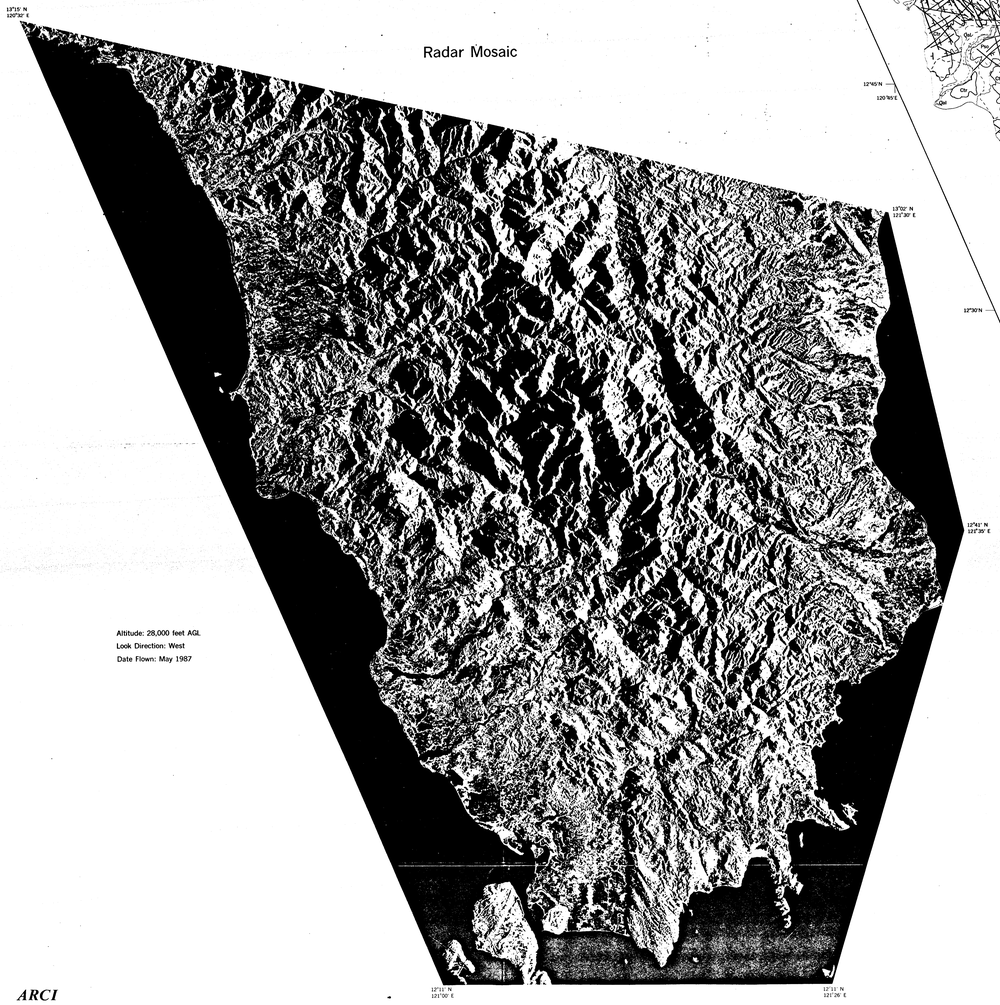

Altitude: 28,000 feet AGL
Look Direction: West
Date Flown: May 1987

Radar-Geologic Interpretation

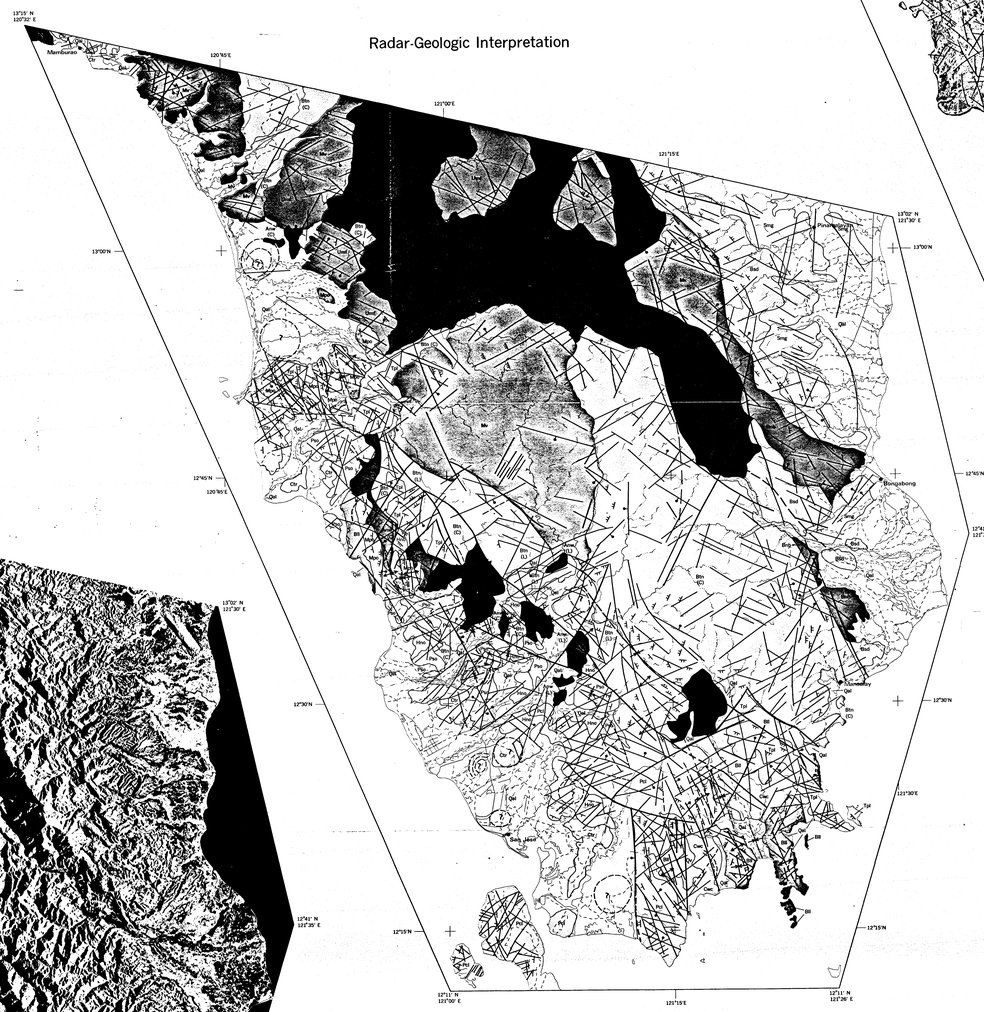

Radar-Lineament Interpretation

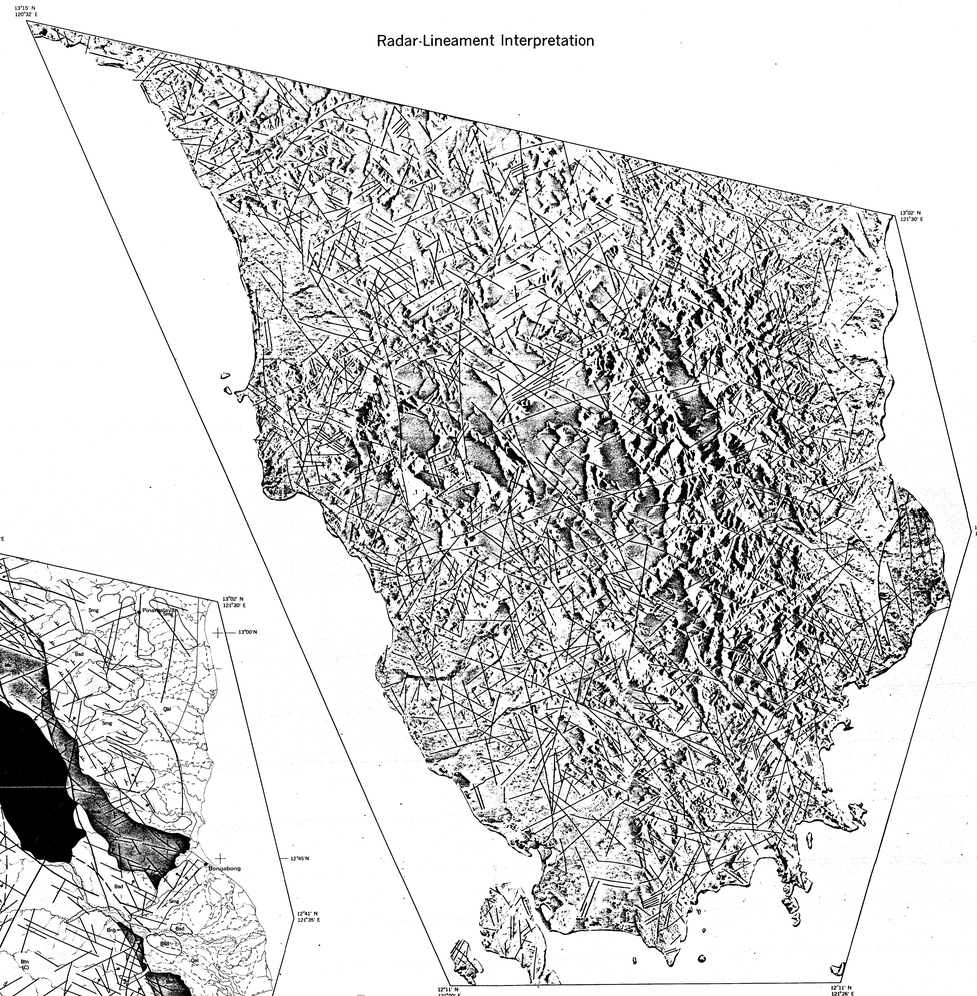

Qal Quaternary alluvium.

Qv Quaternary volcanics; undifferentiated volcanics and pyroclastics.

Ctr Pleistocene clastics; semi-consolidated conglomerate. Central Conglomerate.

Smg Pleistocene pyroclastics. Sumagui Pyroclastics.

Cwc Pliocene clastics; poorly consolidated quartzose sandstone and siltstone with coal seams. Cawacat Coal Measures.

Pcl Pliocene limestone; reefal and shallow water detrital limestone. Paclolo Limestones.

Hno Pliocene clastics; basal planktonic calcisiltites. Hinango Calcisiltites.

Bsd Late Miocene-Pliocene clastics; polymictic conglomerate. Bansud Conglomerates.

Late Miocene-Pliocene limestone; transgressive shelfal limestone. Bongabong Limestones.

Pso Late Miocene clastics; conglomerate with poorly consolidated arkose and terrigenous calcarenite. Punso Conglomerates.

Tpl Middle Miocene limestone; thick-bedded lagoonal and shelfal carbonates and patch reefs. Tusk Peak Limestone.

Bll Early Miocene limestone; undifferentiated carbonates. Bulalacao Limestone.

Mpo Early Miocene clastics; interbedded carbonaceous shale and sandstone, clastic turbidites, hypabyssal micrites. Mompong Turbidites.

Oligocene limestone/clastics; (L)limestone facies; thin-bedded open marine detrital limestone; (C)clastic facies; shallow water sandstone and claystone. Anahawin Fm.

Oligocene metavolcanics; altered pillow basalts and bathyal red argillites.

Ultramafic Oligocene ultramafics; undifferentiated.

Btn(L) Btn(C) Eocene limestone/clastics; (L)limestone facies; biohermal limestone; (C)clastic facies; arkose, shelfal calcarenite, minor quartz arenite with carbonaceous siltstone, claystone, and dark thick shale. Batangan Fm.

Mesozoic-Paleozoic metamorphics; crystalline schist, slate, marble, gneiss, and metavolcanics. Mindoro Metamorphic Fm.

- Lithologic boundary
- Faults (dashed where inferred); ↑ on downthrown side, ⇌ strike-slip
- Anticline (dashed where inferred)
- Syncline (dashed where inferred)
- Dip group less than 15 degrees
- Dip group 15 to 45 degrees
- Dip group greater than 45 degrees
- Structural form lines
- Geomorphic anomaly

ARCI